Synthetic biomaterial microenvironments to modulate paracrine effects of mesenchymal stromal cells for skeletal muscle regeneration

vorgelegt von

M.Sc.

Taimoor Hasan Qazi

geboren in Islamabad, Pakistan

von der Fakultät III – Prozesswissenschaften
der Technischen Universität Berlin
zur Erlangung des akademischen Grades

Doktor der Ingenieurwissenschaften

- Dr.-Ing. –

genehmigte Dissertation

Promotionsausschuss:

Vorsitzender:	Prof. Dr. Jens Kurreck
Gutachter:	Prof. Dr. Roland Lauster
Gutachter:	Prof. Dr. Georg N. Duda

Tag der wissenschaftlichen Aussprache: 08 Februar 2017

Berlin 2017

TABLE OF CONTENTS

For my parents

I. Acknowledgements

This thesis would not have been possible without the support, encouragement, help, assistance, friendship, advice, mentoring, and guidance of a number of individuals who I would like to thank.

I express my sincere gratitude to Prof. Georg Duda for putting his trust in me and believing in me throughout the last four years. He has always extended his full support through every stage of my doctoral studies, and I have gained immensely from interacting with him. I am very grateful to Prof. David Mooney for being a great supervisor and mentor, and for his unconditional support, encouragement, and guidance through good and bad days. He is someone I look up to, and I have benefitted from his words of wisdom. I would also like to thank Prof. Roland Lauster for agreeing to supervise my thesis, and for providing constant support throughout.

I especially thank my mentor Dr. Sven Geißler for his invaluable advice and guidance, and for always having my back. He gave me independence and provided financial support to pursue my interests in the lab, and provided excellent feedback and constructive criticisms. I also thank my clinical mentor Dr. Tobias Winkler, who recognized my potential early on and made every effort to facilitate my training and scientific growth. His constant encouragement and motivational talks spurred me on. I was lucky to have Martin Textor in the lab who introduced me to cell culture and trained me in methods of molecular and cellular biology. His optimism and positive attitude continues to amaze me, and I have thoroughly enjoyed our companionship. I am also grateful to Kristin Strohschein who was my go-to person when I first joined the lab, and who helped me with various personal, administrative, and scientific matters. I thank Janosch, Andrea, Ana, and Julia for making the lab and office a joyful place to do research, and Dorit, Antje, Janine, and Lily for their technical assistance.

Over the years, I have come to interact with a number of surgeons and clinical fellows all of whom have contributed in some way to my scientific growth; I therefore thank Dr. Matthias Pumberger, Dr. Philipp von Roth, and Dr. Michael Fuchs for providing insights into clinical scenarios and for fruitful discussions and collaborations.

There are a number of people at the JWI with whom I have enjoyed working, and who have been extremely helpful and accomodating with my questions and requests. I therefore thank Ansgar, Erik, Sophie, Aaron, Dag, Gabriela, and Mario. I especially thank Dr. Evi Lippens whose contagious optimism, work ethic, passion for science, and ambition have greatly inspired

me, and I am grateful for her unwavering support and encouragement. I will always cherish our discussions, collaborations, and joint mentoring of SH. I am also thankful to Aru for her friendship, for bearing with my crazy collaboration ideas, and for taking my mind off of work especially when I needed it.

I have enjoyed excellent personal and administrative support from the BSRT coordination office, especially Sabine, Janet, and Bianca, and I thank them for their assistance.

I would like to acknowledge financial support from the Friede Springer Stiftung and the Berlin-Brandenburg School for Regenerative Therapies.

I am thankful to the numerous bachelor/master/medical students who I have worked with, and some of whom I have had the pleasure of mentoring, especially Tine, Aline, Shahzad, Miriam, Janina, and Mareike. I also thank collaborators at the MPI (Prof. Sigmar Stricker) and Harvard (Cristina Borselli, Luo, and Katie from the Mooney lab).

Finally, and most importantly, I thank my family (Mama, Papa, Wardah, and Ahmed) and my wife Salwa for all their love, care, encouragement, and support. This is for you guys.

II. Selbständigkeitserklärung / Declaration of authorship

Hiermit erkläre ich, dass ich die hier vorliegende Dissertation selbstständig und eigenhändig und nur unter Verwendung der angegeben Hilfsmittel und Literaturquellen angefertigt habe.

Ich versichere, dass ich diese Arbeit weder in gleicher noch in ähnlicher Form in anderen Prüfungsverfahren vorgelegt habe.

Ich habe die dem Prüfungsverfahren zu Grunde liegende Promotionsordnung der Fakultät III Prozesswissenschaften der Technischen Universität berlin zur Kenntnis genommen.

I hereby declare that this thesis has been written by myself, independently and without the help of third parties. I have not used any other tools or references except for those cited in this work.

The work has not been presented in the context of any other examination procedure.

I have read and understood the underlying doctoral degree regulations of the Faculty III Process Engineering of the Technische Universität Berlin.

III. List of Abbreviations:

µg – microgram

µl – microliter

µM – micro mole

2D – two-dimensional

3D – three-dimensional

ANOVA – analysis of variance

CM – conditioned medium

DAPI – 4',6-diamidino-2-phenylindole

ECM – extracellular matrix

EDC – 1-Ethyl-3-(3-dimethylaminopropyl) carbodiimide

EDTA - ethylenediamine tetraacetic acid

ELISA – enzyme-linked immunosorbent assay

FAP – fibro/adipogenic progenitor cell

FCS – fetal calf serum

g – gram

G_4RGDSP – (Glycine-Glycine-Glycine-Glycine-Arginine-Glycine-Aspartic acid-Serine-Proline)

GAPDH – Glyceraldehyde 3-phosphate dehydrogenase

GF – hIGF + hVEGF

h – hour

H&E – Hematoxylin and Eosin

hIGF – recombinant human IGF-1

HUVEC – Human Umbilical Vein Endothelial Cells

hVEGF – recombinant human $VEGF_{165}$

I – hIGF

I-CM – hIGF stimulated MSC derived conditioned media

IL – interleukin

l – liter

M – mol

M1 – classically activated macrophages (proinflammatory)

M2 – alternatively activated macorphages (anti-inflammatory)

mg – milligram

MHC – myosin heavy chain

min – minute

ml – milliliter

mM – milli mole

MSC – mesenchymal stromal cell

MSC-CM – conditioned media derived from MSCs

MyoD – myogenic differentiation factor

MyoG – myogenin

nAB – neutralization/blocking antibody

NHS – N-Hydroxysuccinimide

Pax7 – paired box protein 7

PFA - paraformaldehyde

qPCR – quantitative polymerase chain reaction

rFGF – fibroblast growth factor secreted by rat MSCs

rHGF – hepatocyte growth factor secreted by rat MSCs

rIGF – insulin like growth factor secreted by rat MSCs

rLIF – leukemia inhibitory factor secreted by rat MSCs

RT-qPCR – real time quantitative polymerase chain reaction

rVEGF – vascular endothelial growth factor secreted by rat MSCs

s – second

SC – satellite cell

TBST – Tris Buffered Saline with Tween® 20

V – hVEGF

V-CM – hVEGF stimulated MSC derived conditioned media

VI – hVEGF + hIGF

VI-CM – hVEGF + hIGF stimulated MSC derived conditioned media

IV. List of Figures:

V. List of Tables:

VI. List of Appendices:

VII. Abstract

While skeletal muscles can recover from minor injuries, severe trauma can often induce irreversible structural damage such as extensive scar tissue formation and damaged muscle fibers. This leads to functional deficits and loss in the quality of life of patients. Effective treatment of severe muscle injuries is currently an unmet clinical need. In such cases, a therapeutic intervention such as cell transplantation can be beneficial. Mesenchymal stromal cells (MSCs) have gained wide attention in regenerative medicine, and have recently been explored in the context of muscle repair.

The hypothesis guiding this thesis was that the paracrine effects of MSCs, by which they can influence the biological function of progenitor cells, can be enhanced by providing MSCs with appropriate microenvironments during transplantation. In this way, the paracrine function of MSCs can be harnessed to stimulate muscle progenitor cells function leading to muscle regeneration.

Comparison of a series of substrates that differed in dimensionality and microstructure revealed that MSCs enhanced their secretion pattern after culture on 3D macroporous scaffolds. In response to MSC conditioned medium, muscle progenitor cells displayed improved proliferation, survival, migration, and differentiation behaviors. Interestingly, MSCs encapsulated in 3D nanoporous hydrogels elicited significantly weaker functional response in myoblasts. MSC paracrine effects depended on the establishment of N-cadherin mediated cell-cell contacts which was facilitated by the macroporous structure of 3D scaffolds, but inhibited by the nanoporous structure of 3D hydrogels.

The ability of MSCs to respond to soluble cues was investigated via transient exposure to recombinant growth factors. MSCs in macroporous scaffolds upregulated their secretion pattern in response to growth factor stimulation. As a result, pro-regenerative myoblast functions were further enhanced. In comparison, encapsulated MSCs showed a much weaker response to growth factor stimulation. Thus, macroporous scaffolds constituted optimal microenvironments that could increase the ability of MSCs to induce muscle regeneration in a paracrine manner.

Autologous MSCs were transplanted near severely injured muscle tissues using porous scaffolds that could provide a sustained, local release of stimulatory factors. From this synthetic niche, the MSCs stimulated muscle regeneration by promoting re-vascularization, muscle fiber formation, and remodeling scar tissue over time. These positive effects on structural regeneration led to restoration of functional strength in the treated muscles. This approach is an

important example of enabling endogenous tissue regeneration without physical engraftment of transplanted cells, and can likely be adapted for the treatment of other injuries and diseases.

VIII. Zusammenfassung

Während minderschwere Verletzungen der Skelettmuskulatur sehr heilen, führen schwere Traumata zu irreversiblen strukturellen Beschädigungen, wie beispielsweise ausgedehnte Narbengewebsbildung und zerstörte Muskelfasern. Dies führt zu funktionellen Defiziten, welche die Lebensqualität des Patienten stark einschränken. Eine effektive Behandlung solcher schweren Muskelverletzungen ist gegenwertig enormer klinischer Bedarf. Mesenchymale Stromazellen (MSCs) haben große Aufmerksamkeit in Bereich der Regenerativen Medizin geweckt und werden seit kurzem im Kontext der Muskelregeneration untersucht.

Die Grundhypothese dieser Arbeit ist die Annahme, dass die parakrine Effekte, über welche MSCs die biologischen Funktionen anderer Vorläuferzellen beeinflussen, durch eine geeignete Mikroumgebung während bzw. nach ihrer Translation verbessert werden kann. Dementsprechend könnte die parakrine Funktion von MSCs dazu genutzt werden Muskelvorläuferzellen zu stimulieren und so Muskelregeneration zu ermöglichen.

Der Vergleich verschiedener Kultivierungsumgebungen, welche sich sowohl in ihrer Dimensionalität als auch in ihrer Mikrostruktur unterscheiden, zeigte dass die Kultivierung in einem 3D makroporösen Trägermaterial die Proteinsekretion von MSCs erhöht. Muskelvorläuferzellen zeigten eine verbesserte Proliferation, Vitalität, Migration und Differenzierung nach der Exposition zu konditioniertem Medium von MSCs. Interessanterweise, führte die Verkapselung von MSCs in einem 3D (nanoporösen) Hydrogel zu einer signifikant geringeren funktionellen Antwort der Myoblasten. Die parakrinen Effekte der MSCs hängen von der Ausbildung von N-Cadherin-vermittelten Zell-Zell-Kontakten ab, was durch die makroporöse Struktur der 3D Trägermaterialen ermöglicht wird, jedoch durch die nanoporöse Struktur der 3D Hydrogele unterbunden wird.

Die Fähigkeit der MSCs auf lösliche Signale zu antworten, wurde mittels kurzzeitiger Exposition zu rekombinanten Wachstumsfaktoren untersucht. MSCs im makroporösen Trägermaterial erhöhten ihr allgemeines Sekretionsmuster in Folge dieser Stimulation und verbesserten dementsprechend auch die pro-regenerativen Funktionen der Myoblasten. Im Vergleich dazu zeigten MSCs im Hydrogel eine wesentlich geringere Antwort auf die Stimulation mit Wachstumsfaktoren. Folglich stellt das makroporöse Trägermaterial eine optimale Mikroumgebung da, welche durch eine anhaltende Freisetzung von stimulierenden Wachstumsfaktoren, die Fähigkeit der MSCs erhöht die Muskelregeneration parakrin zu induzieren.

Autologe MSCs in einem makroporösen Trägermaterial, welches die stimulierenden Wachstumsfaktoren konstant freisetzt, wurden anschließend in die Nähe von schwerverletztem Muskelgewebe transplantiert. Aus dieser synthetischen Nische heraus, stimulierten die MSCs die Muskelregeneration durch die Förderung der (Re-)Vaskularisation, der Bildung neuer Muskelfasern und dem Umbau von Narbengewebe. Diese positiven Effekte auf die strukturelle Regeneration führten zu einer Wiederherstellung der funktionellen Kraft der so behandelten Muskeln. Der beschriebene Ansatz ist ein wichtiges Beispiel für die Aktivierung endogener Geweberegeneration ohne die Notwendigkeit des physischen Einwachsens der transplantierten Zellen und kann sehr wahrscheinlich auch auf die Behandlung anderer Verletzungen und Krankheiten übertragen werden.

1. Introduction:

Loss of muscle function due to trauma can lead to a decline in the quality of life of young and old patients alike. Despite the inherent regenerative capacity of skeletal muscle, severe trauma often leads to formation of scar tissue and loss of structural integrity. From a clinical perspective, the treatment of severe muscle trauma represents an unmet clinical need because current treatments follow a very conservative approach. Even patients with injuries such as complete muscle rupture or volumetric muscle loss are advised icing, rest, and rehabilitation, with surgical intervention being the last resort [1]. If surgical intervention is carried out, the clinical gold standard is the transfer of functional, innervated, autologous muscle tissue. Naturally, this is associated with donor site morbidity, besides requiring long recovery and rehabilitation times.

Basic research studies have sought to stimulate muscle regeneration through different strategies. At the heart of all these strategies is the idea of favorably modulating the basic biological behavior and function of various cell types that can potentially contribute towards regeneration. These cell types could be muscle resident cells, stem cells that home in to the site of injury, or immune cells that are present during inflammation. Perhaps the most widely pursued of these strategies is the intramuscular administration of growth factors such as FGF, IGF, and HGF, among others [2]. However, growth factors have short half-lives, tend to rapidly diffuse away from the site of injury, and, unless delivered locally at an appropriate dosage, may cause undesirable side effects [3, 4]. In the past decade, mesenchymal stromal cells (MSCs) have witnessed a surge in interest for regenerative medicine applications. MSCs represent a promising avenue for muscle regeneration because they can influence the function of other cells via paracrine signaling [5].

Currently, the most commonly used method to deliver any cell type in vivo is bolus injection. Often, bolus delivery of cells does not lead to beneficial outcomes because the large majority of transplanted cells undergo apoptosis within the first 24 hours [6, 7]. This can be due to multiple reasons including lack of engraftment, adverse interaction with immune cells, or incompatibility with host biology [8]. Many of these issues can be overcome by using biomaterials as cell carriers. More importantly, biomaterial properties can be optimized to elicit desirable cell behavior.

The work described in this thesis is an effort to combine the use of biomaterials, MSCs, and growth factors in a way that stimulates skeletal muscle regeneration in cases where it would not heal naturally.

1.1. Skeletal muscle:

1.1.1. Physiology

Skeletal muscles constitute 40-45% of the body mass, and permit essential functions such as locomotion, postural support, and breathing by generating longitudinal contractile forces [9]. Skeletal muscle is a highly organized tissue that consists of muscle fibers, connective tissue that forms the extracellular matrix (ECM), blood vessels, nerves, and distinct cellular populations [10]. The basic structural unit of the skeletal muscle is the muscle fiber (often referred to as myofiber). Myofibers are long, cylindrical structures that are formed when multiple myoblasts fuse together and undergo terminal myogenic differentiation. Each myofiber is surrounded by extracellular matrix that forms the tissue's structural framework, and multiple myofibers are bundled together to form the skeletal muscle. The myofibers are the contractile units of the muscle tissue, and are therefore highly metabolically active. Sufficient supply of oxygen and essential nutrients to the myofiber is ensured by the presence of blood capillaries and larger vessels that form a highly infiltrative vascular network. To permit voluntary movement, each myofiber is connected to the nervous system via neuromuscular junctions that allow the conduction of electrical signals, triggering myofiber contraction. Individual muscle fibers in the skeletal muscle can be classified into either fast or slow, depending on their MHC isoforms (oxidative slow twitch and glycolytic fast twitch) [11]. The slow twitch fibers are primarily responsible for less intense, but more prolonged activities such as long distance running, whereas the fast twitch fibers enable short, but high intensity work such as sprinting. The contractile properties of an individual muscle are determined by the proportion of the two fiber types existing in that muscle. The relative composition of the two fiber types determines the overall functional performance of the muscle.

1.1.2. Injury and Regeneration

Injuries to the skeletal muscle can occur, among other causes, due to surgical intervention (iatrogenic injury), impact trauma, military related injuries, and sports related injuries. Minor damage to the muscle tissue occurs almost on a daily basis, and a classical example is the pain and soreness that people experience when they resume sports or exercise after long periods of inactivity. Importantly, the muscle soreness subsides over a few days indicating that the muscle tissue successfully recovers from the after-effects of sudden bouts of activity. The muscle tissue's inherent regenerative capacity ensures restoration of function and structure after minor injuries. Essentially, this is mediated by local cell populations such as satellite cells that undergo activation in response to injury signals and participate in regeneration.

So far, what remains unknown is the extent of muscle injury that can be repaired via inherent regenerative mechanisms. However, it is clear that beyond a certain injury severity threshold, the regenerative actions by local cell populations prove to be insufficient. Left untreated, such injuries can lead to a permanent loss of muscle function due to the destruction of structural components such as myofibers and blood vessels, and the subsequent manifestation of collagenous scar tissue.

Muscle regeneration after injury follows a series of overlapping phases. These include the destructive/inflammatory phase, the repair phase, and the remodeling phase.

Immediately following acute injury, molecular signals and factors released by necrotic fibers induce the chemotactic recruitment of neutrophils to the site of injury. Neutrophils are the first inflammatory cells that invade the injured area (typically within ~2 hours of injury), where they induce damage to the muscle membrane via the release of enzymes and produce free radicals that target tissue debris for later phagocytosis. Monocytes also reach the injured tissue and give rise to macrophages. Two distinct populations of macrophages (pro-inflammatory CD68+/CD163-, and anti-inflammatory CD68-/CD163+) are involved in the muscle healing cascades. The M1, classically activated macrophages phagocytose apoptotic cells and other cellular debris, and secrete pro-inflammatory cytokines. The M1 macrophages then undergo a phenotypic switch, giving rise to the anti-inflammatory M2 type macrophages. The M2 macrophages have been found to persist in the muscle for a number of days, during which their secreted factors such as IL-10 and others influence the behavior of myogenic cells [12]. For instance, M2 macrophages inhibit excessive proliferation of fibro/adipogenic progenitor (FAP) cells, while promoting the fusion and myogenic differentiation of committed satellite cells [13].

The repair phase of muscle healing often overlaps the inflammatory phase, and is characterized by the activation, proliferation, migration, and eventual fusion of satellite cells. Existing literature points towards a correlation between macrophage phenotype and function of satellite cells. While factors secreted by M1 macrophages have been found to stimulate satellite cell proliferation and migration, and inhibit their differentiation, the M2 macrophages have been reported to induce the myogenic differentiation of satellite cells [14].

The remodeling phase of muscle healing comprises the maturation of contractile muscle fibers, remodeling of fibrous scar tissue, and establishment of neuromuscular junctions. Newly formed myofibers reorganize themselves and fuse with existing ones. In cases of severe injury, the reorganization and maturation of myofibers may be hindered by the formation of scar tissue. This may lead to a decline in muscle function. In these cases, external intervention may be required and research work in this area has largely revolved around the exogenous delivery or transplantation of biological therapeutic agents such as growth factors and cells.

1.1.3. Biological milieu and cellular components

There are several cell populations that reside in the skeletal muscle and make up the muscle microenvironment. However, this section provides a brief introduction to cellular components that play critical roles in determining the response of the muscle to acute injury.

Satellite cells comprise a small population (2-7%) of the adult muscle tissue, but are the primary enablers of muscle maintenance and repair [15, 16]. Initially identified by Mauro [17], satellite cells are normally located in a specialized niche that exists between the sarcolemma and the basal lamina of muscle fibers [18]. Under normal conditions, satellite cells remain in a quiescent state and can be characterized by the expression of the transcription factor paired box protein 7 (Pax7). Responding to signaling factors released upon injury, these cells become activated, undergo proliferation and fuse together to form multinucleated myotubes that ultimately mature into contractile myofibers. In addition to generating functional myofibers, satellite cells also undergo self-renewal to sustain a pool of undifferentiated cells. Satellite cells are notoriously sensitive to their microenvironmental niche, and changes in the properties of the niche associated with age, disease, or injury can critically influence the regenerative capacity of satellite cells [19]. This has, on the one hand, enabled the identification of various chemical, biological, and mechanical properties that exert control over satellite cell quiescence and function, but on the other hand has hindered the ex vivo study of these cells [20]. When isolated

satellite cells are cultured on stiff tissue culture plastic substrates, they quickly become activated and lose their regenerative capacity, thereby making it difficult to expand a therapeutically potent population of these cells for in vivo transplantation [21, 22].

Not so long ago, a new population of fibro/adipogenic progenitor cells (FAPs) resident in skeletal muscle tissues was identified [23, 24]. Similar to satellite cells, FAPs were demonstrated to remain quiescent in healthy muscle, only proliferating in the event of injury. In cases of successful endogenous muscle regeneration, FAPs play a role in creating a pro-myogenic differentiation niche in the muscle that ultimately leads to the fusion of progenitor cells into myofibers. On the other hand, in cases of unsuccessful regeneration, FAPs have been implicated in directly giving rise to fibroblasts and adipocytes that contribute to fatty degeneration and scar tissue formation in adult muscle. Moreover, immune cells especially macrophages and eosinophils that infiltrate the site of injury have been shown to influence fate decisions in FAPs via paracrine signaling of cytokines such as IL-4 and IL-13 [25].

Together, the interaction between immune cells, satellite cells, and FAPs form a complex biological milieu in the injured skeletal muscle (**Fig. 1**). The paracrine communication between different components of this milieu largely determines whether the muscle will undergo remodeling and regeneration, or whether scar tissue formation and lack of muscle progenitor cell differentiation will hinder proper healing [26].

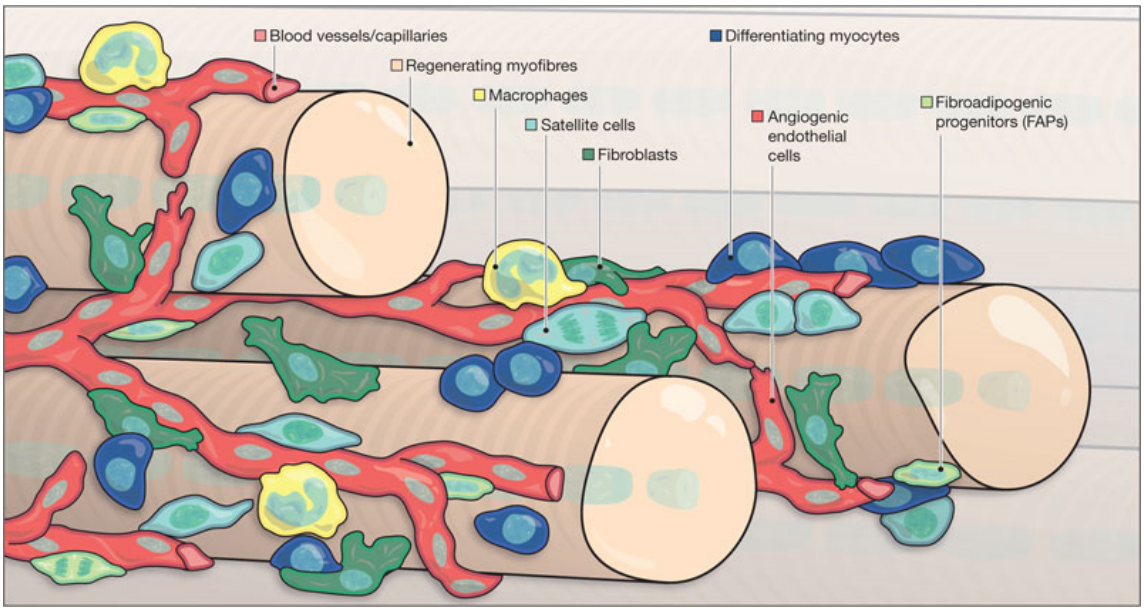

Fig. 1: Cell populations that form the complex biological milieu of regenerating muscle. *Blood vessels infiltrate the interstitial spaces between muscle fibers, providing a route for invading macrophages. Satellite cells become activated and give rise to progenitor myoblasts that fuse to form myofibers. Fibro/adipogenic progenitor cells promote the process of myogenic differentiation by creating a regenerative niche. Reproduced with permission from John Wiley and Sons [26].*

1.2. Mesenchymal stromal cells:

Mesenchymal stromal cells (MSCs) are multipotent cells that can undergo ex vivo differentiation into the osteogenic, chondrogenic, myogenic, tenogenic, and adipogenic lineages [27, 28]. MSCs are present in, and can be isolated from, a number of different tissues in the body such as bone marrow, adipose, umbilical cord blood, and muscle [29, 30]. Isolated cells can be induced to differentiate even after extended *in vitro* culture in their unspecialized state. This has led to a remarkable interest in the use of MSCs for tissue engineering and regenerative medicine applications. In the body, tissue resident MSCs or those that home in to the site of injury via vasculature participate in the maintenance, homeostasis, and repair of healthy tissues by participating as progenitor cells or by modulating the function of other cells via paracrine signaling [31]. In 2006, the International Society for Cellular Therapy (ISCT) proposed a minimal set of criteria that cells must fulfil in order to be defined as MSCs. These include: (1) the ability to adhere to plastic during culture in standard conditions, (2) the ability to differentiate into osteoblasts, adipocytes, and chondroblasts *in vitro*, and (3) expression of

the surface markers CD105, CD73, and CD90, and absence of the surface markers CD45, CD34, and CD14 [32].

1.2.1. Application in regenerative medicine

Traditionally, the stemness of MSCs has been related to their trilineage differentiation potential. A large number of studies have supported the use of MSCs based solely on their ability to differentiate into the osteogenic, adipogenic, and chondrogenic lineages. This has made MSCs an attractive cellular candidate for musculoskeletal tissue engineering applications. A great deal has also be learnt about the role of endogenously present stromal cells, which home in to injured tissues and participate in tissue repair and regeneration. Exogenously delivered MSCs that are delivered systemically may get entrapped in other tissues and organs such as the lungs, but reports indicate that some portion of the transplanted cells do manage to engraft at the site of injury. What functions MSCs perform once they are at the site of injury is a topic of intense interest and debate. One of the ways in which MSCs exert their benefit is by integrating into the structure of the injured tissue and physically contributing to regeneration by replacing damaged cells [33, 34]. In an early example, Ferrari et al. showed that labeled bone marrow cells migrated to injured muscle tissue, underwent myogenic differentiation, and contributed to new muscle fiber formation [35]. Similarly, Horwitz et al. demonstrated that allogeneic MSC transplantation in children with osteogenesis imperfecta led to bone formation and increases in bone mineral content after cell engraftment [36]. Similarly, bone marrow derived MSCs have been used to repair cartilage defects [37], and improve clinical outcomes in patients with chronic ischemic cardiomyopathies [38].

However, an ever growing body of work argues that the extremely low engraftment of transplanted MSCs at the site of injury does not correlate or explain the beneficial effects observed [39, 40]. This leads to the other way in which MSCs exert their therapeutic benefits on injured tissues – secretion of paracrine factors and the ability to modulate their environment including the function of other cells. It is well known that MSCs secrete a wide range of cytokines, chemokines, vesicles, mRNA, and growth factors [41]. These paracrine factors are bioactive and can influence other cells by binding to surface receptors and triggering various intracellular signaling pathways, ultimately leading to a modulation of biological function (**Fig. 2**) [42]. In a recent study, Katagiri et al. reported the results of a human clinical study where patients who received collagen sponges soaked in bone marrow MSC derived conditioned

medium (MSC-CM) showed alveolar bone regeneration [43]. Multiple preclinical studies have also demonstrated that a cell-free approach involving the transplantation of materials containing MSC-CM or in vivo infusion of MSC-CM stimulates tissue regeneration [44-47]. MSCs are now increasingly being used for their ability to secrete factors that exert therapeutic benefits and facilitate a multitude of basic biological processes, rather than solely for their differentiation potential [48, 49]. Moreover, MSCs have been shown to exert immunomodulatory effects, actively communicating with cells of the immune system and indirectly contributing towards tissue regeneration [50, 51]. This has led to intense research efforts involving the application of MSCs for treating inflammatory diseases [52, 53].

Excitement generated by properties and benefits of the MSC secretome has recently led scientists to investigate ways by which the paracrine effects of MSCs can be enhanced or amplified. A number of pre-conditioning strategies have been proposed to enhance the secretory properties of MSCs, without genetically modifying the cells. These include hypoxia conditioning, heat shock, co-culture with pro-inflammatory factors, and aggregation of MSCs into spheroids [54, 55]. It is not yet clear how long the effects of pre-conditioning lasts in MSCs that are transplanted in vivo, where they encounter various other biological cues. However, it is quite evident that strategies to modulate the long term paracrine function of MSCs will find utility in tissue engineering and regenerative medicine applications.

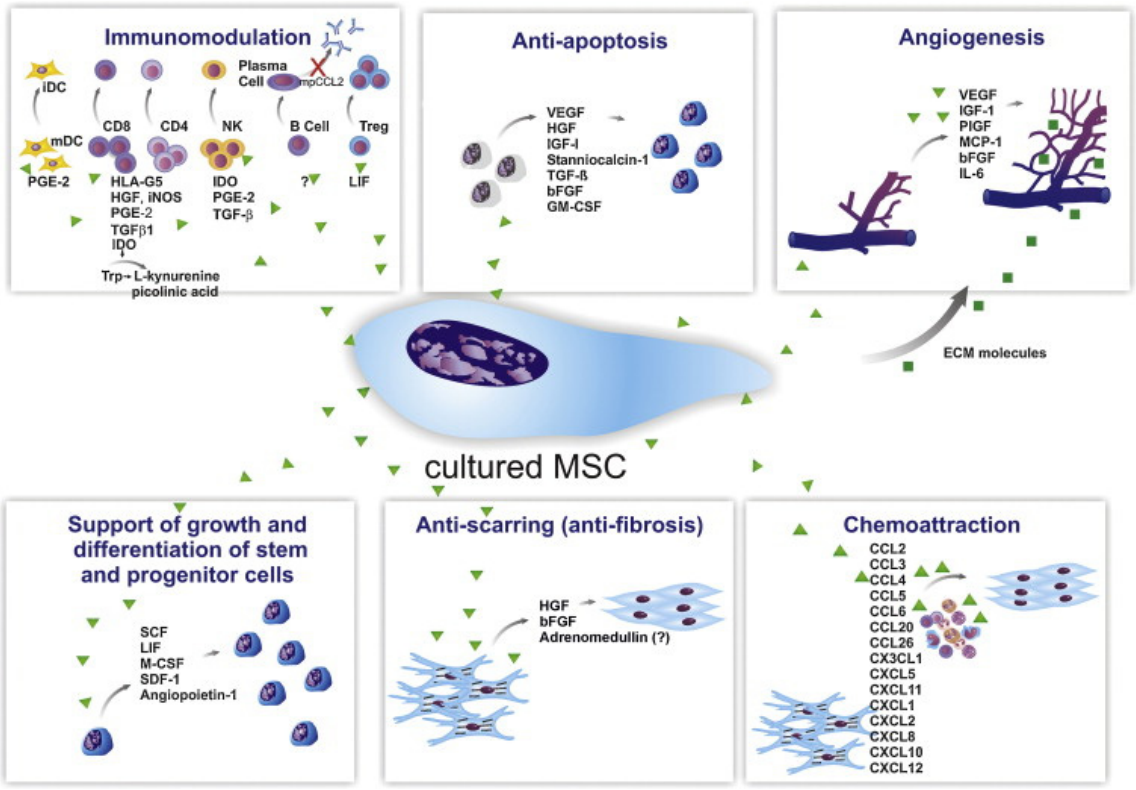

Fig. 2: Control of multiple biological processes by paracrine factors secreted by MSCs. *Cultured MSCs secrete a variety of bioactive cytokines, chemokines, and growth factors that can interact with and modulate the immune environment, prevent cellular apoptosis, promote angiogenesis, stimulate proliferation and differentiation of progenitor cells, prevent scar tissue formation, and attract other cells to the site of injury via chemoattraction. Reproduced with permission from Elsevier [41].*

1.2.2. Application in muscle regeneration

Based on the evident success of MSC therapy in the regeneration of musculoskeletal tissues such as bone and cartilage, researchers have also investigated the efficacy of MSC transplantation for skeletal muscle regeneration. A number of groups have demonstrated the myogenic differentiation capacity of MSCs *in vitro* [56, 57], and other studies have reported rare fusion events of transplanted MSCs with host myofibers [58, 59]. In a series of studies at the Charité, Matziolis, Winkler, von Roth, and colleagues demonstrated that the intramuscular bolus transplantation of autologous, bone marrow derived MSCs can lead to improvement in muscle contractile strength [60-62]. While the jury is still out on whether transplanted MSCs differentiate into myofibers, it is clear that MSCs do stimulate muscle regeneration. Because integration and fusion events are so low that they do not correlate with the benefits reported,

there has been a general consensus that MSCs most likely promote muscle regeneration via paracrine mechanisms.

1.3. Biomaterials:

A biomaterial, in its most basic sense, is any material that interacts with a biological system. The earliest documented use of a biomaterial was almost 32000 years ago when sutures were used to secure open wounds by early Egyptians [63]. Sometime later, the Mayans fashioned dental implants out of sea shells and unknowingly achieved bone integration [64]. Up until the latter half of the 20th century, biomaterials were used as replacement devices to support diseased or damaged tissues such as broken bones.

1.3.1. Evolution of biomaterials for tissue engineering

The main criteria for the first generation of biomaterials was that they be non-toxic, not provoke an immune response, and essentially be as inert as possible while carrying out a load bearing or supporting function [65, 66]. Examples of these include metallic implants used for fixation of bone fractures, coronary stents, and rigid intraocular lenses fabricated from polymers. In the latter half of the 20th century, biomaterial scientists began to develop materials that could actively interact with biological systems and induce a favorable response such as tissue integration. Perhaps the most renowned example of this second generation of biomaterials is the ceramic hydroxyapatite (HA), the chemical structure of which resembles that of native bone. HA, like other bioactive ceramic biomaterials, binds to bone, and has been used as coatings for orthopedic and maxillofacial implants [67]. Another feature of some second generation biomaterials was their ability to resorb or degrade over time. Created using polymers, ceramics, or metals, resorbable biomaterials performed a specific reparative function before undergoing degradation and excretion from the body [68]. Being resorbable or biodegradable avoided any long term undesirable reactions from the host. At the turn of the 21st century, Hench and Polak described what came to be known as third generation biomaterials that could not only interact with bodily tissues, but could also influence, by either promotion or inhibition of processes at the molecular level, the genetic expression and function of cells [69].

The field of biomaterials science has come a long way over the past few decades [70]. Increasingly sophisticated biomaterial systems have been developed, which are not just

biocompatible, but can additionally perform specific functions. These include, but are not limited to, degradation at defined rates in vivo [71], interaction with the host immune system [72], and delivering biological molecules in a controlled manner [73]. With the exponential increase in knowledge of ways to manipulate cells using chemical, physical, and other properties, biomaterials have been designed to promote and render control over cell delivery [74], differentiation [75], migration [76], and paracrine secretion [77].

Biomaterials for tissue engineering applications have not only been used as carriers for cells, but also as synthetic mimics of native ECM, which provides cells with specific information in order to evoke desirable processes such as differentiation [78]. Modifications of chemical, physical, electrical, and mechanical properties of biomaterials have allowed scientists to mimic various aspects of the ECM [79]. Many of these modifications require materials to be modifiable and have a certain degree of flexibility.

1.3.2. Hydrogels and alginate

While metallic (e.g. hip implants) and ceramic (e.g. bone grafts) biomaterials are still widely used, their core material properties are often difficult to manipulate. Polymers, on the other hand, can be customized in a variety of ways, and therefore give scientists ample space for innovation [80]. Polymeric biomaterials can be made of naturally derived materials such as collagen, hyaluronic acid, spider silk, and alginate, or can be chemically synthesized such as in the case of polylactic acid, polyglycolic acid, poly glycerol sebacate, and polycaprolactone [81-84].

Hydrogels are cross-linked networks of water soluble polymers that have generated tremendous interest in the biomaterials and tissue engineering communities [85, 86]. Hydrogels can be formed into various shapes and sizes, have simple crosslinking chemistries, are easy to handle, are biocompatible, and most importantly can be manipulated to have a wide range of physical, chemical, and mechanical properties [87-89]. Alginate is one such type of hydrogel, naturally derived from brown algae, and purified for use in biomedical applications. It is perhaps the most widely employed hydrogel for tissue engineering applications due to its versatility, low cost, wide availability, gentle crosslinking, and low toxicity. Other naturally derived hydrogels such as hyaluronic acid and collagen are essentially ECM components, and have inherent biological properties. In contrast, alginate in many ways represents a blank slate with no inherent biological characteristics, and is thus a popular material used to study basic cell-

material interactions. Due to its hydrophilic nature, alginate does not allow cell attachment but it can be rendered cell-interactive by the conjugation of cell adhesive peptide sequences and other signaling cues on its polymeric backbone. Oxidation of its structure renders alginate hydrolytically degradable, allowing researchers to tune the degradation rate of scaffolds and gels in vivo. Moreover, alginate can be crosslinked either ionically or covalently, resulting in materials that exhibit significantly different mechanical behaviors including linear elasticity (covalently crosslinked) or viscoelasticity (ionically crosslinked). For these reasons, alginates have been widely used for drug delivery and tissue engineering applications.

1.3.3. Biomaterials in skeletal muscle tissue engineering

Biomaterials have been used in a wide variety of ways to induce skeletal muscle regeneration, and different types of synthetic and natural polymeric biomaterials have been employed to do so.

One strategy involves employing biomaterials that promote the myogenic differentiation and myotube formation of muscle progenitor cells [90]. These biomaterial scaffolds are typically macroporous and degradable, allowing sufficient space for seeded myoblasts to proliferate and undergo fusion, before resorbing in the body to facilitate the integration between newly formed and host tissues [91]. Fusion of myoblasts is enhanced when cells lie end-to-end in an orientated fashion, such as in native anisotropic skeletal muscle. For this reason, 2D and 3D biomaterials have been formed which provide contact guidance cues to seeded cells via surface or 3D topography. These contact guidance cues, varying from nanometers to micrometers, can stimulate various myoprogenitor cell populations into exhibiting greater functional outcomes including cytoskeleton alignment, striated myotube formation, and expression of myogenic proteins [92-94]. Efforts to incorporate topographical cues in three-dimensional scaffolds have been made using freeze drying and phase separation techniques [95]. These techniques can be applied to a variety of polymers, and result in micro/macro-tubular porous structures which can guide muscle fiber formation. As an example, Jana and colleagues fabricated chitosan scaffolds with tubular pores to guide cell alignment, fusion, and differentiation into large myotubes [96]. The chitosan concentration was optimized to produce scaffolds with mechanical properties similar to those of native muscle, and the concentration was found to significantly influence myotube diameter, and expression of MHC. In a study by Kroehne et al., collagen sponges with longitudinal porous structure were seeded with murine myoblasts and cultured *in vitro*, before

being transplanted into a muscle defect site in mice [97]. Two weeks after transplantation, newly formed myofibers could be seen in the outer regions of the collagen scaffold, whereas major contribution to contractile forces was made by donor myotubes inside the scaffold.

Besides topographical guidance, biomaterial scaffolds can be designed to incorporate mechanical and electrical cues which can be sensed by adherent cells [98, 99]. In this regard, electrically conducting polymers such as polyaniline (PANI) and polypryyole (PPy) have been blended with other synthetic and natural polymers, and electrospun into fibers to simultaneously deliver electrical and topographical cues to seeded cells [100]. Jun et al. showed that myoblast differentiation can be stimulated by culturing on PANI containing poly(L-lactide-co-ε-caprolactone) (PLCL) electrospun fibers [101]. The presence of the conducting polymer PANI was found to have a significant effect on myotube number and length, as well as the expression of myogenic genes myogenin, troponin T, and MHC. Similar conclusions were drawn by other groups studying PANI-PCL fibers [102, 103], indicating that synergistic effects of nanofiber alignment and electroactivity has great potential in skeletal muscle tissue engineering applications [104].

Another reported strategy is to combine ex vivo cultured progenitor cells with a biomaterial that, when transplanted in vivo, promotes the outward migration of cells which then participate in the regeneration process at the site of injury [105]. Borselli et al. reported that when used as porous cryogels, drug releasing alginate scaffolds promoted outward migration of myoblasts which integrated into the muscle structure by forming new myofibers, and led to restoration of muscle contraction forces [106]. Indeed the outward migration of muscle cells has been shown to be of vital importance on subsequent muscle regeneration. For example, Hill et al. used wire porogens to fabricate highly porous alginate scaffolds that would promote outward migration of cells, and observed greatest muscle regeneration when myoblasts were activated by growth factors and migrated out of the scaffold to repopulate the injured muscle tissue and form new muscle fibers [107, 108].

Table 1: Various properties of biomaterials used for skeletal muscle tissue engineering.

Biomaterial property	Benefits	Key parameters for optimization	Ref.
Porosity	- Cell proliferation. - Cell migration. - Cell ECM deposition.	- Pore size, interconnectivity. - Cell adhesive cues	[107-110]
2D Topography	- Cell alignment. - Cell shape. - Cellular mechanotransduction. - Myotube fusion, maturation.	- Groove width, depth. - Island spacing, clustering. - Chemical composition. - Fiber orientation.	[111-124]
3D Topography	- Contact guidance. - ECM deposition in 3D - Large diameter myotubes	- Channels to facilitate fusion events. - Ensuring properties don't change due to degradation and/or swelling.	[96, 97]
Injectability	- Minimally invasive delivery. - Immune protection.	- Hydrogel composition. - Ensuring sufficient nutrient diffusion to encapsulated cells.	[125-131]
Presentation of growth factors	- Sustained, long-term release. - Influence behavior of cells in tissue as well as on biomaterial.	- Growth factor release kinetics. - Loss of bioactivity - Chemical conjugation/steric hindrance.	[107, 109, 132]

Overall, biomaterials have not only been used to locally deliver drugs and cells to injured muscle, but have also been formulated with properties that promote the myogenic differentiation of progenitor cells. Thus, several properties of biomaterials have been considered important for eliciting desirable cell behavior for tissue regeneration (**Table 1**).

2. Hypothesis & Aims:

The main hypothesis of this work is that mesenchymal stromal cells (MSCs) can stimulate muscle regeneration via paracrine mechanisms when delivered in a biomaterial that enhances their ability to secrete pro-regenerative cytokines.

To test the hypothesis, the following aims were devised:

1. Characterize the paracrine response of MSCs when cultured on alginate biomaterials with distinct microenvironments.
2. Investigate the effects of paracrine factors secreted by MSCs on myoblast function.
3. Determine the effectiveness of MSC transplantation using an optimal biomaterial in a clinically relevant model of muscle injury.

3. Experimental details:

A detailed list of materials, chemicals, cells, proteins, antibodies, and reagents used in the work described in this thesis is provided in Appendix A.

3.1. Alginate processing

To create degradable alginates, high molecular weight (MVG) and low molecular weight (LVG) alginates were mixed together in powder form and dissolved in distilled water to a final concentration of 1 % w/v. The alginate was oxidized using sodium periodate in the dark for 16 hours, after which the reaction was quenched using ethylene glycol. The alginate solution was dialyzed over 2 days using distilled water, frozen at -20 ºC, lyophilized until dry, and stored at -20 ºC until further use.

Carbodiimide chemistry was used to chemically attach cell-adhesive RGD peptide sequences to the alginate polymers, using a procedure adapted from Rowley et al. and Kong et al. [133, 134]. Briefly, high molecular weight (MVG) and low molecular weight (LVG) alginates were mixed together in powder form and dissolved in MES buffer (pH 6.5) to obtain a final concentration of 1 % w/v. NHS, EDC, and G_4RGDSP were added, in that order, to the alginate to achieve a theoretical degree of substitution of 20 (20 RGD peptides per alginate chain) and the mixture was allowed to stir for 20 hours. The reaction was quenched using hydroxylamine hydrochloride. The modified alginate solution was dialyzed against distilled water containing a decreasing amount of sodium chloride over 3 days. The purified alginate was removed from dialysis tubes, decolored using activated charcoal for 30 minutes, sterile filtered, frozen at -20 ºC, and lyophilized until dry.

3.2. Substrate fabrication

To fabricate macroporous scaffolds, reconstituted alginate was rapidly mixed with 48.8 mM calcium sulfate slurry (from a stock of 1.22 M $CaSO_4$ in dH_2O) to a final concentration of 2 % w/v, cast between two glass plates separated by 3 mm spacers, and allowed to crosslink for 45 minutes. Smaller gels measuring 8 mm x 3 mm x 3 mm were punched out and frozen at -80 ºC overnight before being lyophilized. To create growth factor releasing scaffolds, desirable quantities (5 ng/scaffold for *in vitro*, 3 µg/scaffold for *in vivo*) of hIGF and hVEGF were mixed with the alginate prior to crosslinking with calcium sulfate slurry.

To fabricate cell encapsulating hydrogels, desirable amount of cells were trypsinized, centrifuged, resuspended in media and mixed with alginate prior to crosslinking. The cell+alginate mixture was cast between glass plates separated by spacers, and allowed to crosslink for 30 minutes. Smaller sized gels were then punched out and placed in well plates containing full culture media.

To fabricate 2D alginate films, the alginate was crosslinked with calcium sulfate slurry and cast between two glass plates separated by 1 mm spacers. After 45 minutes, the gels were transferred to well plates and supplemented with full culture media. Cells were seeded onto the 2D films the next day.

3.3. Cell culture

Routine cell culture for rat bone marrow derived MSCs and C2C12 myoblasts was carried out on tissue culture treated flasks or well plates. Culture media consisted of 10 % v/v FCS, 1 % v/v penicillin/streptomycin, and 1 % v/v glutamax. MSCs were not used beyond passage 5. C2C12 myoblasts were typically trypsinized at a confluency of 80 %, and were not used beyond passage 12. FCS concentration was reduced to 5 % v/v to induce myogenic differentiation of C2C12 myoblasts.

3.4. N-cadherin blocking

N-cadherin blocking in MSCs was carried out using a protocol modified from Lee et al. [135]. Trypsinized MSCs were incubated with 20 μg/mL of N-cadherin blocking antibody (clone GC-4, Sigma) for 15 minutes, washed twice with PBS, and seeded on the appropriate substrate. Before MSC-CM collection, the biomaterial+cell constructs were incubated in 4 mM EDTA for 5 minutes to break up calcium mediated cell-cell contacts, washed with PBS and placed into a well plate containing serum free DMEM with additional supplemented N-cadherin blocking antibody (10 μg/μL).

3.5. Cell loading

In order to normalize the ELISA and cytokine array intensities to cell number, MSCs present on the different substrates at the time of conditioned media collection were counted. For TCP and 2D film substrates, the cells were trypsinized, re-suspended in medium and counted using a hemocytometer after staining with Trypan blue. For 3D hydrogels and 3D scaffolds, the biomaterial+cell constructs were washed with PBS, and the alginate was dissolved using sterile 50 mM EDTA solution for 15 minutes at 37 ºC. After the alginate had dissolved, the cells were

centrifuged, re-suspended in medium and counted with a hemocytometer after staining with trypan blue.

3.6. Cell outward migration

To determine cumulative outward migration of MSCs from 3D scaffolds, cell seeded scaffolds (1×10^5 MSCs/scaffold) were placed in separate wells of a 24 well plate. After every 24 h, the scaffolds were shifted to new wells, and the number of cells that had colonized the wells over the previous 24 h was quantified using the CyQUANT® cell proliferation assay kit.

3.7. Cell morphology

Morphology of MSCs on different substrates was assessed by fluorescence microscopy. Briefly, cells were fixed with 4% PFA for 10 minutes, and permeabilized using 0.1% Triton-X-100 in PBS. Cells were then stained with Alexa Fluor® 488 Phalloidin and DAPI, and imaged with an inverted microscope (DMI6000B, Leica, Germany).

3.8. N-cadherin immunofluorescence

MSCs on various substrates were fixed with PFA containing 0.1 % of Triton and Tween, blocked in 1% BSA-PBS containing 5% v/v of normal rabbit serum, and incubated with primary antibody for N-cadherin (1:200; H-63, Santa Cruz Biotechnology) overnight at 4 ºC on an orbital shaker. Secondary antibody (Alexa Fluor® 546 goat anti-rabbit; 1:1000) was added for 1 hour at room temperature. Cells were then incubated with PBS containing DAPI. Fluorescence was detected using an inverted microscope.

3.9. Growth factor release kinetics

Release of hIGF and hVEGF from alginate scaffolds was determined using ELISA kits following the manufacturer's instructions. Growth factor loaded scaffolds were placed in 1 mL of serum free culture media. The media was collected, and refreshed, at various time points (days 1, 3, 7, 14, 21, and 28), centrifuged to remove debris, and stored at -80 ºC for later detection by ELISA.

3.10. Conditioned media generation

MSCs were cultured on the appropriate substrate for 2 days prior to conditioned media collection. First, cells were washed with PBS twice, and 1.5 mL of serum free media was added to the well plates. 24 hours later, the conditioned media was collected, centrifuged at 500g to remove cellular debris, passed through a sterile filter, and stored at -80 ºC until use.

To prepare conditioned media for cytokine arrays, a large volume of conditioned media collected from cell numbers suggested by the supplier was concentrated using Amicon ultracentrifugal filters, and was rediluted to a final volume of 1 mL.

For conditioned media from growth factor stimulated MSCs, 50 ng/mL of hVEGF and/or 50 ng/mL of hIGF (unless stated otherwise) were added to the serum free media in the well plates containing the samples. Conditioned media was collected 24 hours later, and processed in the same manner as described earlier.

3.11. Analysis of protein and cytokine secretion

Protein content of MSC conditioned media from various groups was determined by Comassie or DC protein assay. Rat MSC secreted rHGF, rbFGF, rIGF, rLIF, and rVEGF in the conditioned media were determined using ELISA kits following the manufacturers' instructions.

A wider analysis of cytokines secreted by the rat MSCs was carried out by using cytokine arrays following the manufacturer's instructions. The intensities were detected using G:BOX imager (Syngene). Intensities were normalized to the positive control of every array to account for inter-array differences.

3.12. Cell viability

MSCs from various substrates were harvested by trypsinization and dissolution of the alginate substrate with 50 mM EDTA. The cell suspension was mixed with a mixture of Calcein AM and Ethidium homodimer (Live/Dead imaging kit) and imaged with a fluorescence microscope after a 15 minute incubation period. The number of live (green) and dead (red) cells were counted using ImageJ.

3.13. qPCR

The following primers (Invitrogen) were used for qPCR analysis:

Table 2: List of primers.

Gene	Forward Primer	Reverse Primer
Cdh1 (E-Cadherin)	ACCCCCTGTTGGCGTTTTCA	CATCACGGAGGTTCCTGGAAGAG
Cdh2 (N-Cadherin)	GGAGCCGATGAAGGAACCACA	TGAAGATGCCCGTTGGAGGC
Eef1α (Elongation factor) [Housekeeping gene]	CCCTGTGGAAGTTTGAGACC	CTGCCCGTTCTTGGAGATAC
GAPDH (Glyceraldehyde 3-phosphate dehydrogenase) [Housekeeping gene]	ATGGGAAGCTGGTCATCAAC	GTGGTTCACACCCATCACAA

RNA was isolated from MSCs cultured on different substrates by using the Trizol® reagent according to the manufacturer's instructions. Mechanical disruption was carried out using an Ultra-Turrax® homogenizer. RNA concentration was determined using a Nano-Drop spectrophotometer. The iScript™ Reverse Transcription Supermix was used to transcribe RNA into cDNA. SYBR Green dye was used to detect fluorescence. The amplification plot was used to determine threshold cycle values. Values (ddCT) for the genes of interest were normalized to the housekeeping gene (Eef1α).

3.14. In vitro functional assays with myoblasts:

3.14.1. Migration (scratch assay)

A scratch wound healing assay was employed to investigate the migration behavior of C2C12 myoblasts [136]. 1.45 x 10^5 myoblasts were seeded in each well of a 24 well plate and allowed to attach for 24 hours. A yellow pipette tip was used to create a horizontal scratch in the confluent monolayer of cells. The cells were washed with PBS and 400 μL of the appropriate serum free media was added. The plate was placed inside the chamber of a live-cell microscope, and various regions of interest were marked for image acquisition over 20 hours. Closure of the scratch over time was evaluated and quantified using T-scratch software [137]. The empty area values over time obtained from the software were normalized to the reading at t=0 (initial empty area =100%). To analyze migration distance, displacement, velocity, and directionality, single cell tracking (ImageJ) was carried out. Images from each region of interest were stacked

together and the manual tracking feature of ImageJ was used to track the movement of multiple cells from independent wells and conditioned media groups. The data file was uploaded into the Chemotaxis and cell migration tool available for download from the ibidi website. Values obtained from this software package were then compiled into a single file and used for analysis.

3.14.2. Proliferation

C2C12 myoblasts were seeded at a density of 2.5 x 10^3 cells/well of a 48 well plate, and allowed to attach overnight. After attachment, the cells were washed with PBS, and appropriate serum free media were added. One plate with seeded myoblasts was frozen at the time of media addition to the other plates (t=0). At each evaluation time point (24 or 48 hours), media was aspirated from the wells, and the well plates were transferred to -80 ºC for at least 24 hours. CyQUANT® cell proliferation assay was used to assess changes in cell number relative to day 0. Briefly, CyQUANT dye (1:400) and lysis buffer (1:20) were added to distilled water to create a master-mix. 150 µL of this master-mix was then added to each well of the thawed well plates. The reaction was allowed to continue for 7.5 minutes before fluorescence values were acquired using a plate reader.

3.14.3. Survival/Anti-apoptosis

C2C12 myoblasts were seeded at a density of 2.5 x 10^4 cells/well of a 48 well plate, and allowed to attach overnight. After attachment, a horizontal scratch was induced in the cell monolayer using a yellow pipette tip. The cells were washed with PBS, and appropriate serum free media or media supplemented with growth factors was added. 24 hours later, the supernatants were collected into separate Eppendorf tubes. The cells on the plate were washed with PBS, trypsinized, and collected into Eppendorf tubes marked earlier. The intention was to collect any detached cells. The cell suspension was mixed 1:1 (v/v) with Trypan blue and the number of live and dead cells were counted using a hemocytometer.

Apoptosis was evaluated with Caspase-Glo® 3/7 assay according to the manufacturer's instructions. Briefly, myoblasts were seeded in white-walled 96 well plates with a cell density of 1 x 10^4/well. After overnight attachment a scratch was made and appropriate media were added. After a further 24 h, a 1:1 mixture of the Caspase-Glo® buffer and substrate was added into the wells and luminescence was detected using a plate reader. Measurements were normalized to cell number determined by CyQUANT®.

3.14.4. Myogenic Differentiation

3.14.4.1. Western Blot

To monitor the influence of MSC's conditioned media on myoblast differentiation behavior, 4 x 10^5 C2C12 cells were seeded in each well of a 6 well plate. After overnight attachment and the formation of a confluent layer, the appropriate conditioned media were added. Four-five days after induction of differentiation, C2C12 cells were washed with PBS, and lysates were generated using SDS lysis buffer. Protein content was determined using DC protein assay (BioRad). The Novex NuPAGE® system (Invitrogen) was used according to manufacturer's instructions followed by semi-dry transfer. Primary antibodies for Myosin heavy chain (Clone # MF20, R&D Systems, Catalog # MAB4470) (1:500), Myogenin (Clone # F5D, Abcam, Catalog # ab1835) (1:500), MyoD (Clone # 5.8A, Thermo Scientific, Catalog # MA1-41017) (1:500), and the house keeping gene GAPDH (Clone # 6C5, Abcam, Catalog # ab8245) (1:10000) were used with TBST+5% milk. Anti-mouse horseradish peroxidase (GE Healthcare) (1:7000) was utilized as the secondary antibody. Using ECL substrate (GE Healthcare) pictures were acquired using the G:BOX imager (Syngene). Analysis was performed using band intensities normalized to GAPDH and quantified by NIH ImageJ.

3.14.4.2. Fluorescence microscopy

Cells were seeded at a density of 1 x 10^5/well of a 24 well plate. Differentiation was induced by addition the appropriate serum free media supplemented with 5% v/v FCS. Media was refreshed every alternate day. Five days later, cells were washed with PBS, fixed with 4% paraformaldehyde, permeabilized with 0.1% saponin in 3% PBS-BSA solution, and stained with anti-Myosin heavy chain (1:200), and DAPI (1:1000). Goat anti-mouse Alexa Fluor® 488 was used as the secondary antibody. Cells were imaged with an inverted fluorescence microscope (Leica). Myotube length and density were determined by manual counting in ImageJ. Fusion index was calculated by counting the number of nuclei inside myotubes and the total number of nuclei in the region of interest. Fusion index = (nuclei in myotubes/total nuclei in ROI)*100.

3.15. In vivo work:

3.15.1. Animal care and handling

Four month old female Sprague Dawley rats (Charles River laboratories), weighing between 200 and 250 g were used for this study. All animal experiments were carried out in compliance with the policies and principles established by the Animal Welfare Act, the NIH Guide for Care and Use of Laboratory Animals, and the national animal welfare guidelines. The study was approved by the local legal representative (Landesamt für Gesundheit und Soziales, Berlin: Registration number: G0119/12).

3.15.2. Study design

Animals were randomly assigned to one of four test groups: (1) alginate scaffold; (2) alginate scaffold + hIGF + hVEGF; (3) alginate scaffold + MSCs; or (4) alginate scaffold + MSCs + hIGF + hVEGF. Muscle force measurement and tissue harvest were carried out at three time points: (1) one week; (2) four weeks; and (3) eight weeks. Assessment of the effectiveness of Group 2 (alginate scaffold + hIGF + hVEGF) was discontinued after the four week time point due to restrictions from the animal ethics committee.

3.15.3. Bone marrow biopsies

Bone marrow biopsies were obtained, under anesthesia, from the tibiae of every animal two weeks after its arrival into the animal housing facility. After harvesting the bone marrow, the wounds were closed using sutures and the animals were allowed a minimum rest time of two weeks before further procedures. The biopsy was mixed with full culture medium in semi-sterile conditions, transported to the laboratory, and seeded on tissue culture flasks. Culture media was refreshed every second day and colonies of stromal cells were observed under the microscope. MSC phenotype and differentiation potential was confirmed as described earlier [138]. Briefly, cell surface marker expression was validated using flow cytometry. MSC populations were positive (≥95% of total counts) for CD29, CD44, CD105, CD73, CD166, CD90, and RT1A, and negative (≥98%) for CD45, CD34 and RT1B. Differentiation potential upon stimulation with adipogenic or osteogenic media was confirmed via Nile red and Alizarin Red staining, respectively.

3.15.4. Injury model

The muscle injury model consisted of multiple crush trauma performed using plastic covered surgical forceps at three distinct locations along the length of the soleus muscle. The neurovascular bundle was spared from any trauma. The injuries were always inflicted on the lower left limb. The soleus muscle in the lower right limb of every animal was uninjured, and served as internal control to normalize muscle forces.

3.15.5. Transplantation of scaffolds, cells, and growth factors

Autologous MSCs were seeded on porous scaffolds four hours prior to surgery and cultured in the incubator at 37 ºC and 5% CO_2. Prior to transplantation, the scaffolds were washed three times in saline before being placed on top of the injured muscle tissue.

3.15.6. Muscle force measurement

After an initial isoflurane narcosis, rats were anesthetized by intraperitoneal injection of a mixture of xylazine and ketamine in saline before proceeding with the muscle force measurement and muscle harvesting. Fast twitch and slow twitch (tetanic) forces of the treated and contralateral uninjured muscles were measured as described earlier [62]. Briefly, after anesthetizing the animals, the sciatic nerve and the soleus muscle were exposed whilst care was taken to protect the neuromuscular junctions and the neurovascular bundle. The Achilles tendon was severed and the lower extremity was connected to the muscle force measuring device using a silk suture. Subsequently, the sciatic nerve was electrically stimulated and the contraction forces were recorded using a force transducer. After the muscle force measurements, the animals were sacrificed. The soleus muscles were detached from surrounding tissues and connected, via the Achilles tendon, to a force transducer and recording device. The sciatic nerve of the animal was electrically stimulated and the responsive force generated by the soleus muscle was measured and recorded.

3.15.7. Tissue histology

Soleus muscles embedded in Tissue-Tek® O.C.T.™ compound (Sakura), were divided into 9 segments along the length of the muscle, and 10 consecutive slices (7 µm sections) from each segment were sectioned and fixed onto glass slides (Marienfeld). Sections undergoing H&E and Picrosirius red staining were post-fixed with 4% formaldehyde. To identify collagenous scar tissue (Sirius red), the sections were stained with Direct Red 80 (Fluka, Germany) by incubation in Sirius red solution (1% w/v in saturated picric acid) for 60 min. Differentiation

was reached with two washes in diluted acetic acid. Dehydration was carried out by immersion in a graded series of ethanol before being incubated in xylol (T. J. Baker) twice for 5 min. The amount of fibrosis in muscle sections was quantified using a custom built macro in NIH ImageJ software package. The fibrotic area in the treated muscle was expressed as a percentage of the total section area, and normalized to the percentage of connective tissue in the uninjured control. Muscle sections were stained with Hematoxylin and Eosin (Merck, Germany) for visualization of myofiber nuclei and cytoplasm. For nuclei staining, sections were incubated in Hematoxylin for 7 min then washed twice in distilled water. Differentiation was achieved by shortly placing the sections in 0.25% HCl-ethanol solution (Merck, Germany) followed by washing under tap water for 10 min. For cytoplasm staining, sections were placed in 2% Eosin (CHROMA) for up to 3 s and dehydrated in graded series of ethanol and finally incubated in xylol twice, each time for a duration of 5 min. The number of fibers with centrally located nuclei was counted manually and expressed as a percentage of the total section area. Muscle fibers expressing slow myosin were detected with monoclonal anti-myosin (skeletal, slow) antibody (1:10000) (Sigma-Aldrich, clone # NOQ7.5.4D, catalog # M8421). Blood vessels were detected with CD31 monoclonal antibody (1:50) (abcam, clone # TLD-3A12, catalog # ab64543). For both stainings, air dried sections were fixed in cold acetone for 20 min and washed in 10% PBS twice for 5 min each. Sections were blocked in 2% horse serum (Biozol) diluted in 2% BSA-PBS for 30 min at room temperature. The primary antibodies were then applied with overnight incubation at 4 °C. After washing twice with PBS, the secondary antibody (Biotinylated Horse Anti-Mouse IgG Antibody, rat adsorbed, Biozol) was applied (1:50) for 30 min. The sections were washed twice with PBS and the avidin-biotin complex was applied for 50 min at room temperature (AP-Standard kit AK 5000; Vector). After washing, sections were then incubated with Alkaline Phosphatase substrate (Red Alkaline Substrate Kit I, SK-5100, Vector) for up to 8 min. Finally, sections were counter-stained following the Mayers Haemalum method. Slow fibers were quantified using a custom built macro in NIH ImageJ software package. For quantification, positively stained blood vessels were manually counted from regions of interest generated randomly from the entire muscle section. For all stained sections, images were captured using a light microscope (Leica Microsystems, Germany) equipped with a digital camera (AxioCam MRc, Carl Zeiss MicroImaging, Germany).

3.15.8. Structural analysis of skeletal muscle

Muscle fiber density was determined by manually counting the total number of fibers in the muscle cross-sections. The number of fibers was normalized to the total area of the cross-section, which was determined using NIH ImageJ.

The total number of centrally located nuclei were counted manually for each muscle cross-section, and was normalized to total cross-section area.

CD31+ capillaries were counted manually from at least 3 regions of interest (ROI) that were determined from the muscle cross-sections using a random ROI generator in NIH ImageJ.

Blood vessels that were positively stained for Factor VIII were counted manually from entire muscle cross-sections.

Muscle fibrosis was determined by using a custom-built ImageJ macro that calculated Sirius red positive area as a percentage of the total muscle cross-section area.

The ratio between fast and slow type fibers was determined by counting the number of fibers that were positive for myosin fast using a custom-built macro in NIH ImageJ.

3.16. Statistical Analysis

All values are depicted as mean ± standard deviation. A minimum of three independent experiments were performed for all *in vitro* studies, often with multiple biological replicates. This information is included in figure legends. Statistical analysis was carried out in GraphPad Prism 7.0 (GraphPad Software Inc., USA). The Shapiro-Wilk test was used to test normality for experiments with $n>15$. If the data was normally distributed, two-tailed student's t-test (two groups) or one-way ANOVA with Tukey's or Bonferroni's post-hoc test (> two groups) was used. If normality could not be confirmed, the Mann Whitney U test (two groups) or the Kruskal-Wallis test with Tukey's or Bonferroni's post-hoc test (> two groups) was used. $P<0.05$ was considered statistically significant.

4. Results:

4.1. Proof of concept: Myoblast function is influenced by paracrine factors secreted by MSCs

To investigate MSC paracrine effects on myoblasts, conditioned media from MSCs cultured on TCP well plates was collected, and used further to study myoblast behavior in an indirect co-culture setup (**Fig. 3a**). Myoblast functions such as survival, migration, and proliferation are essential for regeneration and can determine the healing outcome, and were therefore analyzed in corresponding *in vitro* assays. The *in vitro* experiments were carried out in serum free conditions to prevent exogenously supplemented serum from masking the effects of the paracrine factors present in MSC-CM.

The effects of MSC-CM on the migration behavior of myoblasts was investigated in a scratch wound healing assay with live cell imaging. The kinetics of scratch closure (**Fig. 3b**) indicates that the rate of scratch closure by myoblasts was elevated in the presence of MSC-CM than the control group. This difference between the groups became apparent only 5 hours after the addition of MSC-CM and indicates the quick response of myoblasts to paracrine factors present in MSC-CM. At the end of the experiment (20 h), myoblasts in the MSC-CM group had repopulated a significantly greater area of the scratch (~80%) compared to control (~40%) (**Fig. 3c**).

Cell apoptosis is a major hindrance to regeneration in a harsh post-injury environment. An *in vitro* survival assay was established to evaluate the viability of myoblasts in injury mimicking conditions. In the absence of serum, myoblast viability dropped to ~40% after 24 hours. In contrast, MSC-CM prevented myoblasts from undergoing apoptosis, as a significantly higher number of viable cells (~75%) were detected in the MSC-CM group, suggesting that paracrine factors secreted by MSCs may exert anti-apoptotic benefits (**Fig. 3d**).

Next, the proliferative behavior of myoblasts was assessed over 48 hours (**Fig. 3e**). In comparison to control, a significantly higher number of myoblasts were found in the MSC-CM group at both time points tested. Relative to day 0, cell numbers declined in the control group, likely due to the absence of nutrients normally present in serum.

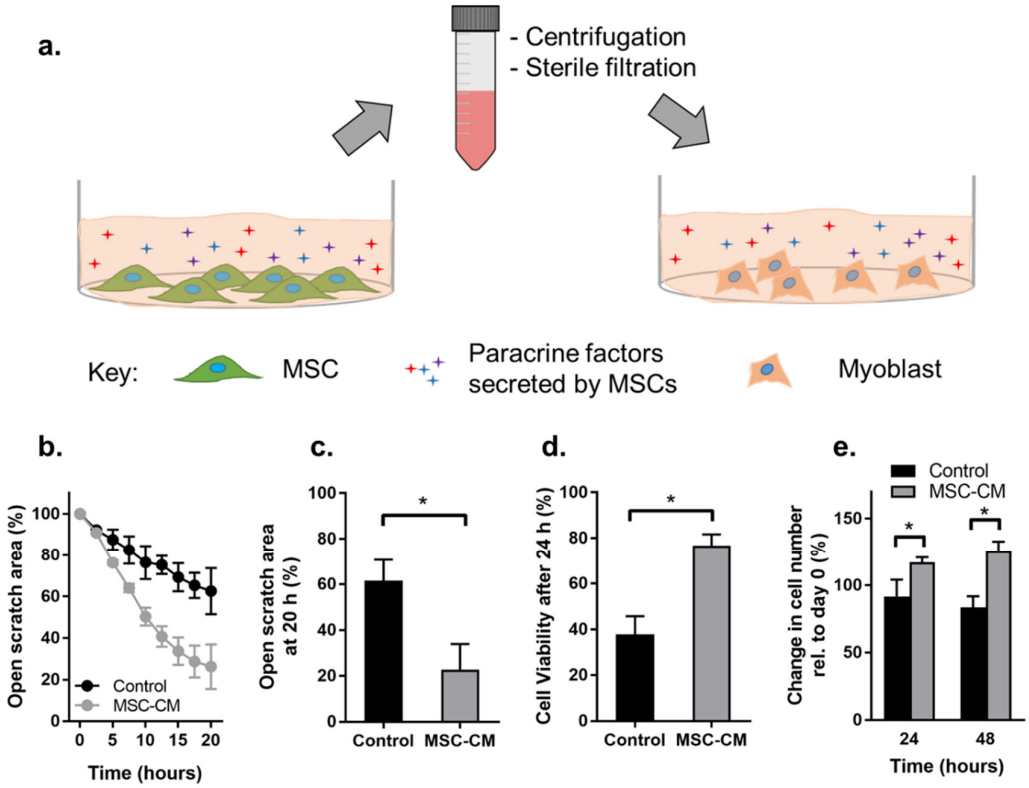

Fig. 3: MSC paracrine effects on myoblast function.

(a) Schematic depicting the procedure of conditioned media collection from MSCs (MSC-CM) seeded on TCP well plates, and its subsequent exposure to myoblasts for functional assessment. The migration of myoblasts in the presence of MSC-CM was determined using a scratch wound healing assay. (b) Kinetics of scratch closure by myoblasts revealed a faster repopulation of the scratch in the presence of MSC-CM. (c) Evaluation of open scratch area at the end of the experiment (20 h) revealed greater migration in the presence of MSC-CM [n=4, two-tailed student's t-test]. (d) MSC-CM enhanced the viability of myoblasts in serum-free conditions, suggesting anti-apoptotic benefits [n=4, two-tailed student's t-test]. (e) MSC-CM promoted myoblast proliferation in serum-free conditions, whereas cell numbers decreased over time in the control group [n=5, two-tailed student's t-test].

4.2. Behavior of MSCs on alginate substrates

Biomaterials for cell transplantation are typically used in the form of 3D injectable hydrogels or 3D porous scaffolds. The microenvironments that these biomaterials offer are starkly different to normal cell culture substrates such as TCP and glass coverslips. MSCs are known to be environmentally-responsive, therefore it was pertinent to determine if their paracrine secretion pattern and the subsequent effects of secreted factors on myoblasts are altered when culture dimensionality changes from 2D to 3D and when substrate microenvironment changes from nanoporous (hydrogels) to macroporous (scaffolds).

Alginate is a widely used hydrogel in the field of tissue engineering. Its versatile nature allows the formation of substrates that provide cells with distinct microenvironments without the need to alter chemical or mechanical properties. Alginate is frequently employed to deliver cells via injectable formulations or via porous sponge-like scaffolds. It thus represented a suitable candidate biomaterial for this study.

Alginate was rendered biocompatible by the covalent conjugation of cell-adhesive RGD peptide sequences, and ionically crosslinked to fabricate three distinct substrates: (1) flat 2D films, (2) 3D cell-encapsulating hydrogels, and (3) 3D porous scaffolds. TCP was used throughout for comparison (**Fig. 4a**).

4.2.1. Cell morphology

Morphological evaluation of MSCs on the different substrates was carried out by staining with phalloidin (actin filaments) and DAPI (nuclei) (**Fig. 4b**). MSCs displayed typical spread out morphology with prominent actin filaments on TCP. Culture on relatively compliant 2D alginate films resulted in MSCs adopting an elongated morphology and multiple cells were found clustered together in close proximity. In contrast, when the cells were encapsulated in 3D hydrogels, they displayed a round morphology which is typically observed when the surrounding matrix does not provide enough space for cell spreading. In a 3D scaffold, large interconnected pores (80-150 μm) allowed cell spreading on the pore walls and facilitated the formation of cell-cell contacts as multiple nuclei were observed in close proximity.

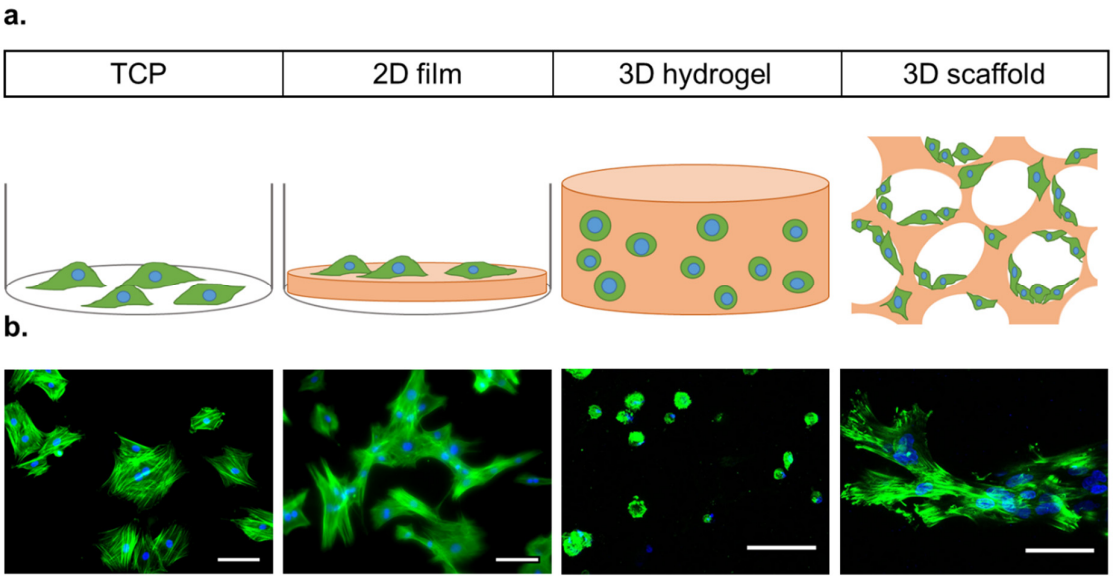

Fig. 4: MSCs adopt distinct morphologies on biomaterial substrates.
(a) Schematic representation of MSCs cultured on tissue culture plastic (TCP), an alginate film (2D film), encapsulated in a 3D alginate hydrogel, and seeded on a 3D macroporous alginate scaffold. (b) Representative images of MSCs stained with phalloidin (actin filaments) and DAPI (nuclei) show that MSCs adopt different morphologies on the four substrates tested. [Scale bar: TCP, 2D film, 3D hydrogel = 100 µm; 3D scaffold = 50 µm].

4.2.2. Cell viability

Due to their synthetic nature, many biomaterials do not support the long term viability of cells. Alginate, in its unmodified form, does not support cell attachment due to the absence of cell binding sites, but facilitates cellular adhesion and subsequent functions after the covalent attachment of cell-adhesive RGD peptides.

Viability of MSCs on the different substrates was evaluated by harvesting the cells either via trypsinization and/or dissolution of alginate, followed by a LIVE/DEAD cell viability assay (**Fig. 5**). Cells in all groups maintained high viability over the time points evaluated. Although encapsulation in 3D hydrogels is relatively stressful for the cells due to the higher shear forces compared to 2D or 3D scaffold cultures, no detrimental effects on viability were observed in this setup. The viability can be affected by viscosity of the material, frequency and harshness of mixing, and by the diffusion co-efficient of the material that determines the rate of nutrient diffusion to the cells. Importantly, MSCs remained highly viable in 3D hydrogels for up to 14

days *in vitro* (**Fig. 5b**), which indicated that the alginate matrix did not inhibit nutrient diffusion to the cells and that the lack of cell spreading did not have a detrimental effect on MSC fate.

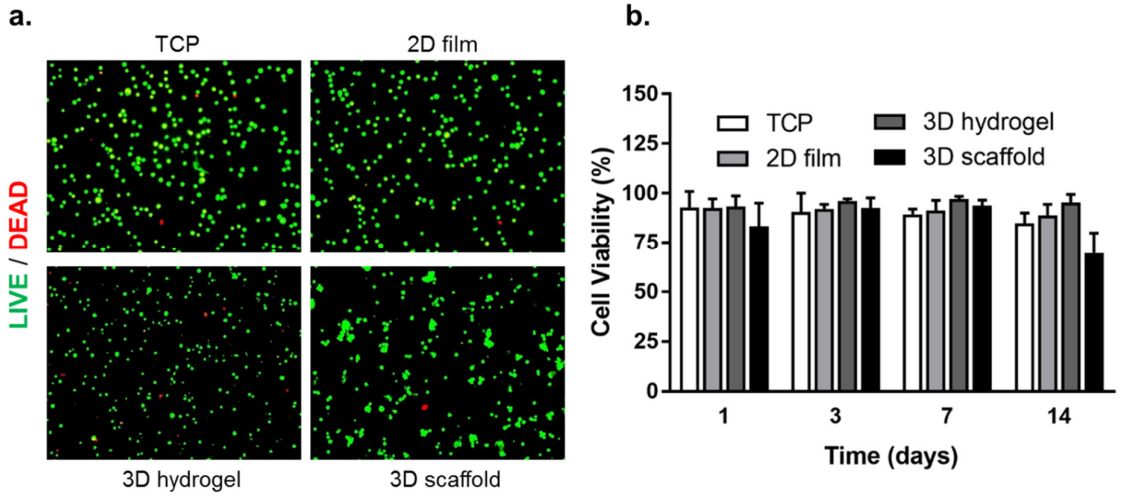

Fig. 5: MSCs remain highly viable on biomaterial substrates in vitro.
(a) Representative fluorescence images of trypsinized MSCs stained with calcein AM (green = live cells), and Ethidium homodimer-1 (red = dead cells) after 7 days of culture on the indicated substrates. (b) Quantification of MSC viability at 1, 3, 7, and 14 days [n=4].

4.2.3. Paracrine secretion

To assess whether differences in substrate microenvironments influence the paracrine function of MSCs, a cytokine array kit was employed which concurrently detects 90 different cytokines in cell culture supernatants (**Fig. 6**). This array was chosen because it permitted the detection of a wide range of secreted factors and could therefore provide a generalized, qualitative impression of MSC secretion pattern. The heatmap in **Fig. 6** shows intensities of the indicated cytokines normalized to cell number. Cytokine secretion from MSCs was found to strongly depend on the culture substrate. The highest cytokine intensities were detected in CM from MSCs that were cultured in 3D porous scaffolds. CM from 2D films also led to relatively higher detection intensities. In stark contrast, CM from MSCs in TCP and 3D hydrogels had the lowest intensities for a large number of cytokines, which are represented as dark spots in the heatmap.

Some of the cytokines detected on the array are known to play a role in muscle development and regeneration. For instance, Adiponectin is a well-known regulator of several metabolic functions in skeletal muscle, and has also been reported to promote the myogenic differentiation of muscle cells [139]. Basic-FGF, which was detected in relative higher intensities in the 2D-

film and 3D scaffold CM, has been reported to be a vital stimulatory factor of muscle resident satellite cells' activation and proliferation [140]. Ciliary neurotrophic factor (CNTF), a higher intensity of which was detected in 3D scaffold-CM compared to the other groups, has been reported to improve the viability of muscle progenitor cells [141].

Interestingly, cytokines such as MMP-13 (matrix metalloproteinase 13), TIMP-3 (tissue inhibitor of metalloproteinase-3), and BDNF (Brain-derived neurotrophic factor) were highly secreted by MSCs in all four substrate conditions. Others, such as IL-2, 3, and 6 (Interleukin-2, 3, and 6), and PDGF-AA (platelet derived growth factor) were highly secreted only by MSCs cultured on TCP. On the other hand, IL-13 was highly expressed only by MSCs in 3D hydrogels. Taken together, the cytokine array analysis reveals that paracrine secretion from MSCs can be modulated by engineered microenvironments.

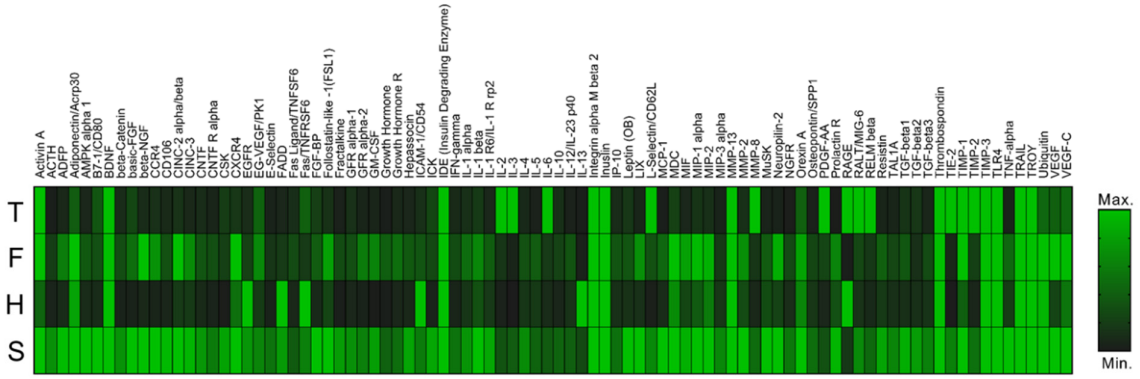

Fig. 6: Modulation of MSC cytokine secretion by biomaterial substrate.

Heatmap comparing the secretion of 90 cytokines by MSCs when cultured on TCP (T), 2D film (F), 3D hydrogel (H), and 3D scaffold (S) substrates. In general, MSCs cultured on 2D films and 3D scaffolds secreted high amounts of many cytokines tested, whereas lower secretion was observed for MSCs cultured on TCP or encapsulated in 3D hydrogels. Conditioned media obtained from MSCs were tested with a Ray-Biotech cytokine array kit. Intensities were normalized to cell numbers that were determined immediately after CM collection [n=4 biological replicates].

To gain insight into the secretion of paracrine factors relevant for muscle regeneration, rat specific ELISA kits were employed to quantify the secretion of Vascular endothelial growth factor (rVEGF), Leukemia inhibitory factor (rLIF), Insulin like growth factor (rIGF), Hepatocyte growth factor (rHGF), and Fibroblast growth factor (rFGF) (**Fig. 7**).

VEGF is a potent angiogenic factor and, along with other pro-angiogenic molecules, plays an important role in stimulating blood vessel formation in injured muscle tissues. MSCs cultured on TCP and 3D scaffolds secreted the highest amounts of rVEGF (**Fig. 7a**). Among the three alginate based substrates, 3D scaffold-CM contained significantly higher concentrations of rVEGF than 2D film-CM and 3D hydrogel-CM.

LIF is well known for its role in maintaining the pluripotency of embryonic stem cells, but has also been implicated in the modulation of myoblast proliferation and differentiation [142, 143]. ELISA based detection revealed that MSC-CM from 3D scaffolds contained significantly higher concentrations of rLIF than all other CM groups (**Fig. 7b**).

IGF is a potent myogenic factor that stimulates satellite cells, promotes their myogenic differentiation, increases muscle mass and strength, and has been implicated in the timely onset of the anti-inflammatory phase after injury [144]. Surprisingly, only 3D scaffold-CM was found to contain high amounts of rIGF, whereas the secretion in the other groups was negligible in comparison (**Fig. 7c**).

HGF, also known as scatter factor, is known to stimulate the motility and migration of cells. In skeletal muscle, HGF has been shown to stimulate the function of satellite cells and is considered a potent therapeutic factor for muscle regeneration strategies [145]. Significantly higher concentrations of secreted rHGF were detected in 3D scaffold-CM compared to all other groups (**Fig. 7d**).

FGF has also been implicated to play an important role in the regenerative phase following muscle injury. Members of the FGF family have been shown to activate muscle satellite cells and stimulate their proliferation [146]. Although MSCs in general secreted low amounts of rFGF, differences were observed between the groups. 2D film-CM and 3D scaffold-CM contained similar amounts of rFGF, whereas 3D hydrogel-CM and TCP-CM contained significantly lower amounts of rFGF compared to 3D scaffold-CM (**Fig. 7e**).

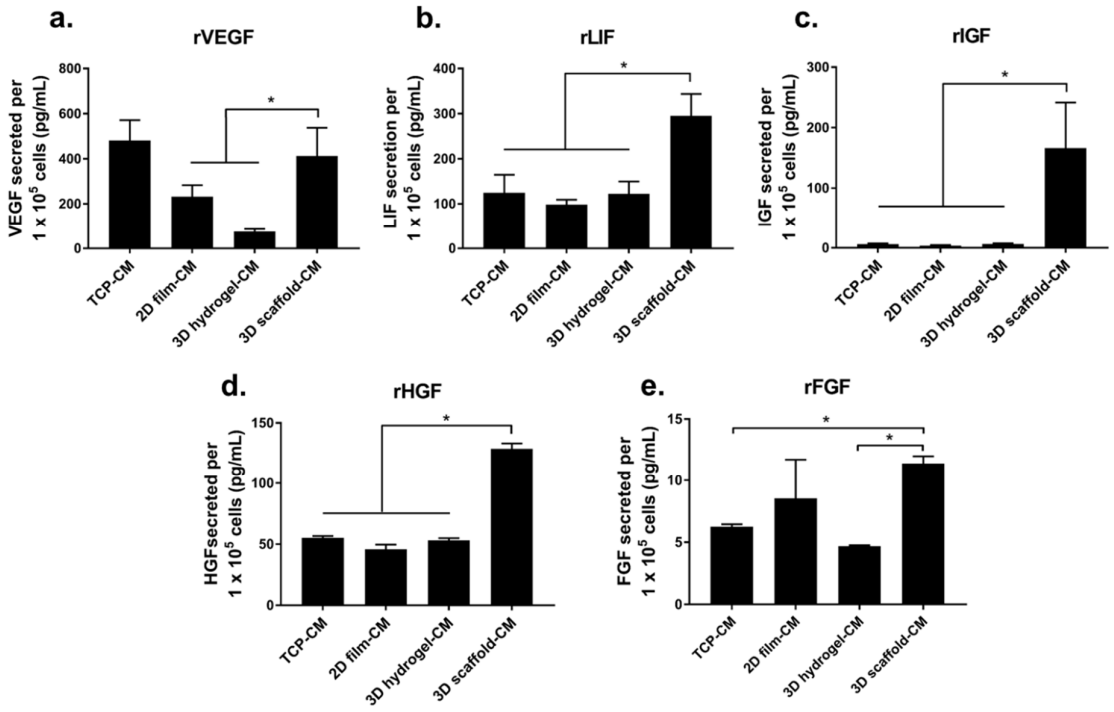

Fig. 7: Secretion of muscle relevant growth factors from MSCs.

Based on the differences in secretion observed with the cytokine array, more precise rat specific ELISA kits were used to detect the secretion of (a) Vascular endothelial growth factor (rVEGF), (b) Leukemia inhibitory factor (rLIF), (c) Insulin like growth factor (rIGF), (d) Hepatocyte growth factor (rHGF), and (e) Fibroblast growth factor (rFGF). Compared to 3D hydrogels, MSCs in 3D scaffolds secreted significantly higher amounts of all growth factors tested. [n=4 biological replicates, one-way ANOVA with Tukey's correction for multiple comparisons].

4.3. Biomaterial substrate dictates the paracrine effects of MSCs on myoblast function

The substrate microenvironment clearly modulated the paracrine secretion from MSCs, but does this alteration lead to varying effects on the function of muscle progenitor cells? Investigating the influence of MSC-CM from different culture conditions on the pro-regenerative function of myoblasts could lead to a rational selection of appropriate biomaterial substrates for skeletal muscle regeneration strategies using MSCs.

4.3.1. Survival

The anti-apoptotic or cytoprotective effects of MSC-CM from different substrates was assessed in a myoblast survival assay (**Fig. 8**). Under serum deprived conditions, the viability of myoblasts in the control group dropped to ~50% after 24 hours. The addition of any kind of (serum free) MSC-CM significantly improved myoblast viability (>70%). However, a significantly higher percentage of viable cells were detected in the presence of CM from 3D scaffolds compared to CM from 3D hydrogels.

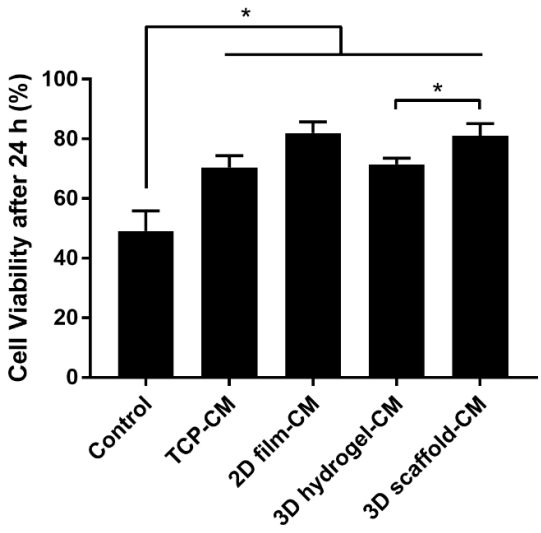

Fig. 8: Anti-apoptotic property of MSC-CM obtained from different substrates.
Addition of any type of CM significantly enhanced the survival (viability) of myoblasts compared to the control (serum free culture media). [n=8, one-way ANOVA with Dunnett's correction]. More specifically, MSC-CM from 3D scaffolds supported significantly higher survival of myoblasts than CM obtained from 3D hydrogels [n=8, two-tailed student's t-test].

4.3.2. Metabolic activity and proliferation

The ability of CM from different substrates to stimulate the metabolic activity and proliferation of C2C12 myoblasts was evaluated over two days. The metabolic activity (normalized to cell number) remained consistent between the different groups after the first 24 hours, but significant differences emerged after 48 hours (**Fig. 9a**). CM from the two 3D substrates significantly increased the metabolic activity of myoblasts relative to all other groups.

Myoblasts proliferated significantly in response to all CM groups relative to control media at both time points. Typically, in response to a reduction in the serum concentration, myoblasts

exit the cell cycle and start to undergo myogenic differentiation. However, in completely serum free conditions, no cell fusion was observed and myoblasts underwent cell death. This explains the negative change in cell number after 48 hours in the proliferation assay (**Fig. 9b**). Despite also being serum free, MSC-CM from different substrates stimulated an increase in cell number. After 48 hours, a higher number of myoblasts were detected in the presence of 3D scaffold-CM and 2D film-CM compared to 3D hydrogel-CM.

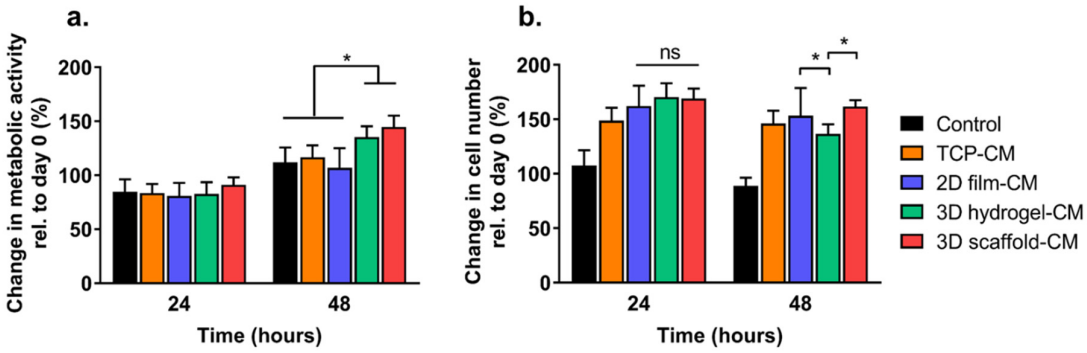

Fig. 9: Influence of MSC-CM from different substrates on the metabolic activity and proliferation of C2C12 myoblasts.

(a) Metabolic activity was comparable between the groups after 24 hours, but showed significant enhancement in the 3D scaffold-CM and 3D hydrogel-CM groups after 48 hours. [n=12, one-way ANOVA with Tukey's correction for multiple comparisons] (b) Proliferation of C2C12 myoblasts was significantly higher in all CM groups relative to control at both time points. However, after 48 hours, significantly higher myoblasts were detected in the 3D scaffold-CM and 2D film-CM groups compared to 3D hydrogel-CM. [n=12, one-way ANOVA with Tukey's correction for multiple comparisons].

4.3.3. Collective cell migration

The migration behavior of myoblasts was characterized using a scratch wound healing assay (**Fig. 10a**). The kinetics of scratch closure (**Fig. 10b**) revealed that, as expected, myoblasts had the slowest rate of migration in the presence of control media. MSC-CM from TCP and 3D hydrogel substrates stimulated almost identical rates of scratch closure. Scratch closure in response to 3D scaffold-CM was the quickest up to 10 hours, but slowed down until the end of

the experiment. The fastest rate of scratch closure was observed in the presence of 2D film-CM.

At the end of the experiment (**Fig. 10c**), ~70% of the scratch area remained empty in the control group. Due to paracrine effects, ~40-45% of the scratch area remained empty in the TCP-CM and 3D hydrogel-CM groups. Scratch closure was significantly higher in the 3D scaffold-CM group compared to 3D hydrogel-CM and TCP-CM groups. The fastest kinetics of scratch closure in the 2D film-CM also led to most of the scratch area being repopulated by myoblasts at the end of the experiment (significant to all other groups).

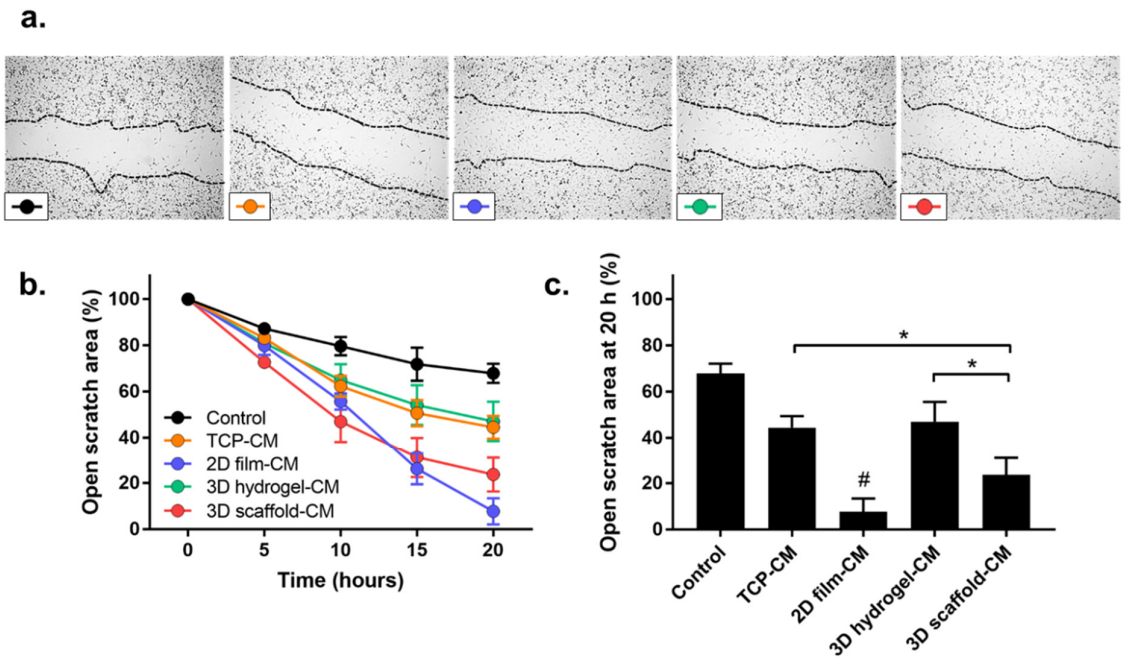

Fig. 10: Collective myoblast migration in response to MSC-CM from different substrates.
(a) Representative bright field images of regions of interest showing myoblasts populating the open scratch area. Dashed lines indicate initial scratch boundary. (b) Kinetics of scratch closure revealed that the highest migration rate was maintained by myoblasts in the presence of 2D film-CM. (c) At the end of the experiment (20 h), myoblasts in 2D film-CM had repopulated a significantly higher area of the scratch than any other group. [n=4, one-way ANOVA with Tukey's correction for multiple comparisons; # significant compared to all other groups].

4.3.4. Migratory behavior of single cells

The readouts in **Fig. 10** provide information on the rates and extent of scratch closure; this may be due to collective myoblast migration, but can also be due to simultaneous myoblast proliferation, especially in the absence of any proliferation inhibitors. The assay did not reveal whether single cells migrate faster or slower, maintain a direction, or cover larger distances in response to the paracrine factors present in the different CM groups. To investigate these aspects, manual single tracking of cells in a scratch assay setting was performed.

Single cell tracking of myoblasts revealed detailed information regarding total distance migrated, net displacement within the timeframe of the experiment, migration velocity, and directionality, in the presence of MSC-CM from different substrates (**Fig. 11**). Total distance migrated by myoblasts in control media was significantly lower than all other groups, which corresponded to the earlier observation that >60% of the scratch area remained unpopulated at the end of the experiment. Myoblasts that were exposed to 2D film-CM and 3D scaffold-CM, on average, traveled the greatest distance (~500 μm), whereas myoblasts covered a significantly lesser distance in the presence of 3D hydrogel-CM (**Fig. 11a**).

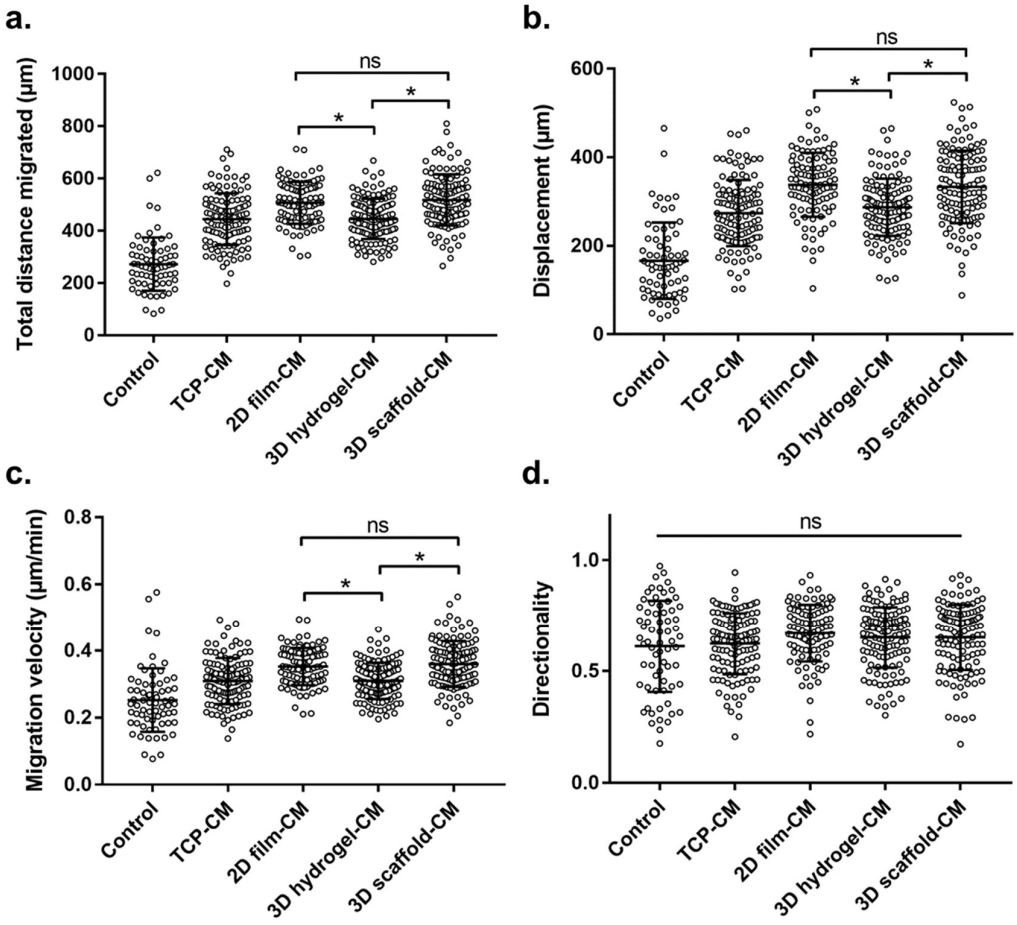

Fig. 11: Single cell migratory behavior in response to MSC-CM from different substrates. *Quantitative analysis by single cell tracking of C2C12 myoblasts in the presence of different MSC-CM groups revealed differences in (a) total distance migrated, (b) net displacement, (c) migration velocity, and (d) directionality. Each dot in the dot plots is representative of one cell. [n=68-129 from at least 4 independent experiments, a-c: one-way ANOVA with Bonferroni's correction for multiple comparisons; d: Kruskal-Wallis test with Dunn's correction for multiple comparisons].*

Unlike in many chemotaxis assays, cells in a scratch assay do not only move in one direction but may change course randomly; the net displacement is, therefore, an important readout to define how far the cells migrated from their starting position. Similar to the total distance traveled, the mean displacement of the myoblasts was largest in the presence of 3D scaffold-CM and 2D-film CM (~350 µm), whereas it was considerably lower (~270-300µm) in the TCP-CM and 3D hydrogel-CM groups (**Fig. 11b**).

Migration velocity, which is vital for progenitor cells that migrate to the site of injury *in vivo*, also showed differences in response to MSC-CM from different groups (**Fig. 11c**). Myoblasts had the highest mean velocity of ~0.35 μm/min in the presence of 3D scaffold-CM and 2D film-CM, whereas the migration velocity in the presence of 3D hydrogel-CM was significantly lower.

No significant differences between the groups was observed for directionality (**Fig. 11d**). This was an expected outcome in the absence of any chemical gradient or contact guidance cues that would induce directed migration of cells.

4.3.5. Myogenic differentiation

The influence of CM from the different substrates on the myogenic differentiation and *in vitro* myotube formation of C2C12 myoblasts was determined in two ways: (1) via fluorescent staining of MHC and subsequent analysis of myotube density and length (**Fig. 12**); and (2) using Western Blot to quantify the expression of myogenic differentiation markers MHC and MyoG (**Fig. 13**).

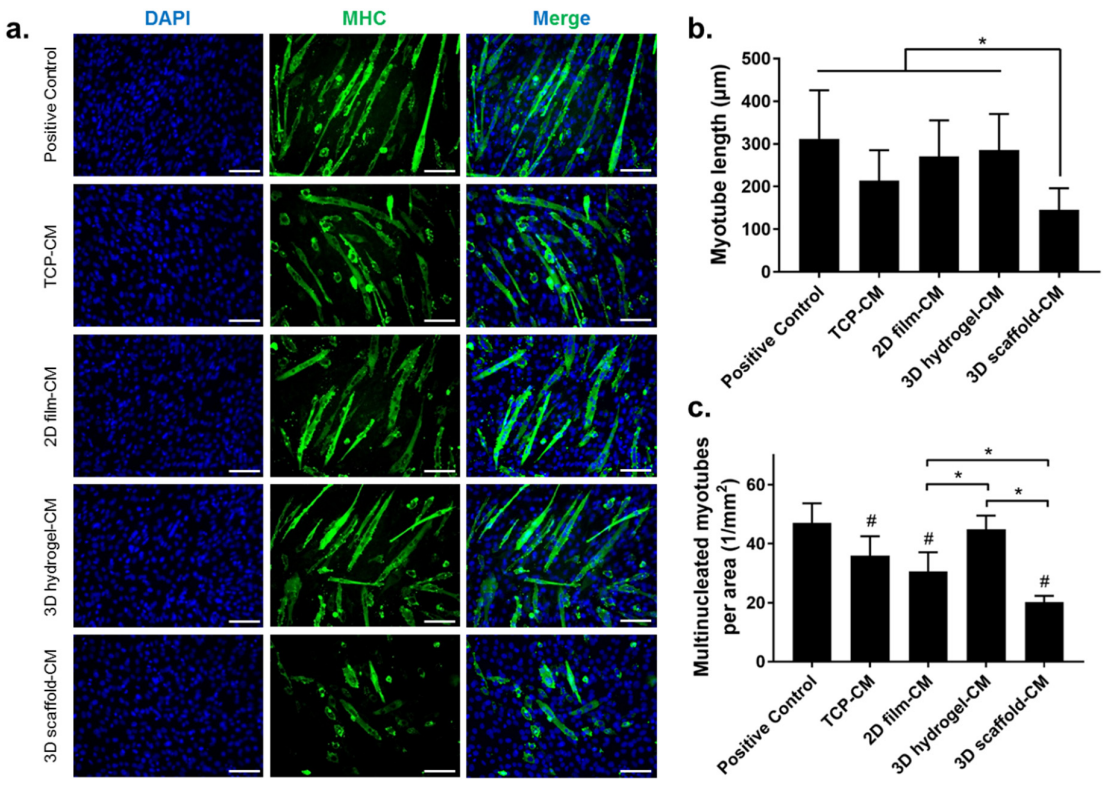

Fig. 12: Myogenic differentiation in response to MSC-CM from different substrates (immunofluorescence).

(a) Fluorescent images of myoblasts expressing the differentiation marker myosin heavy chain (MHC=green) five days after induction of differentiation.[Scale bar = 100 µm]. Several regions of interest were used to quantify: (b) mean myotube length [n=63, Kruskal-Wallis test with Dunn's correction for multiple comparisons] and (c) number of multinucleated myotubes per area [n=5, one-way ANOVA with Tukey's correction for multiple comparisons; # significant compared to positive control].

The positive control in **Fig. 12a** shows fusion of myoblasts to form myotubes five days after induction of differentiation by reducing the serum content. CM from MSCs cultured on TCP, 2D films, and 3D hydrogels similarly supported myotube formation *in vitro* within the same time frame. However, the addition of 3D scaffold-CM notably inhibited or delayed myotube formation. Several regions of interest were then used to quantify myotube length and myotube density. The mean myotube length in the positive control was ~300 µm. Although the myotube length varied in the presence of TCP-CM (~200 µm), 2D film-CM (~275 µm), and 3D hydrogel-CM (~275 µm), no significance was reached due to large deviations (**Fig. 12b**).

However, myotube length was significantly lower in the 3D scaffold-CM group (~150 μm) compared to all other groups.

Quantification of myotube density revealed that 3D hydrogel-CM, similar to the positive control, supported myoblast fusion and myotube formation (~42-45/ mm^2). Culture in TCP-CM, 2D film-CM, and 3D scaffold-CM significantly reduced myotube density relative to the positive control (**Fig. 13c**). However, myotube density was significantly lowest in the 3D scaffold-CM group compared to all other groups.

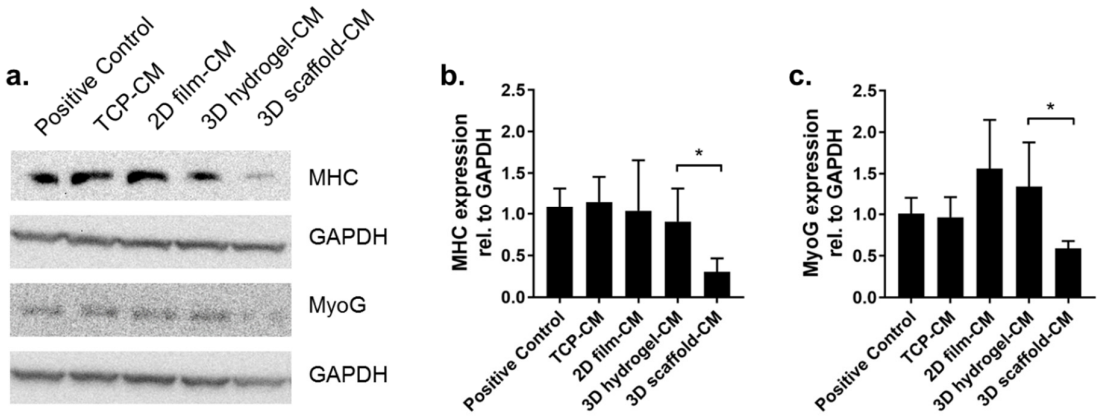

Fig. 13: Myogenic differentiation in response to MSC-CM from different substrates (Western blot).

Whole cell lysates were analyzed for the detection of myogenic differentiation markers MHC and MyoG. *(a) Detection of myosin heavy chain (MHC) and myogenin (MyoG) in cell lysates obtained from myoblasts cultured in the presence of MSC-CM from different groups. Protein loading was determined using GAPDH. Relative expression of (b) MHC, and (c) MyoG was quantified using densitometry [n=4, two-tailed student's t-test].*

Western blot analysis from four biological replicates confirmed that CM from MSCs cultured in 3D scaffolds significantly inhibited or delayed myogenic differentiation, as assessed by the relative expression of the myogenic differentiation markers MHC and MyoG.

4.4. N-cadherin expression modulates MSC paracrine effects

Based on paracrine factor secretion, and the results of the functional assays on myoblasts using MSC-CM from different substrates, it can be concluded that a 3D scaffold represents a microenvironment, distinct from the other substrates, that not only promotes the enhanced secretion of paracrine factors from MSCs, but these paracrine factors also exert beneficial functional effects on muscle progenitor cells.

The question that naturally followed was: what geometrical or structural cues were the 3D porous scaffolds providing the MSCs that the other alginate groups were not, despite being chemically and mechanically similar? The difference in dimensionality between the 2D and 3D groups may have played a role, but this does not account for the differences observed between 3D scaffold and 3D hydrogel CM. One of the clues may be in the way the MSCs were morphologically organized in a 3D scaffold compared to a 3D hydrogel (**Fig 4**). MSCs in the 3D scaffold were in close physical proximity, almost as if clustered together, whereas they were physically separated by an alginate matrix in a 3D hydrogel. A proposed hypothesis was that the porosity of the 3D scaffold allowed MSCs to establish cell-cell contacts possibly via cell adhesion molecules such as N-cadherin and E-cadherin. The formation of cadherin junctions, in turn, may have resulted in enhanced paracrine factor secretion and subsequent effects on myoblast function. Previous studies have reported high expression of E- and N- cadherins in spheroid cultures of MSC, and have correlated it with enhanced trophic factor secretion [147, 148].

4.4.1. Substrate dependent expression of N-cadherin in MSCs

In a first step towards testing this hypothesis, the expression of E- and N-cadherin was determined using immunofluorescence and qPCR experiments (**Fig. 14**). Immunofluorescent detection showed that MSCs in all substrates expressed N-cadherin regardless of cell-cell contact. In 2D films and 3D scaffolds, cells were observed to be clustered together as multiple nuclei were found in close proximity. In 3D hydrogels, N-cadherin was detected in only a fraction of the encapsulated MSCs (**Fig. 14c**). These observations were then quantified using qPCR analysis, which revealed that MSCs in 3D scaffolds registered an almost 10-fold higher expression of N-cadherin (Cdh2 gene) relative to MSCs encapsulated in 3D hydrogels (**Fig. 14 f**). However in 2D culture, MSCs had lower expression of N-cadherin in 2D films compared to TCP substrate (**Fig. 14 e**). E-cadherin (Cdh1 gene) expression was not detected for MSCs on

the alginate substrates, and very low expression (late amplification) was observed for MSCs cultured on TCP (data not shown).

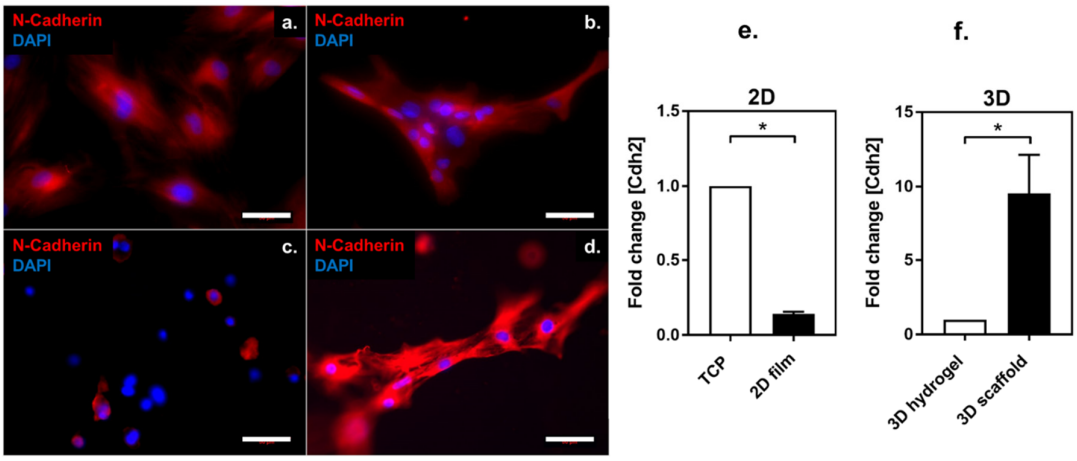

Fig. 14: N-cadherin expression in MSCs cultured on different substrates.
MSCs cultured on (a) TCP, (b) 2D film, (c) 3D hydrogel, and (d) 3D scaffold, stained with N-cadherin (red), and DAPI (blue). Clustering of cells with numerous nuclei in close proximity was observed on 2D films and 3D scaffolds. Only faint N-cadherin signals were observed on cells encapsulated in 3D hydrogels [Scale bar = 50 µm]. Quantification with qPCR revealed a downregulation of the N-cadherin gene Cdh2 on 2D film relative to TCP, whereas an almost 10-fold increase in Cdh2 expression was observed in MSCs on 3D scaffolds relative to 3D hydrogels [n=3, two-tailed student's t-test].

To test whether altered expression of N-cadherin, especially in 3D culture conditions, influenced the paracrine effects of MSCs, cells on all four substrates were treated with an N-cadherin blocking antibody. Conditioned media from MSCs treated with the blocking antibody was then analyzed for detection of paracrine factors, and used in functional assays with myoblasts.

4.4.2. N-cadherin blocking alters MSC secretion profile

To get an indication of how the paracrine secretome is altered in MSCs that are treated with an N-cadherin blocking antibody (+nAB), a cytokine array kit that permitted the detected of 34 cytokines was used. Conditioned media was generated from 3 biological replicates in each substrate condition (TCP, 2D film, 3D hydrogel, and 3D scaffold) with and without N-cadherin blocking. Due to the representative and semi-quantitative nature of the cytokine array, CM from biological replicates were pooled together into one. **Fig. 15** shows fold difference in the intensity of the cytokines detected in N-cadherin blocked samples relative to non-blocked samples. A value below 0 indicates that less of the cytokine was detected after N-cadherin blocking. Despite the fold difference not being greater than 1 or lower than -1, it can be seen that all the cytokines in the 3D scaffold-CM group showed a downregulation after N-cadherin blocking. In comparison, 6 cytokines showed a slight upregulation after N-cadherin blocking in 3D hydrogel-CM as well as 2D film-CM. Similarly, 25 cytokines were upregulated after blocking N-cadherin in MSCs cultured on TCP. One should be cautious in deriving definitive conclusions from this array readout; however, the data supports the hypothesis that blocking N-cadherin mediated cell-cell junctions has a negative effect on paracrine factor secretion by MSCs in a porous scaffold that permitted cell clustering. In a 3D hydrogel substrate, where cells are separated from each other by the alginate matrix, formation of physical cell-cell contacts did not play an important role in determining the secretion of bioactive factors, and therefore blocking N-cadherin did not have as strong an effect.

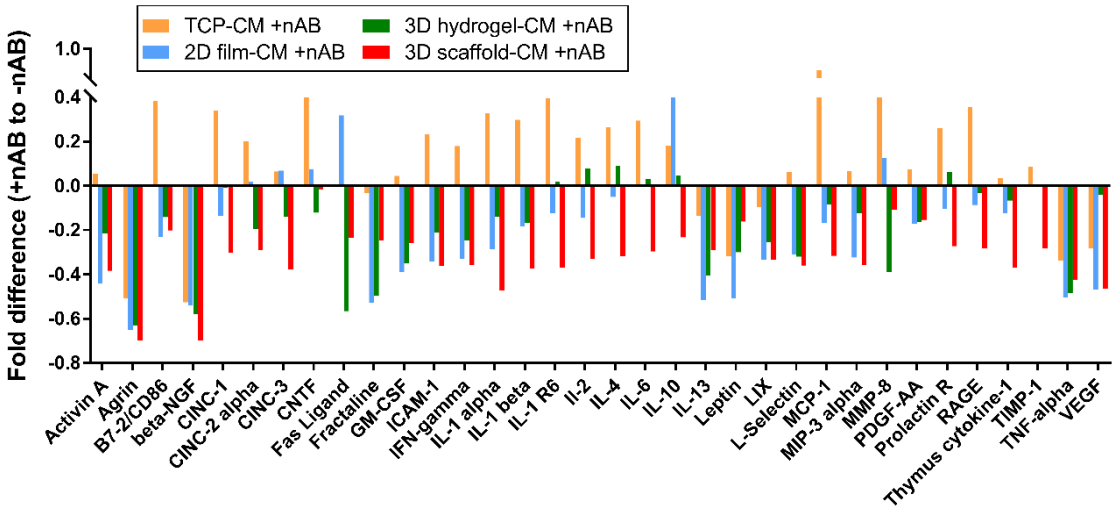

Fig. 15: Cytokine secretion profile of MSCs after N-cadherin blocking.

Fold difference in the secretion of 34 cytokines by MSCs treated with N-cadherin blocking antibody and subsequently cultured on different substrates, relative to MSCs that were not treated with the blocking antibody. Serum free conditioned media from 3 biological donor MSCs were pooled together for the experiment. Intensity values were determined used the Protein Analyzer plugin for ImageJ, and normalized to internal positive controls to compensate for inherent differences between the arrays.

4.4.3. N-cadherin blocking in MSCs alters their paracrine effects on myoblast function

To determine whether the alteration in paracrine secretion from MSCs treated with N-cadherin blocking antibody is reflected in functional behavior of myoblasts, the previously established assays for migration and proliferation were performed.

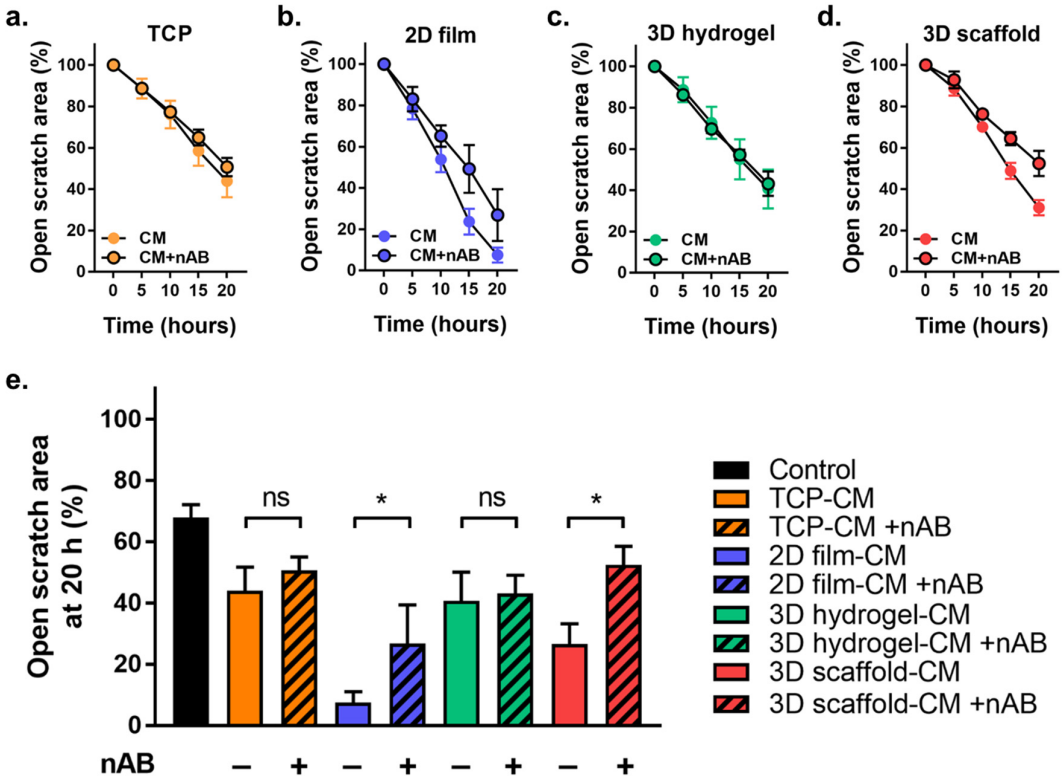

Fig. 16: Collective myoblast migration is affected by N-cadherin blocking in MSCs.
Kinetics of scratch closure in response to CM from N-cadherin treated and non-treated MSCs cultured on (a) TCP, (b) 2D film, (c) 3D hydrogel, and (d) 3D scaffold substrates. (e) Scratch area remaining unpopulated by myoblasts at the end of the experiment (20 h) [n=4, two-tailed student's t-test].

A scratch wound healing assay was performed using MSC-CM from four substrates with and without N-cadherin blocking (**Fig. 16**). The kinetics of scratch closure demonstrate that the rate of collective myoblast migration was not altered by N-cadherin blocking in MSCs on TCP and 3D hydrogel substrates (**Fig. 16a, c**). However, N-cadherin blocking in MSCs cultured on 2D film and 3D scaffold substrates affected the paracrine effects on myoblasts by altering their kinetics of scratch closure (**Fig. 16b, d**). **Fig. 16e** shows the unpopulated scratch area remaining at the end of the experiment. Significantly greater area remained unpopulated in the presence of N-cadherin blocked MSC-CM from 2D film and 3D scaffold substrates, compared to untreated counterparts.

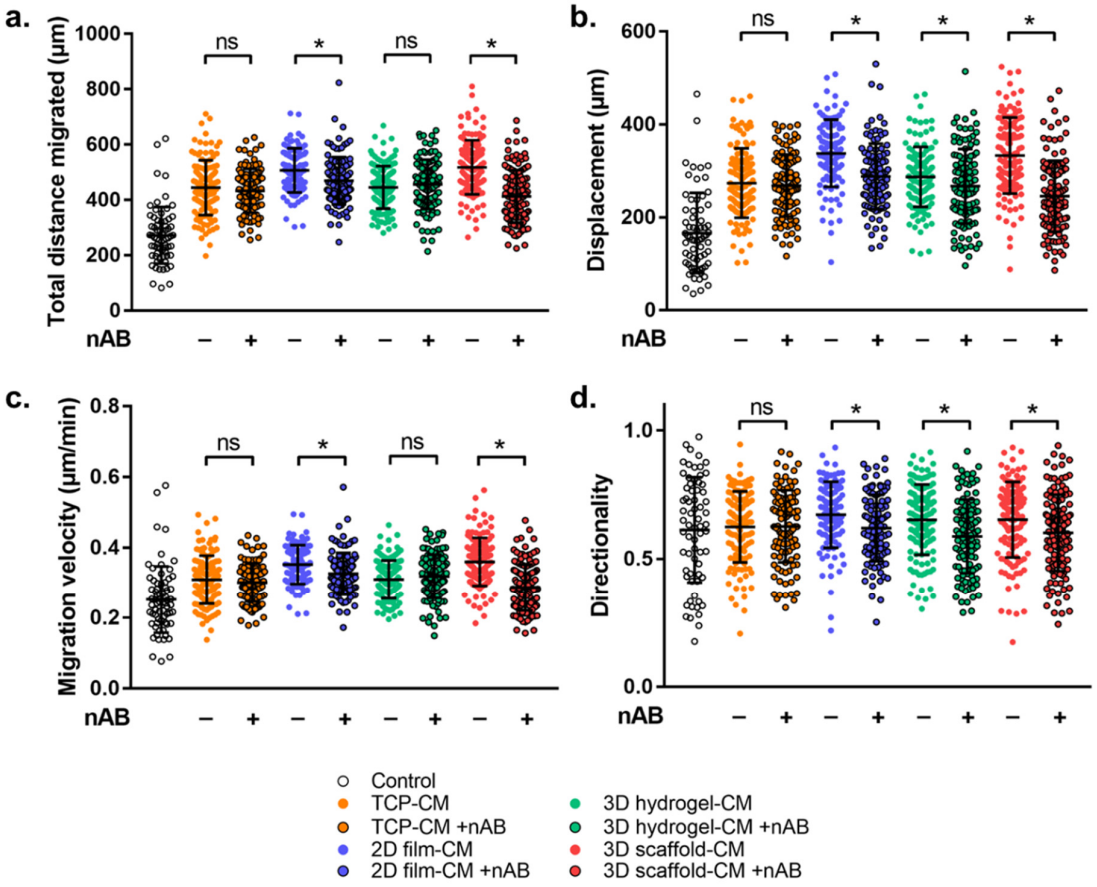

Fig. 17: Single cell migratory behavior after N-cadherin blocking in MSCs.

Single cell tracking revealed that blocking N-cadherin in MSCs prior to CM collection influenced the (a) total distance migrated, (b) net displacement, (c) migration velocity, and (d) directionality of C2C12 myoblasts. [n=68-129, two-tailed Mann-Whitney U test].

Single cell tracking of myoblasts during the migration experiment also revealed significant reduction in total migrated distance and migration velocity after N-cadherin blocking of MSCs in 3D scaffold and 2D film groups, whereas no difference was observed in the TCP and 3D hydrogel groups (**Fig. 17a, c**). This indicated that blocking N-cadherin in MSCs cultured on e.g. porous scaffolds either prevented or downregulated the secretion of paracrine factors that would otherwise stimulate myoblast functions such as migration. However, mean displacement and directionality were significantly reduced after N-cadherin blocking in all groups except TCP-CM (**Fig. 17b, d**).

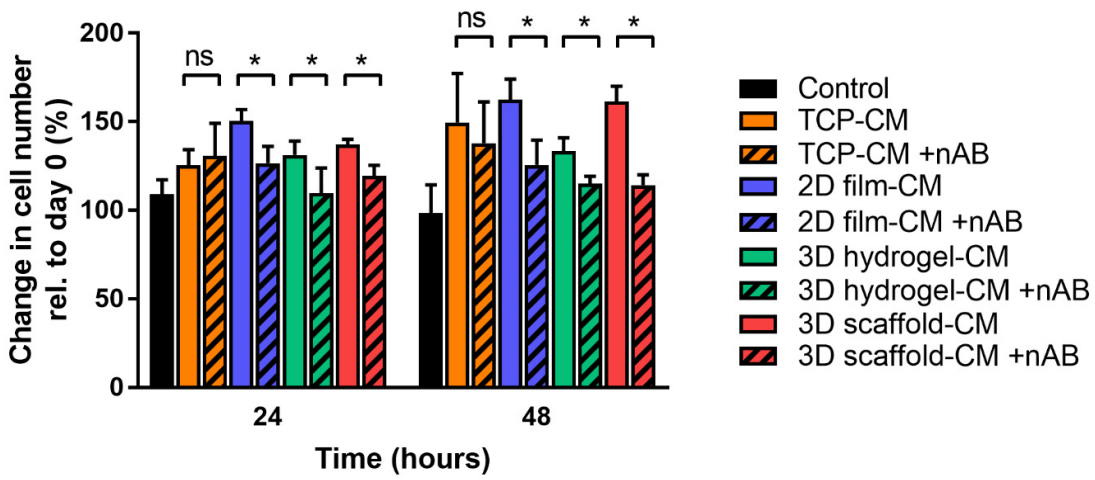

Fig. 18: Myoblast proliferation affected by N-cadherin blocking in MSCs.
Proliferation of myoblasts was significantly reduced in presence of CM from MSCs treated with N-cadherin blocking antibody from all alginate based substrates, but not from TCP. [n=4, two-tailed student's t-test].

To determine whether N-cadherin blocking also affects the proliferative response of myoblasts to MSC-CM, changes in cell number over two days was assessed using a CyQUANT® assay (**Fig. 18**). The results show that at both time points tested, proliferation is negatively influenced in the presence of CM from MSCs that were treated with N-cadherin blocking antibody compared to untreated counterparts. At both time points, no different due to N-cadherin blocking was observed for MSC-CM from TCP substrates.

4.5. Proof of concept: Growth factors enhance paracrine effects of MSCs

In the previous sections, the 3D scaffold emerged as a suitable candidate for skeletal muscle regeneration applications because it enhanced the paracrine secretion of MSCs compared to other substrates by promoting N-cadherin mediated cell-cell contacts. Moreover, the paracrine effects of MSCs seeded in 3D scaffolds also proved to be beneficial for myoblast function.

MSCs transplanted *in vivo* often encounter soluble cues in the injury environment such as pro-inflammatory cytokines. Previous studies have shown that the paracrine effects of MSCs can be modulated by stimulation with these soluble factors. Thus, it was of interest to investigate if

the sensitivity of MSCs to perceive and respond to soluble cues is altered by culture conditions. Another intriguing question was whether certain growth factors encountered in a skeletal muscle environment, such as pro-myogenic IGF and pro-angiogenic VEGF, could stimulate the paracrine secretion of MSCs.

As a first experiment, MSCs cultured on TCP well plates were exposed to 5 ng/mL of recombinant human growth factors hVEGF and hIGF. The conditioned media of unstimulated and GF (GF = hVEGF+hIGF) stimulated MSCs were collected and analyzed using rat specific ELISAs for rHGF, rFGF, rVEGF, and rIGF (**Fig. 19**). After exposure to the two growth factors, MSCs were found to secrete significantly higher total protein, and upregulate the secretion of rHGF, rFGF, and rVEGF. The secretion of rIGF was not altered after hGF stimulation.

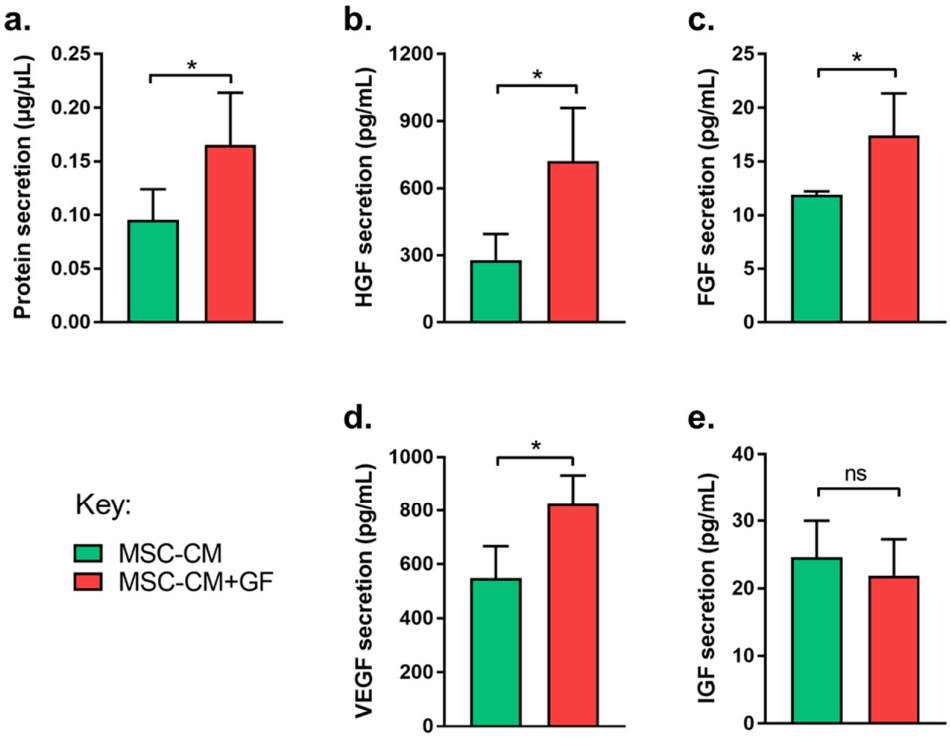

Fig. 19: Recombinant growth factor exposure enhances MSC paracrine secretion.
Treatment of MSCs cultured on TCP with 5 ng/mL of hIGF and hVEGF stimulated significantly increased secretion of total protein and several other growth factors by the MSCs. [n=4, two-tailed student's t-test].

To investigate if increased secretion also exerts benefits on myoblast function, the conditioned media from unstimulated and GF stimulated MSCs were used in previously established *in vitro*

assays (**Fig. 20**). Scratch closure due to collective myoblast migration was significantly enhanced in the presence of CM from GF stimulated MSCs (MSC-CM+GF), whereas the application of GF alone also stimulated greater scratch closure compared to control media. However, no significant effects of MSC-CM+GF were observed in the improvement of cell survival or myoblast proliferation compared to unstimulated MSC-CM (**Fig. 20 a, c, d, f**). The application of GF alone significantly improved cell survival relative to control media.

At a first glance, the improvement in cell migration in response to MSC-CM+GF seemed like an additive effect of growth factors and MSC-CM in combination. To test whether this is the case, the recombinant growth factors present in MSC-CM+GF were neutralized using neutralization antibodies for hVEGF and hIGF, before application in the functional assays. The potency and specificity of the neutralization antibodies was confirmed using ELISA (**Appendix B**). When the cell survival and migration assays were repeated, the previously significant effect of GF alone was diminished, confirming the efficacy of neutralization. However, the positive effects of the MSC-CM+GF group on myoblast migration remained significant over the MSC-CM group (**Fig. 20 b, e**). This confirmed that at least one functional aspect (myoblast migration) was significantly influenced by the enhanced secretion of paracrine factors from GF stimulated MSCs.

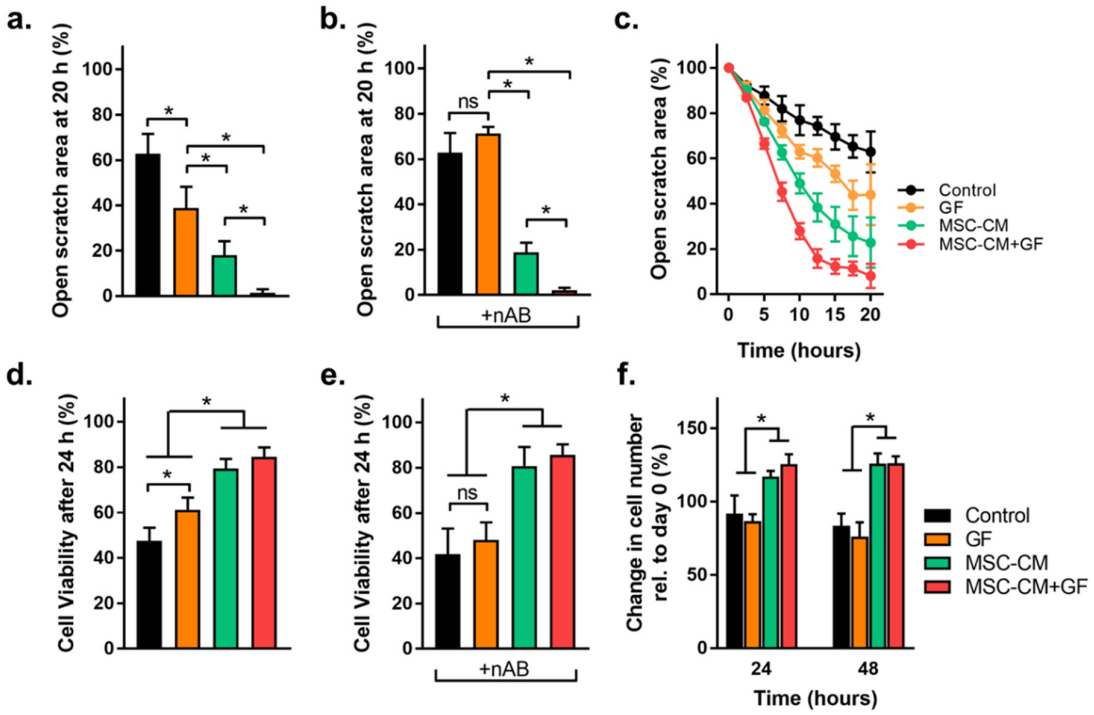

Fig. 20: Conditioned media from growth factor stimulated MSCs enhances myoblast function.

(a) C2C12 myoblasts migrated significantly faster in the presence of MSC-CM+GF. (b) This was not an additive effect of growth factors and MSC-CM in combination, as confirmed by neutralizing the recombinant human growth factors present in MSC-CM+GF. (c) Kinetics of scratch closure confirmed the fast migration rate of myoblasts in the presence of MSC-CM+GF. (d) MSC-CM+GF prevented myoblasts from undergoing apoptosis, and (e) this was further confirmed not to be due to the additive individual effects of GF and MSC-CM. (f) Myoblast proliferation remained high in the presence of MSC-CM+GF. [n=8, one-way ANOVA with Tukey's correction for multiple comparisons].

4.6. Substrate dependent paracrine response of MSCs to growth factor stimulation

Next, the experiments were conducted with MSCs cultured in 3D hydrogels and 3D scaffolds. Furthermore, it became important to determine whether hVEGF or hIGF are equally potent at stimulating MSC secretion individually or in combination. For these experiments, 2D films were excluded because their fragile nature and the possibility of damage to cells during handling renders them a suboptimal transplantation vehicle for *in vivo* studies. To limit the groups, TCP was also not studied further as a substrate.

To evaluate the paracrine response of 3D cultured MSCs after being stimulated with hVEGF and/or hIGF, a cytokine array was performed. Intensities were normalized to cell number and the heatmap in **Fig. 21** shows the fold change in the intensities after stimulation with growth factors relative to unstimulated CM. The results show that stimulation with growth factors provokes a stronger paracrine response from MSCs in 3D scaffolds compared to 3D hydrogels. Additionally, whereas stimulation with both hVEGF and hIGF caused an equally intense increase encapsulated MSC secretion, hIGF was found to be more potent than hVEGF at stimulating paracrine secretion in 3D scaffolds (**Fig. 21 a**).

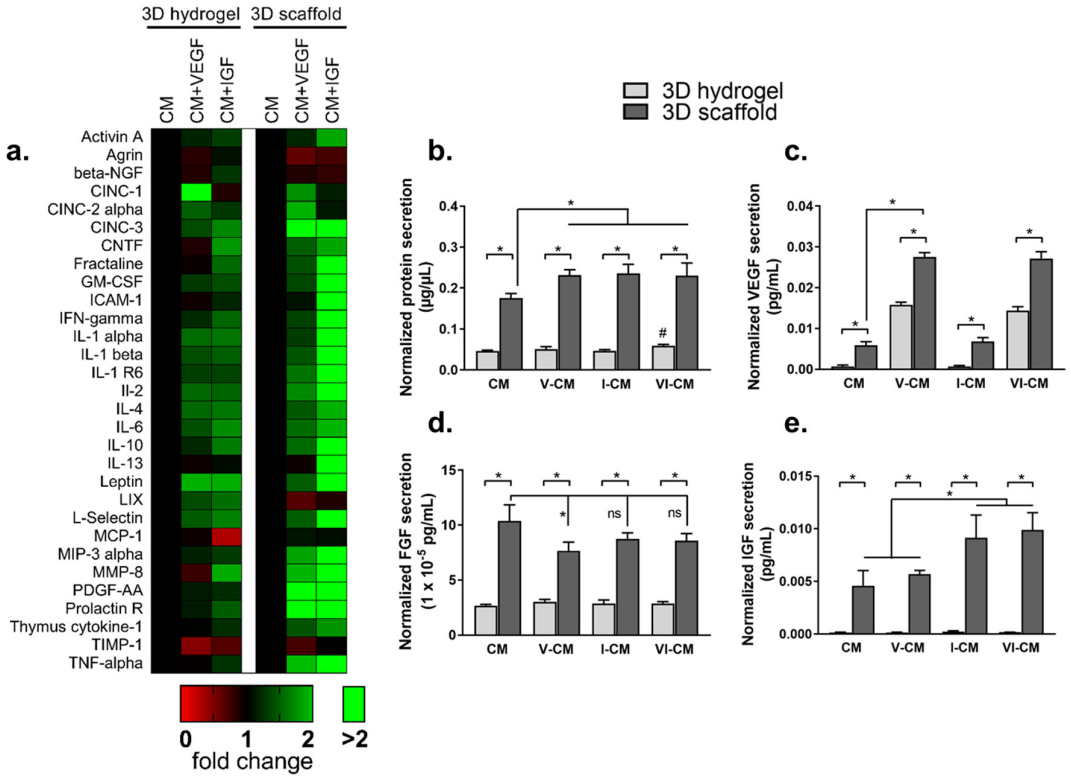

Fig. 21: Recombinant growth factors provoke paracrine response in 3D cultured MSCs.
Secretion of cytokines and growth factors in response to hVEGF and hIGF stimulation is strongly enhanced by MSCs in 3D scaffolds, but not as intensely by MSCs in 3D hydrogels. (a) A heatmap of 30 cytokines showing the fold change in the secretion of cytokines by MSCs in 3D hydrogels and 3D scaffolds with stimulation by growth factors [n=3 biological replicates pooled together]. (b) Normalized protein secretion from unstimulated and growth factor stimulated MSCs in 3D hydrogels and 3D scaffolds. Detection of muscle relevant growth factors (c) rVEGF, (d) rFGF, and (e) rIGF detected using rat specific ELISA kits. [b-e: n=4, differences between secretion in 3D hydrogel and 3D scaffold groups assessed with two tailed

student's t-test; differences between stimulated and non-stimulated values were assessed with one-way ANOVA with Tukey's correction for multiple comparisons].

For more specific measurements, the total protein content in the different CM groups was determined, and ELISAs were performed for the detection of rat specific rVEGF, rFGF, and rIGF (**Fig. 21 b-e**). In 3D scaffolds, stimulation by hVEGF and hIGF, alone or in combination, significantly enhanced the total protein content secreted by MSCs (**Fig. 21 b**). In a 3D hydrogel, enhancement was detected only after stimulation with both hVEGF and hIGF (VI-CM). Furthermore, for both unstimulated and stimulated MSCs, protein secretion was significantly higher from MSCs in a 3D scaffold compared to a 3D hydrogel. This was observed in the ELISAs for rVEGF, rFGF, and rIGF as well. ELISA for rVEGF indicated that stimulation with hVEGF enhances the secretion of rVEGF by the MSCs in both 3D hydrogels and 3D scaffolds (**Fig. 21 c**). ELISA for rFGF suggested that stimulation with either hVEGF or hIGF did not alter the secretion of rFGF from the MSCs in 3D hydrogels, whereas in 3D scaffolds rFGF secretion was reduced after stimulation with hVEGF (**Fig. 21 d**). ELISA for rIGF showed that stimulation with hIGF significantly enhanced the secretion of rIGF by the MSCs in 3D scaffolds. However, no such effect was seen for the 3D hydrogel groups (**Fig. 21 e**). In agreement with previous results, unstimulated MSCs secreted significantly higher amounts of IGF when cultured on 3D scaffolds compared to 3D hydrogels.

4.7. Paracrine effects of growth factor stimulated MSCs on myoblast function

Whether the modulation of MSC secretion pattern after GF stimulation affects functional outcomes in myoblasts was determined by carrying out previously established functional assays.

4.7.1. Collective cell migration

At first, a scratch assay was used to evaluate the kinetics of collective cell migration and scratch area coverage in response to the different CM groups (Fig. 22). Migration was significantly faster than control in the presence of unstimulated and stimulated 3D hydrogel-CM. However, stimulation of 3D encapsulated MSCs with hVEGF, hIGF, or their combination did not

significantly impact migration compared to unstimulated CM (Fig. 22 a, b). In stark contrast, stimulation in 3D scaffolds with hIGF (I-CM) and with the combination of hIGF+hVEGF (VI-CM) resulted in paracrine factors that stimulated significantly faster migration and greater scratch area repopulation (Fig. 22 c, d) compared to the other groups. V-CM was only as effective as unstimulated CM. These results provided the first indication that hIGF stimulated MSCs may exert more potent functional effects on myoblasts. The overall lower secretion of proteins and growth factors observed in Fig. 21 in the 3D hydrogel substrate corresponded to the slower /lesser migration results seen here.

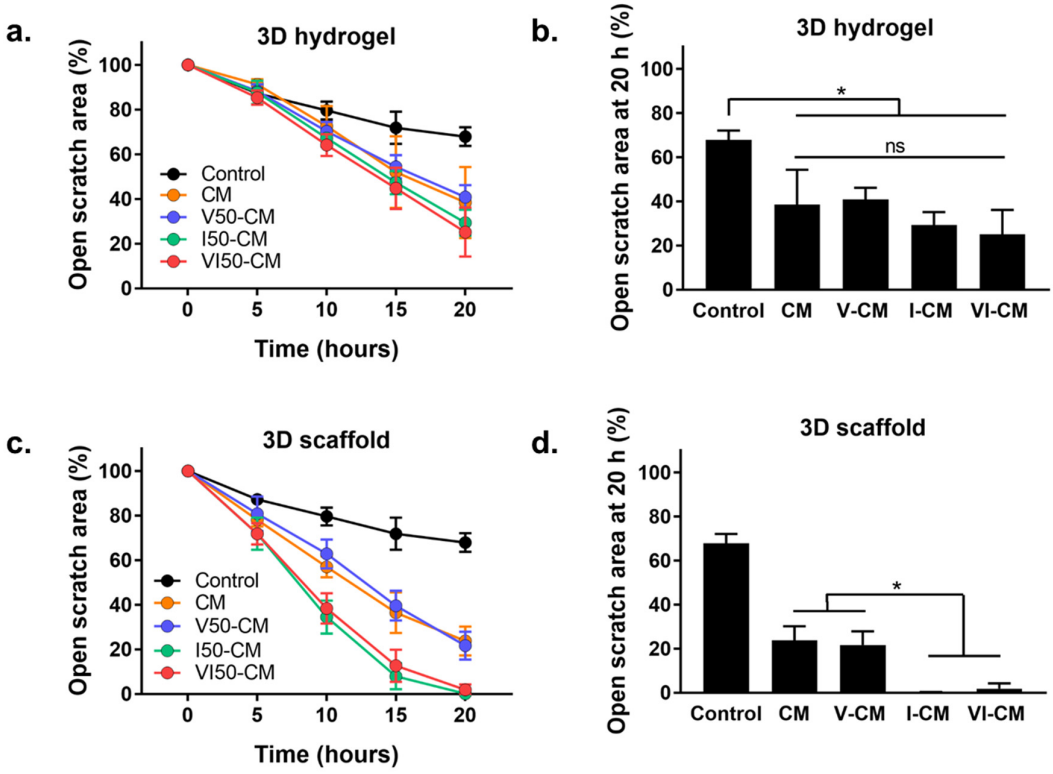

Fig. 22: Collective myoblast migration modulated by paracrine effects of 3D cultured MSCs after GF stimulation.

(a, b) In 3D hydrogels, MSC secretion in response to growth factor stimulation did not significantly influence myoblast migration in a scratch assay. (c, d) In 3D scaffolds, MSC secretion in response to hIGF stimulation significantly enhanced myoblast migration [n=4, one way ANOVA with Tukey's correction for multiple comparisons].

4.7.2. Migratory behavior of single cells

Next, single cell tracking was used to analyze if total distance migrated, migration velocity, displacement, and directionality of myoblasts is affected in the presence of different CM groups (**Fig. 23**). When supplemented in serum free media, hVEGF and hIGF caused significantly increased net displacement and enhanced directionality of myoblasts compared to control (**Fig. 23 Controls c, d**).

In 3D hydrogels, GF stimulation did not alter total migrated distance or migration velocity (**Fig. 23 3D hydrogel a, b**), and only VI-CM stimulated higher net displacement and directionality (**Fig. 23 3D hydrogel c, d**). In a 3D scaffold substrate, stimulation with growth factors resulted in much more pronounced differences in all aspects of myoblast migration (**Fig. 23 3D scaffold a-d**). In the presence of hIGF and the combination of hIGF+hVEGF stimulated CM, myoblasts displayed significantly enhanced total migrated distance, migration velocity, and net displacement, compared to unstimulated CM and V-CM. The net displacement of myoblasts in the presence of 3D scaffold I-CM was significantly higher than VI-CM, indicating that hIGF alone can induce a potent paracrine response from MSCs in 3D scaffolds (**Fig. 23 3D scaffold c**). The directionality of myoblasts was also significantly improved in the presence of I-CM compared to unstimulated CM and V-CM (**Fig. 23 3D scaffold d**).

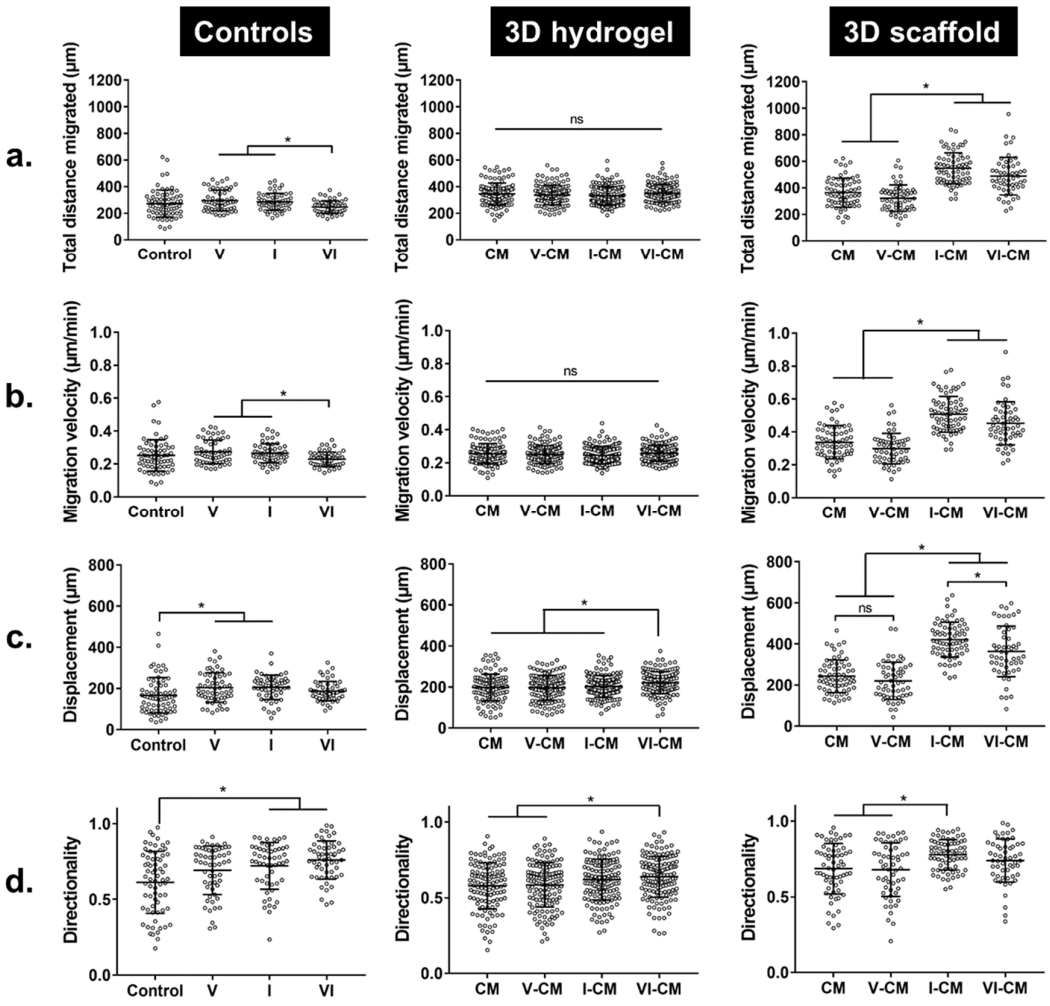

Fig. 23: Myoblast migratory behavior in response to GF stimulated MSC-CM from 3D hydrogels and 3D scaffolds.

Single cell tracking of myoblasts to evaluate (a) total distance migrated, (b) migration velocity, (c) net displacement, and (d) directionality, in response to growth factors alone, or CM from unstimulated and stimulated MSCs in 3D hydrogels and 3D scaffolds. Strong functional modulation was observed when CM from hIGF stimulated MSCs in 3D scaffolds was used, whereas the effect of GF stimulation of MSCs in 3D hydrogels was much less pronounced. [n=54-70, Kruskal-Wallis test with Dunn's correction for multiple comparisons].

4.7.3. Proliferation

Proliferation assays were performed using CyQUANT® to evaluate the effects of CM from 3D cultured, unstimulated and stimulated MSCs on cell growth. Supplementation of hVEGF and hIGF, alone or in combination, in control media did not influence the proliferation of C2C12 myoblasts over two days (**Fig. 24 a**). Of the CM generated from MSCs in 3D hydrogels, hIGF and hIGF+hVEGF stimulated groups significantly improved proliferation compared to unstimulated CM after 24 hours. However, after 48 hours, this improvement diminished, and significance was reached only between VI-CM and V-CM (**Fig. 24 b**). Of the CM generated from MSCs in 3D scaffolds, I-CM and VI-CM significantly increased cell numbers compared to unstimulated CM and V-CM at both time points tested

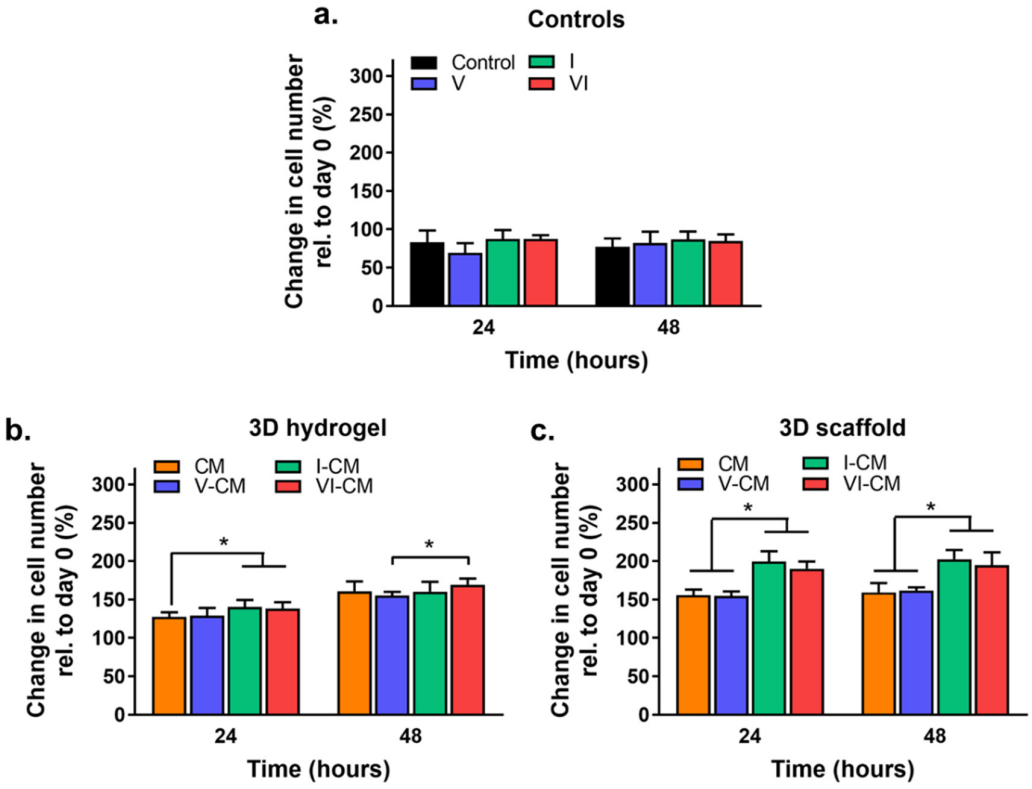

Fig. 24: Myoblast proliferation in response to 3D cultured, GF stimulated MSC-CM.

(a) Direct addition of hVEGF, hIGF, or their combination to myoblasts did not influence proliferation over two days. MSC-CM strongly affected myoblast proliferation, but the effect depended on the substrate MSCs were cultured in [n=12, one-way ANOVA with Tukey's correction for multiple comparisons].

4.7.4. Myogenic differentiation

The potential of CM from different groups to stimulate or inhibit the myogenic differentiation and in vitro myotube formation of myoblasts was investigated by calculating the myoblast fusion index. Representative fluorescent images show fused myoblasts stained with MHC (green) and DAPI (blue) in the different groups (Fig. 25 a, c, e). Multiple images were used to quantify myoblast fusion index (Fig. 25 b, d, e).

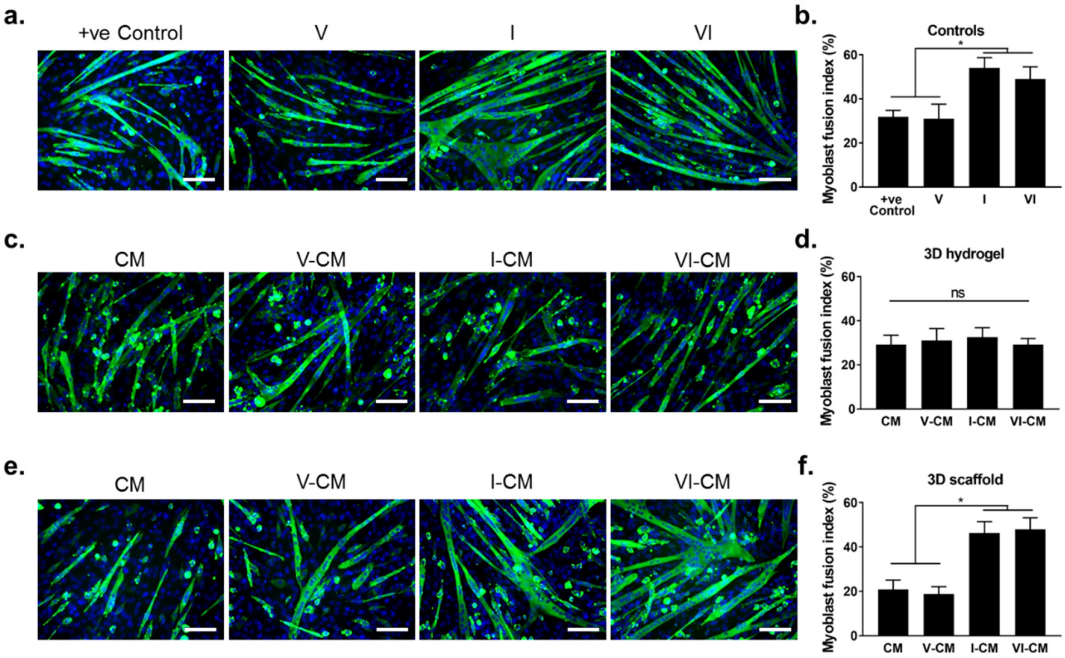

Fig. 25: Modulation of myogenic differentiation by CM from 3D cultured, GF stimulated MSCs.

Representative fluorescent images of myoblasts stained for differentiation marker MHC and DAPI after culture in (a) control media with and without GF supplementation, (c) CM from unstimulated and stimulated MSCs in 3D hydrogels, and (d) CM from unstimulated and stimulated MSCs in 3D scaffolds [Scale bar = 100 µm]. (b, d, f) corresponding quantification of myoblast fusion index from several regions of interest [n=6, one way ANOVA with Tukey's correction for multiple comparisons].

IGF is a known myogenic factor that is potent at promoting myogenic differentiation. In line with this, a significantly higher fusion index was observed for groups where positive control media was supplemented with hIGF and hIGF+hVEGF (~50-55%) compared to positive

control media alone or supplemented with hVEGF (~30-32%) (**Fig. 25 b**). hVEGF alone was unable to induce enhanced myotube formation relative to control.

In order to prevent the recombinant growth factors present in stimulated MSC-CM from interfering with the differentiation assays, neutralization antibodies specific for recombinant hVEGF and hIGF were added to the GF stimulated MSC-CM groups for 3 hours prior to application. When myoblasts were induced to differentiate in CM from unstimulated and stimulated MSCs from a 3D hydrogel substrate, no significant changes in fusion index were observed between the groups (**Fig. 25 c, d**). The low fusion index in I-CM and VI-CM confirmed that the recombinant growth factors, especially hIGF, had been successfully neutralized and did not influence myotube formation.

Strikingly, in the 3D scaffold groups, I-CM and VI-CM significantly enhanced myotube formation and corresponding fusion index (~45%) compared to unstimulated CM and V-CM (~20%) (**Fig. 25 e, f**). Again, V-CM did not significantly alter the fusion index compared to unstimulated CM.

4.7.5. Survival

A cell survival assay was carried out to determine if CM from MSCs stimulated in 3D scaffolds rendered any improved anti-apoptotic benefit on myoblasts compared to its counterparts in 3D hydrogels (**Fig. 26**). The addition of CM from all groups significantly enhanced cell survival compared to control media, but no significant differences were observed between any of the CM groups.

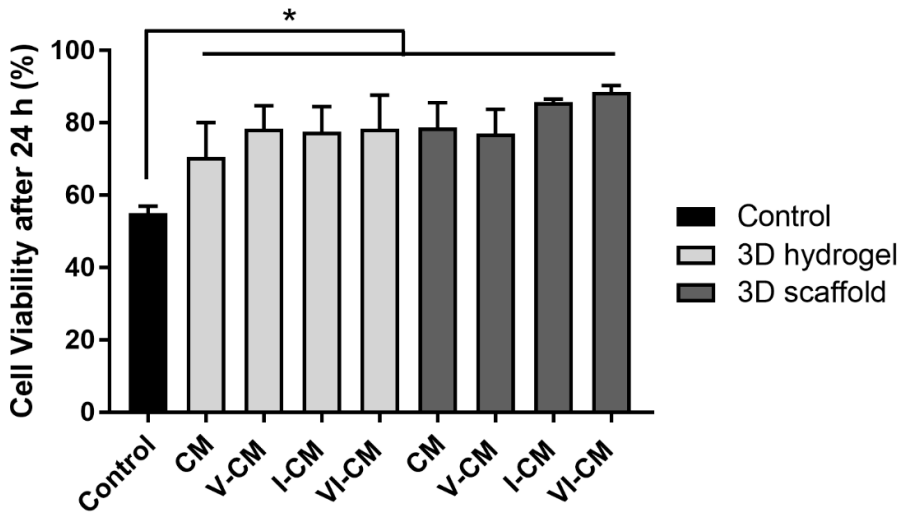

Fig. 26: Cell survival in response to 3D cultured, GF stimulated MSC-CM.
All CM groups enhanced the survival of myoblasts in serum free conditions relative to control. [n=3, one-way ANOVA with Tukey's correction for multiple comparisons].

4.8. A role for N-cadherin in substrate dependent influence of GF stimulation on MSC paracrine effects

Based on the analysis of MSC paracrine secretion after stimulation with growth factors, and its functional effects on myoblasts, it became evident that MSCs encapsulated in 3D hydrogels do not respond to GF stimulation as strongly as MSCs seeded on 3D porous scaffolds. To determine if cell-cell contacts mediated by N-cadherin play a role in the observed phenomenon, conditioned media was collected from N-cadherin blocked MSCs that were stimulated with growth factors in 3D scaffold substrates. The conditioned media was used to assess myoblast functions. Experiments were not performed with MSCs in 3D hydrogel substrates.

The scratch area remaining unpopulated at the end of a migration experiment is depicted in **Fig. 27**. As shown previously, N-cadherin blocking in MSCs reduces the migratory effects that the paracrine factors exert on myoblasts. Interestingly, it was also found that the migratory effects of paracrine factors secreted by GF stimulated MSCs are also mitigated by N-cadherin blocking. MSCs which were not treated with an N-cadherin blocking antibody exerted enhanced paracrine

effects on collective myoblast migration, especially after stimulation with hIGF (I-CM) and hVEGF+hIGF (VI-CM), as also shown previously. However, when N-cadherin blocked MSCs were stimulated with the same dosage of hIGF, hVEGF, and their combination, a significantly higher scratch area remained empty, indicating less migration of myoblasts (striped bars in **Fig. 27**).

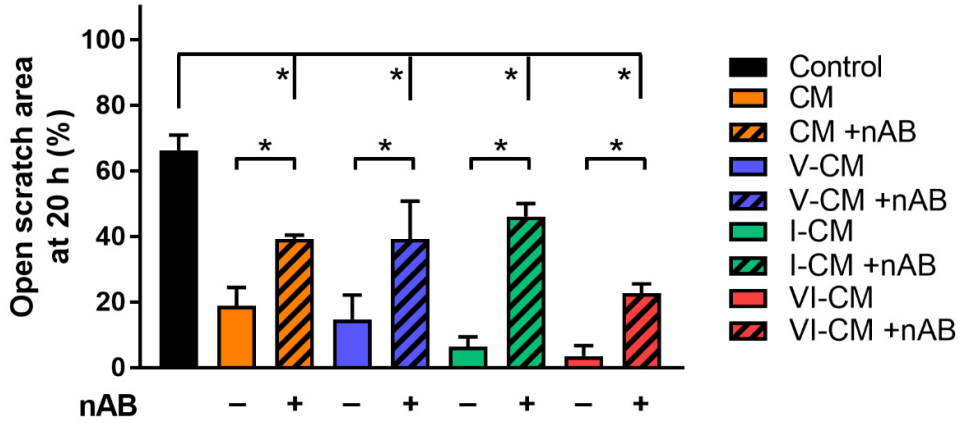

Fig. 27: Collective myoblast migration affected by N-cadherin blocking in GF stimulated MSCs.

The graph shows unpopulated scratch area at the end of the migration experiment. The beneficial effects of CM from GF stimulated MSCs were reduced when MSCs were treated with N-cadherin blocking antibody. [n=3, two-tailed student's t-test. One-way ANOVA with Tukey's correction for multiple comparisons].

Single cell tracking of myoblasts revealed that the total distance migrated, net displacement, and migration velocity of myoblasts were also significantly reduced in the presence of CM from N-cadherin blocked MSCs, despite stimulation with growth factors. The directionality of myoblasts was reduced significantly only in I-CM+nAB (**Fig. 28 d**).

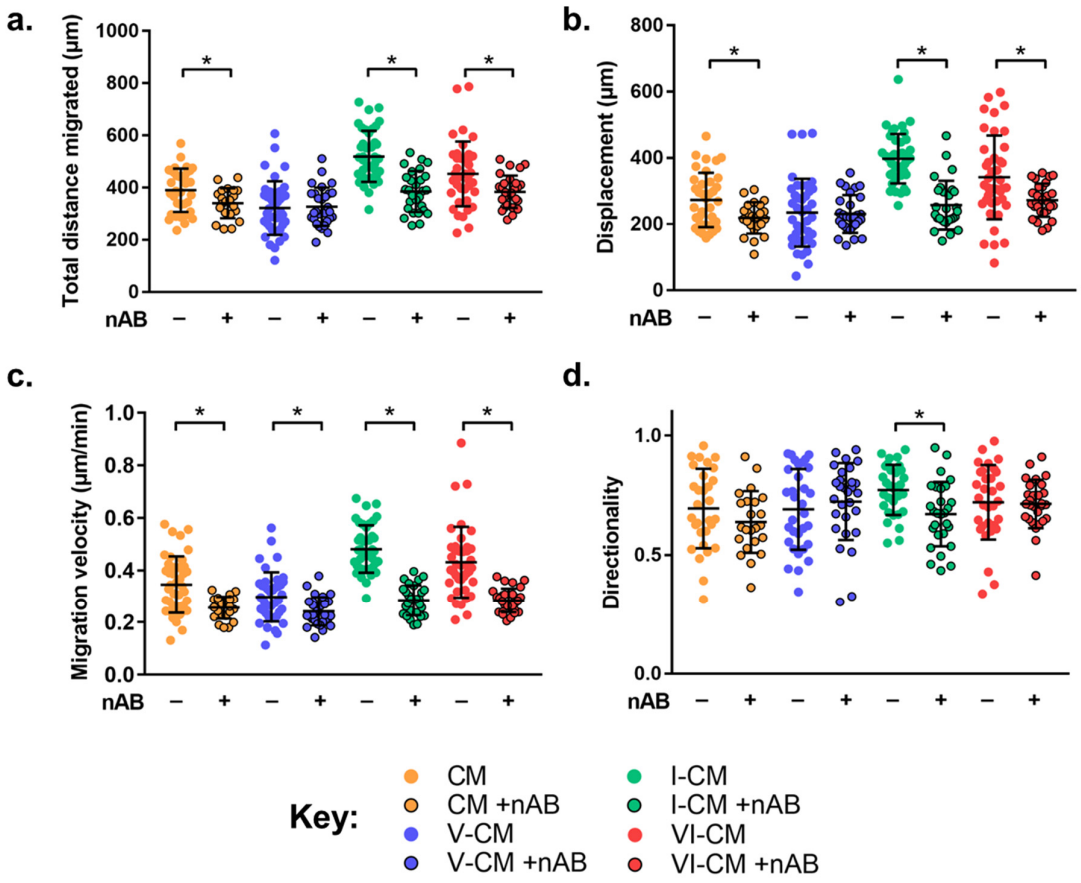

Fig. 28: Single cell migratory behavior after N-cadherin blocking in GF stimulated MSCs. *Single cell tracking of myoblasts to assess (a) total distance migrated, (b) net displacement, (c) migration velocity, and (d) directionality in the presence of CM from MSCs cultured in 3D scaffolds with or without treatment with N-cadherin blocking antibody. [n=23-40, Mann-Whitney U test].*

To determine if the modulation of myogenic differentiation observed with I-CM and VI-CM from MSCs in 3D scaffolds is affected by N-cadherin blocking, myoblasts were induced to differentiate in the presence of different CM groups (+ and – nAB MSCs) and myoblast fusion index was calculated (**Fig. 29**). Surprisingly, no differences in fusion index was observed between the unstimulated and GF stimulated MSC-CM when the MSCs were treated with an N-cadherin blocking antibody (**Fig. 29 b**). Moreover, a significant drop in the fusion index was witnessed in the I-CM and VI-CM groups after N-cadherin blocking.

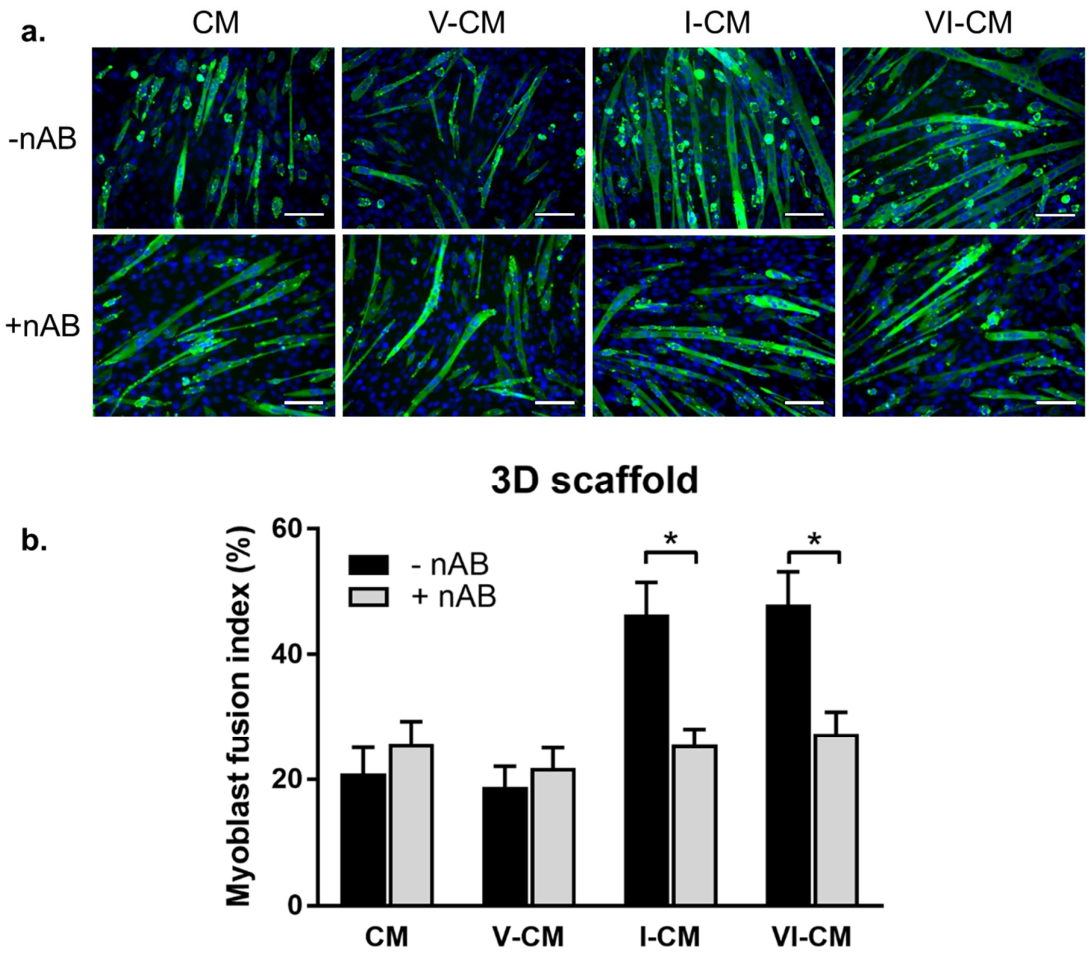

Fig. 29: Modulation of myogenic differentiation by N-cadherin blocking of MSCs.
In vitro myogenic differentiation of C2C12 myoblasts is affected by blocking N-cadherin in MSCs prior to CM collection. (a) Representative images of fused myoblasts expressing the differentiation marker myosin heavy chain (MHC) [Scale bar = 100 µm]. (b) Quantification of fusion index shows loss in the ability of CM to modulate myogenic differentiation after N-cadherin blocking [n=6, two-tailed student's t-test].

Lastly, a cell survival assay carried out using CM from unstimulated and stimulated MSCs with and without N-cadherin blocking revealed that cell survival was not negatively affected by N-cadherin blocking of MSCs in the unstimulated, hVEGF stimulated, and hIGF stimulated groups, but was significantly reduced by N-cadherin blocking in the hVEGF+hIGF stimulated condition (**Fig. 30**).

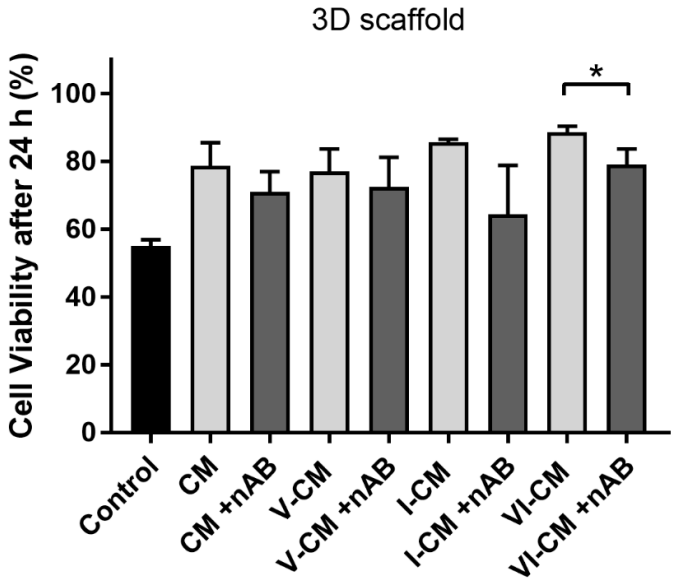

Fig. 30: Anti-apoptotic property of MSCs after N-cadherin blocking.
In vitro myoblast cell survival in the presence of CM from GF stimulated MSCs in 3D scaffolds with and without N-cadherin blocking. [n=3, two-tailed student's t-test].

4.9. In vivo strategy for muscle regeneration

Based on the results of all the *in vitro* studies, the following conclusions could be drawn:

- MSCs show a strong potential to stimulate skeletal muscle regeneration via their paracrine effects on muscle progenitor cells.
- The biomaterial microenvironment that MSCs are transplanted in can potentially impact the outcome of a regeneration strategy.
- A 3D porous scaffold creates an environment for MSCs that facilitates enhanced paracrine factor secretion by permitting cell-cell contacts, whereas a 3D injectable hydrogel inhibits these effects.
- Growth factors, particularly hIGF, stimulates MSCs leading to heightened paracrine factor secretion, and the secreted factors have intense effects on myoblast functions.
- These functions include proliferation, migration, differentiation, and cell survival – all of which are desirable during muscle regeneration.

In light of these results, an *in vivo* study was carried out to evaluate the translational efficacy of the *in vitro* findings, and to test if the transplantation of MSCs in a 3D scaffold that provides a sustained local release of growth factors would stimulate muscle regeneration in a clinically relevant injury model (**Fig. 31**).

Four study groups were planned:

(1) An empty scaffold served as a control (**Fig. 31 a**).
(2) A scaffold that delivers hIGF and hVEGF (**Fig. 31 b**).
(3) A scaffold that delivers MSCs (**Fig. 31 c**).
(4) A scaffold that delivers both MSCs and growth factors (**Fig. 31 d**).

It was our intention to not place the scaffolds intramuscularly, although that has been explored by others as a tissue engineering strategy. Instead, the scaffolds were placed next to the injured muscle tissue to investigate MSC paracrine effects on regeneration, without their engraftment onto the tissue.

Although no beneficial effects of individual GF supplementation were observed *in vitro*, these potent pro-angiogenic ($hVEGF_{165}$) and pro-myogenic (hIGF-1) factors have been shown to induce muscle regeneration in an ischemic injury model. It was therefore considered pertinent to test its efficacy in a crush trauma injury model. Moreover, group (2) acted as a control for group (4).

In line with guidelines from the animal ethics committee, all groups were tested for 7 and 28 day time points. However, for the 56 day evaluation only those groups that showed significant effects at day 28 were allowed to be continued with along with the control group. The GF group (2) was therefore excluded from the 56 day evaluation time point.

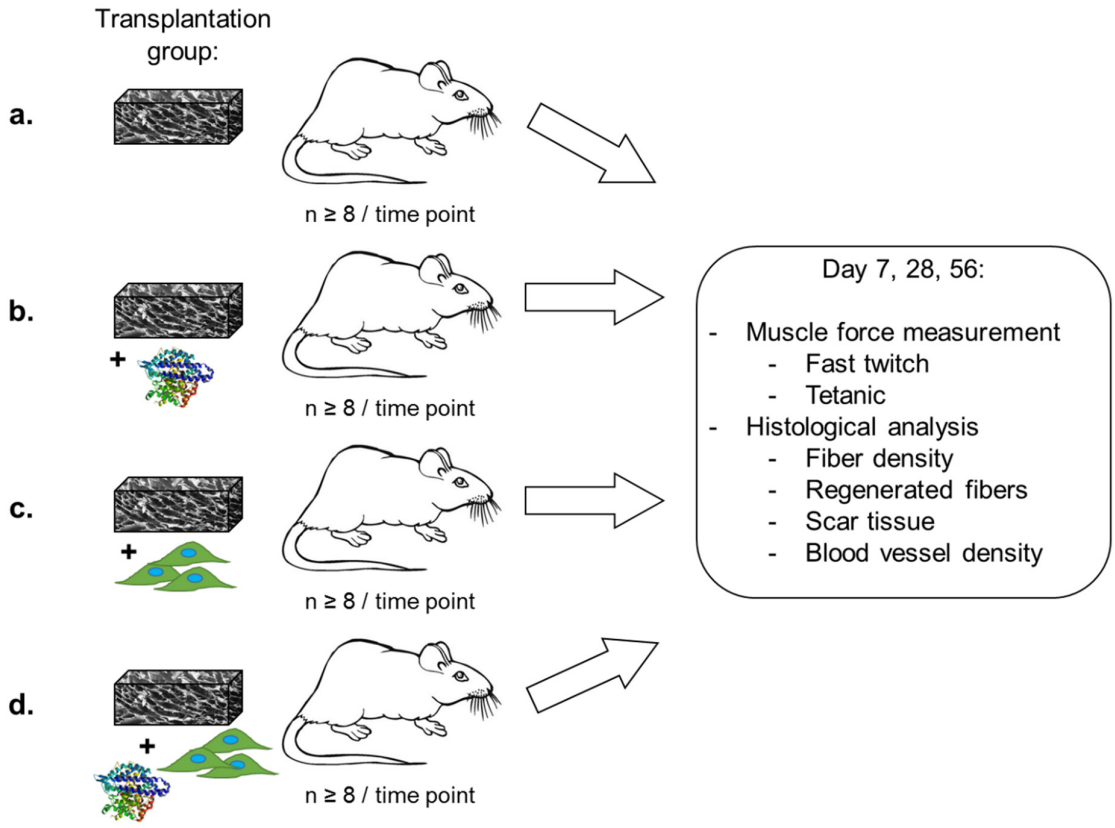

Fig. 31: In vivo study design.

Sprague Dawley rats were randomly allocated to one of four different groups: (a) empty scaffold, (b) scaffold + growth factors, (c) scaffold + MSCs, and (d) scaffold + MSCs + growth factors. At three different time points, functional assessment was carried out by measuring fast twitch and tetanic contractile forces. The muscles were then harvested for histological analysis.

4.9.1. Characteristics of employed scaffolds

The general characteristics of the scaffold used *in vivo* are represented in **Fig. 32**. The scaffold showed a highly porous structure with interconnected porosity and pore size in the range of 100-200 µm (**Fig. 32 a**). MSCs seeded onto the scaffold infiltrated throughout the porous structure (**Fig. 32 b**). The growth factors hIGF and hVEGF were incorporated into the walls of the scaffold during fabrication, and release kinetics (**Fig. 32 c**) showed that after a typical burst release in the first few days, hIGF was released in a sustained manner over 28 days whereas most of the hVEGF was released from the scaffold within one week. To assess whether the porous nature of the scaffold promoted outward migration of the MSCs, an *in vitro* outward cell migration assay was used. The results showed that in GF loaded scaffolds ~3% of the total

seeded cells migrated out of the scaffold over seven days, whereas ~5% of the total seeded cells migrated out of the blank scaffolds (**Fig. 32 d**).

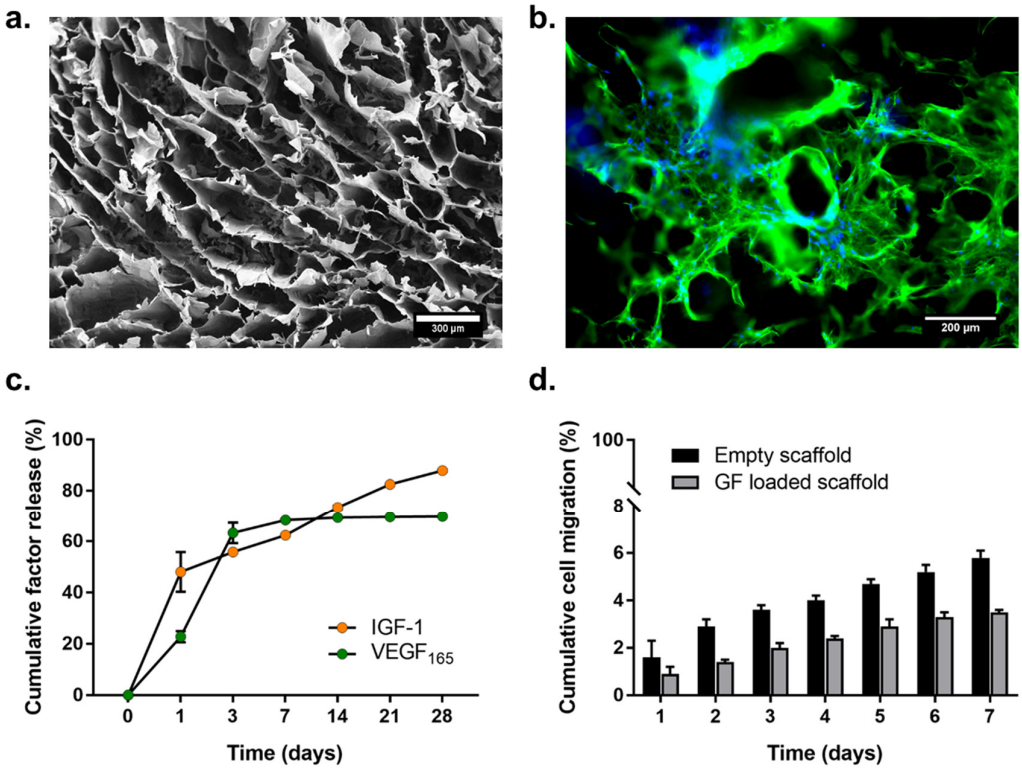

Fig. 32: Characterization of scaffolds used for in vivo studies.
(a) SEM image showing the interconnected porosity of alginate scaffolds [Scale bar = 300 µm]. (b) MSCs stained with phalloidin (actin filaments) and DAPI (nuclei) were able to infiltrate the scaffold and establish cell-cell contacts [Scale bar = 200 µm]. (c) The scaffold provided a sustained release of recombinant growth factors hVEGF and hIGF over a period of 28 days. (d) Migration of MSCs out of the scaffold over a period of 7 days was low compared to the total number of cells seeded.

4.9.2. Functional assessment

To assess whether the transplantation of scaffold with GFs, MSCs, or their combination exerted any functional benefits on the injured muscle tissue, fast twitch and tetanic contractile forces were measured using a custom made set up. This set up uses an electrode to electrically stimulate the sciatic nerve which causes the soleus muscle to twitch. The twitching forces are recorded by a force transducer that is physically connected to the Achilles tendon at the end of the soleus muscle. Contractile forces were recorded from the injured muscle (left limb) as well

as the uninjured muscle in the contralateral limb. The measured forces from the injured muscle were normalized to those of the uninjured muscle for each animal as an internal control.

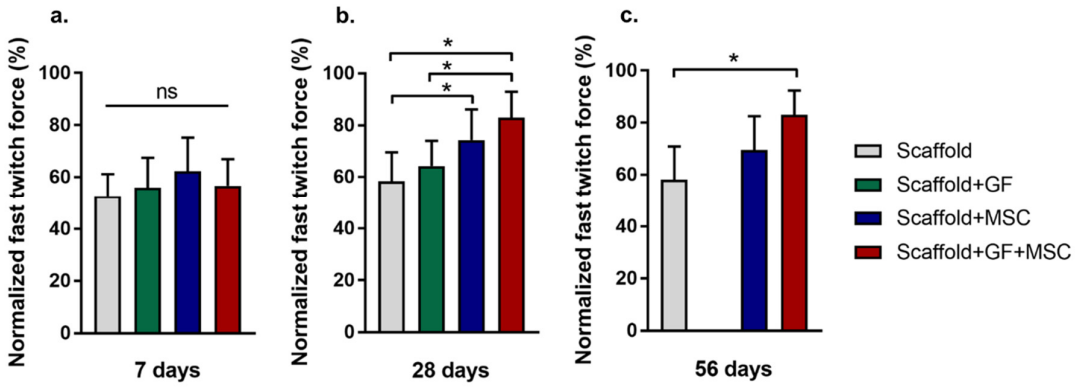

Fig. 33: Quantification of fast twitch forces.

Functional assessment of muscle regeneration by measuring fast twitch forces (a) 7, (b) 28, and (c) 56 days after injury and transplantation of different scaffolds. [n=8, one-way ANOVA with Bonferroni's correction for multiple comparisons].

The normalized fast twitch forces after treatment with different groups over three time points are showed in **Fig. 33**. A value of 100 would indicate that the injured muscle has regained as much functional strength as the uninjured muscle. Early time point assessment (7 days) showed that the severity of the injury caused an almost 40-50 % loss of fast twitch force. Because earlier time points (e.g. few hours after injury) were not assessed, the full effect of the injury may be more severe. After 28 days, differences between the treatment groups became more apparent. It became clear that the delivery of hIGF and hVEGF alone did not cause an improvement in fast twitch forces. However, the transplantation of MSCs registered a significant improvement over the control (empty scaffold) group, whereas the transplantation of MSCs and growth factors together resulted in a significant improvement relative to the control group as well as the GF group. In the long term (56 days), the contractile forces in the GF+MSC group remained significant over the control group, but significance could not be reached with respect to the MSC group.

Over time, the normalized fast twitch forces in the control group increased from ~50% at day 7 to ~57% at day 56. In the MSC group, forces increased from ~60% at day 7 to ~72% at day 28 and decreased slightly to ~70% at day 56. In comparison, forces in the GF+MSC group increased from ~55% from day 7 to ~80% at day 28 and this was maintained at day 56.

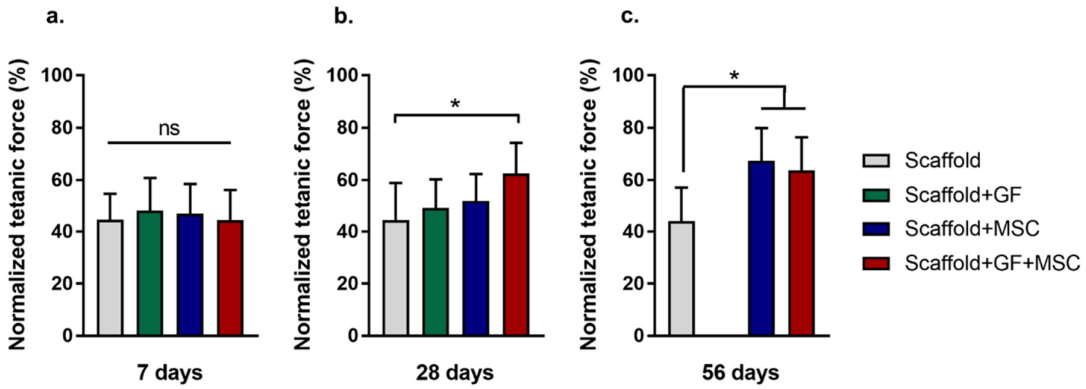

Fig. 34: Quantification of tetanic forces.

Functional assessment of muscle regeneration by measuring tetanic forces (a) 7, (b) 28, and (c) 56 days after injury and transplantation of different scaffolds. [n=8, one-way ANOVA with Bonferroni's correction for multiple comparisons].

Next to fast twitch forces, the tetanic forces were also measured and normalized to the contralateral limb (**Fig. 34**). Once again, early time point assessment showed that the injury caused a 50-60 % loss of functional strength. After 28 days, only the GF+MSC group showed a significant improvement over the control group, whereas in the long term the transplantation of both MSCs and GF+MSC showed a significant benefit over the control group.

It is pertinent to note that in the control group (empty scaffold), no changes in the fast twitch and tetanic contractile forces were observed over the time points tested. In comparison, the transplantation of MSCs showed a gradual improvement in tetanic forces from 7 to 56 days (~42% to ~65%). The forces in the GF+MSC group improved from ~40% on day 7 to ~60% on day 28, and was maintained until day 56.

4.9.3. Histological assessment

To analyze how the transplantation of GF and MSCs, alone or in combination, affected the repair and regeneration of structural elements of the injured skeletal muscle, tissues were harvested from the animals and processed for histological examination. Muscle cross sections were taken from three different regions along the length of the muscle tissue.

Several structural aspects can give an indication about regeneration in muscle tissues. For a thorough analysis of structural regeneration, muscle sections were stained with hematoxylin and eosin (to identify myofibers' cytoplasm and nuclei), picro sirius red (to stain collagenous scar tissue), and CD31 (to identify blood vessels).

4.9.3.1. Muscle fiber density

The density of myofibers in muscle cross-sections can provide vital information on remodeling of the muscle tissue and how it progresses after injury. An increase in the myofiber density may indicate the formation of new myofibers that could contribute to the functional performance of the tissue. Similarly, a decrease in the density of myofibers may suggest insufficient regeneration and may translate to lower functional performance.

Muscle cross-sections that were stained with hematoxylin and eosin were imaged and the total number of myofibers in each section was manually counted. The total number of fibers was then normalized to the section area and represented as myofiber density (**Fig. 35**). The results show that in the control group (empty scaffold), there was a gradual decrease in the myofiber density over time from ~260 myofibers/mm^2 at day 7 to ~190 myofibers/mm^2 at day 56. Delivery of growth factors alone did not improve myofiber density until 28 days, rather a reduction from ~260 myofibers/mm^2 to 200 myofibers/mm^2 was observed. After 28 days, a significantly higher myofiber density was detected in the MSC group and the GF+MSC group compared to the control. In the long term (56 days), significantly higher myofiber density was recorded for the GF+MSC group (~280 myofibers/mm^2) compared to the MSC group (~220 myofibers/mm^2) as well as the control group (~190 myofibers/mm^2).

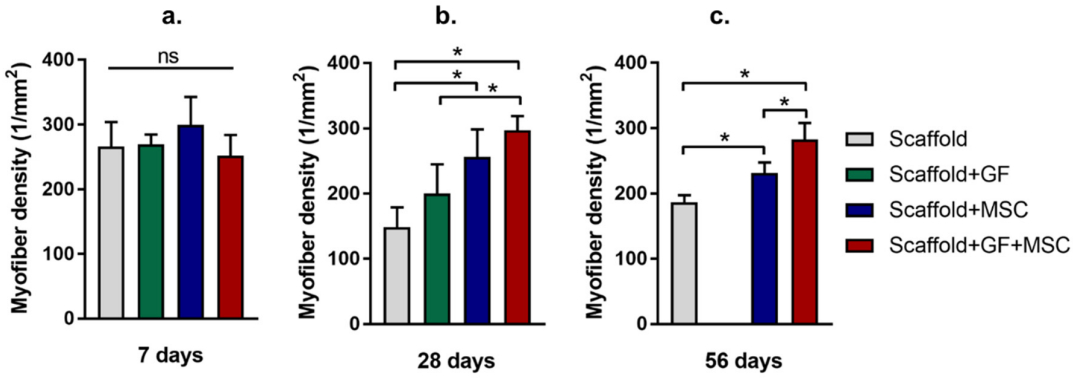

Fig. 35: Quantification of myofiber density.

Structural assessment of muscle regeneration by quantifying myofiber density in histological cross-sections (a) 7, (b) 28, and (c) 56 days after injury and transplantation of different scaffolds. [n=8, one-way ANOVA with Bonferroni's correction for multiple comparisons].

4.9.3.2. Myofiber regeneration

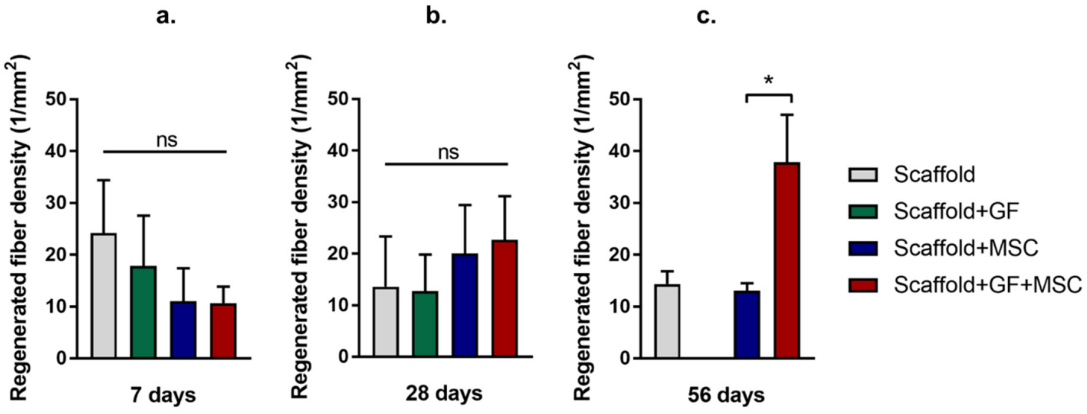

Fig. 36: Quantification of regenerated myofibers.

Structural assessment of muscle regeneration by quantifying regenerated myofiber density in histological cross-sections (a) 7, (b) 28, and (c) 56 days after injury and transplantation of different scaffolds. Myofibers that had centrally located nuclei were considered as regenerated myofibers. [n=8, one-way ANOVA with Bonferroni's correction for multiple comparisons].

The density of regenerated myofibers was determined by manually counting the number of fibers exhibiting a centrally located nuclei in the muscle cross sections, and normalizing it to

section area (**Fig. 36**). Although no significant differences in regenerated fiber density were observed between the groups at 7 and 28 day time points, the GF+MSC group showed a significantly higher number of regenerated myofibers compared to the control and MSC groups at day 56.

4.9.3.3. Angiogenic response

Injury to the skeletal muscle results in the rupture of blood vessels that are essential for the supply of nutrients to contractile myofibers. Therefore, revascularization of the injured tissue must precede successful muscle regeneration. The density of blood vessels in muscle cross sections was assessed by counting the number of CD31+ vessels in several regions of interest (ROI) within each cross-section and normalizing it to the area of the ROI.

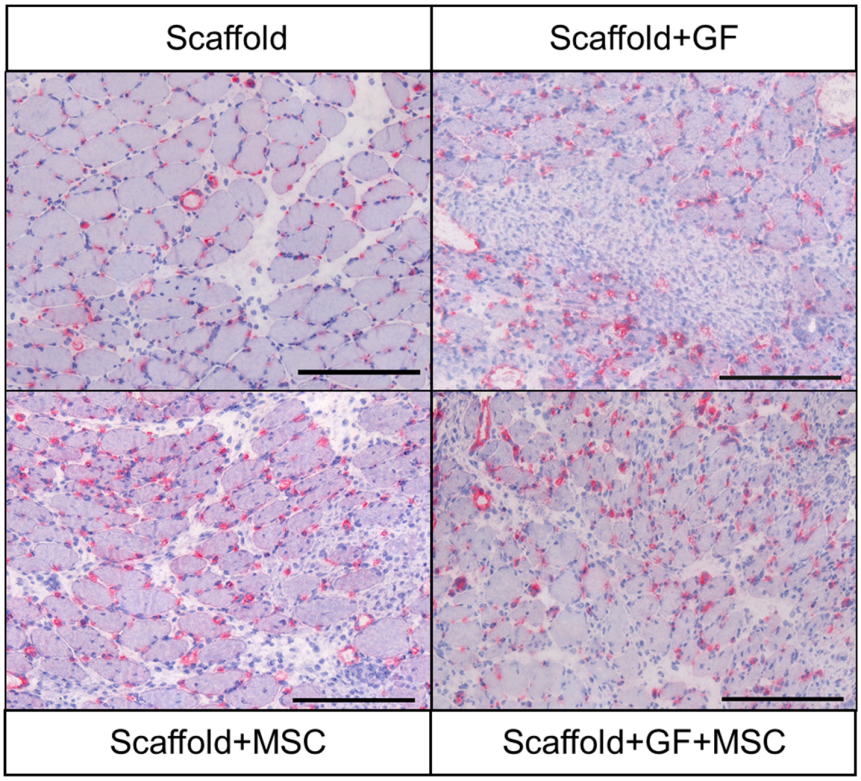

Fig. 37: Early angiogenic response in injured muscles.

Representative histological muscle cross-sections stained with CD31 to identify blood capillaries (red) at the earliest time point (7 days) in response to indicated treatment groups. [Scale bar = 200 µm]

Fig. 37 shows 7 day representative images of muscle cross sections treated with different groups and stained with CD31 (blood vessels in dark red) and counter stained with hematoxylin. Quantitative analysis revealed that a strong early angiogenic response was stimulated by the delivery of GF, MSCs, and their combination (**Fig. 38**). At day 7, the blood vessel density in muscles treated with GF+MSCs (~620 vessels/mm^2) was significantly higher than those in the MSC group (~480 vessels/mm^2). At all time points tested, the control group had a significantly lower blood vessel density compared to all other groups. Despite remaining significantly higher than the control group, the CD31+ vessel density decreased gradually in all groups over time.

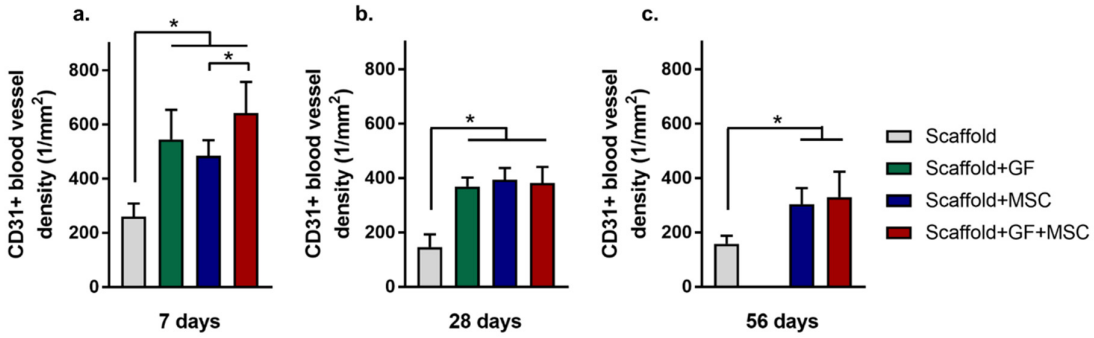

Fig. 38: Quantification of angiogenesis.

Quantitative evaluation of tissue vascularization (a) 7, (b) 28, and (c) 56 days after injury and transplantation of different scaffolds. Random regions of interest from the muscle cross-section were selected based on an ImageJ macro, and positively stained (red) vessels were manually counted. The control group showed significantly lower vessel density than all other groups at all time points tested. [n=8, one-way ANOVA with Bonferroni's correction for multiple comparisons].

4.9.3.4. Scar tissue

Scar tissue is collagenous extracellular matrix (ECM) deposited by fibroblasts after acute injury. In muscle, it does not contribute to the functional performance of the tissue. If left untreated, scar tissue can establish a permanent presence in the muscle tissue, potentially inhibiting the formation of new myofibers or the fusion of existing ones, and can lead to a decline in muscle function.

Fig. 39 shows representative whole muscle cross-sections that were stained with Picro Sirius red to identify scar tissue (dark red). At the earliest time point (7 days), large areas of scar tissue

were detected in all groups. In the control, GF, and MSC groups (**Fig. 39 a-c**) dark red scar tissue areas can be seen distributed within the muscle cross-section at all time points. However, in muscles treated with the combination of GF+MSC, there is a notable reduction in the scar tissue content between days 28 and 56 (**Fig. 39 d**).

The percentage of muscle cross-sectional area that is covered by scar tissue was analyzed using an ImageJ macro. Due to the presence of collagen in the native skeletal muscle ECM, the interstitial matrix between the myofibers also stained positive for Picro Sirius red. Therefore, the mean collagen content detected in uninjured muscle cross-sections (n=33 animals) was subtracted from the scar tissue area detected in injured muscle cross-sections. Quantitative results are shown in **Fig. 40**. At the earliest time point evaluated, there was already significantly less scar tissue in the GF+MSC group (~14%) compared to the GF only group (~23%). At the latest time point tested, expectedly, the control group had the highest scar tissue area (~25%). However, the scar tissue in the GF+MSC group was significantly lower compared to both the control and the MSC groups.

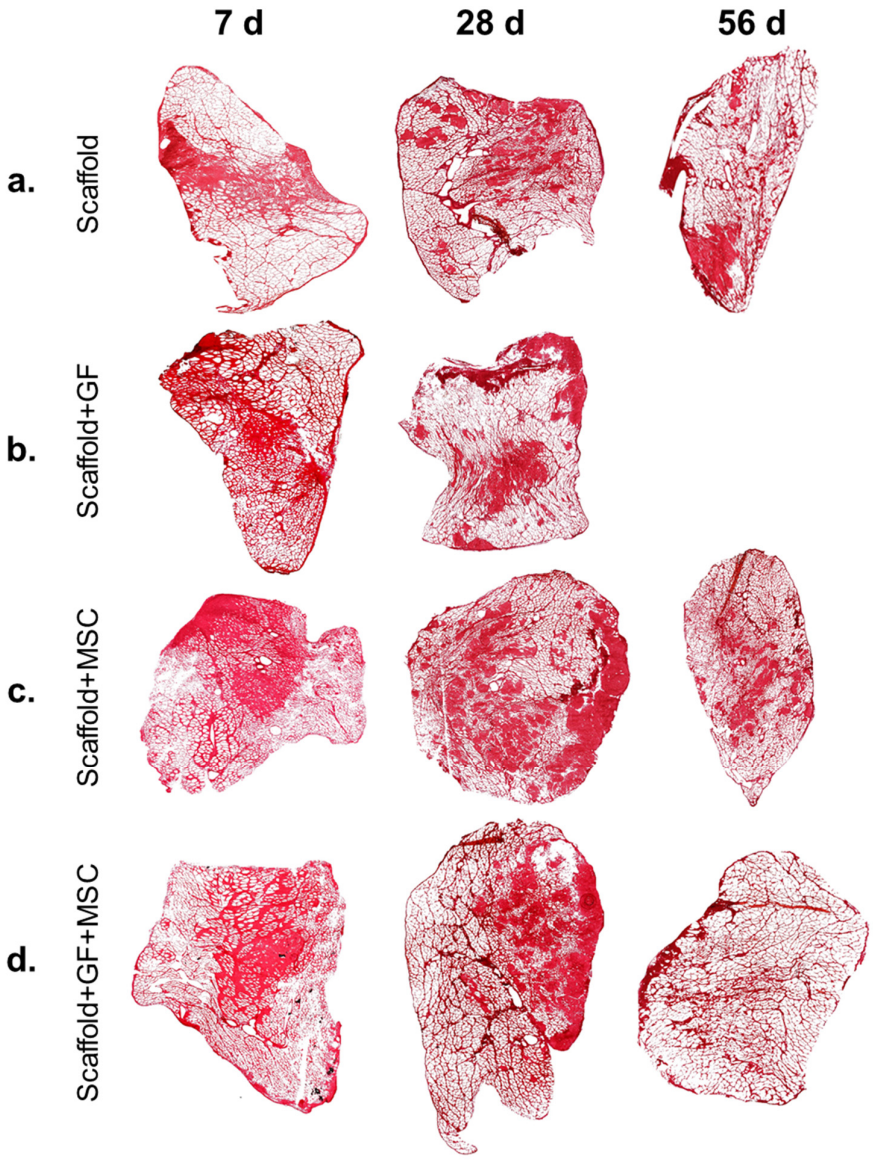

Fig. 39: Scar tissue remodeling.

Representative post-processed images of muscle sections stained with Picro Sirius Red to identify regions of collagenous scar tissue formation in animals treated with (a) scaffold alone, (b) scaffold with growth factors (hIGF and hVEGF), (c) scaffold with MSCs, and (d) scaffold with MSCs and growth factors. Assessment time points from left to right: 7 days, 28 days, and 56 days.

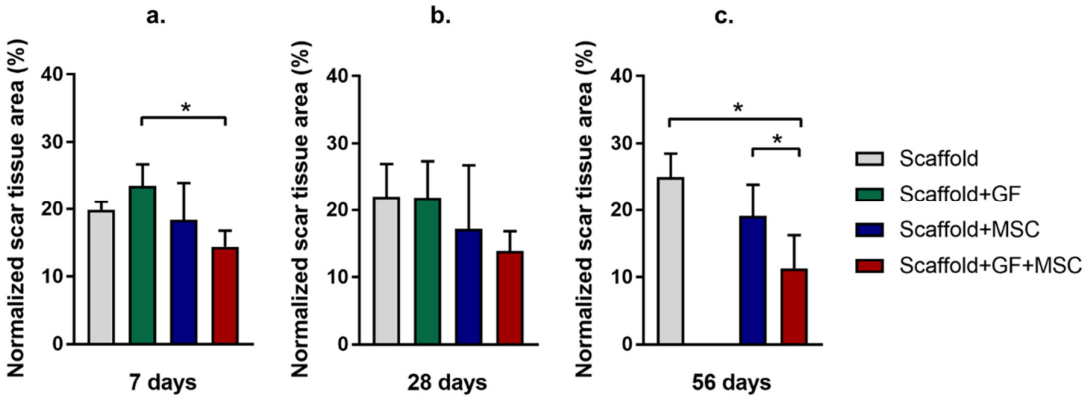

Fig. 40: Quantification of scar tissue area.

Transplantation of scaffold with MSCs and growth factors mitigates scar tissue formation. Quantitative evaluation of scar tissue area in muscle cross sections at day (a) 7, (b) 28, and (c) 56. [n=8, one-way ANOVA with Bonferroni's correction for multiple comparisons].

4.9.3.5. Tissue remodeling

An assessment of tissue remodeling was carried out by evaluating the scar tissue regions of H&E stained muscle cross sections. **Fig. 41** shows areas of muscle cross sections that had a predominant scar tissue presence. On closer inspection, an early regenerative response in the areas of scar tissue was observed in all the groups, characterized by the presence of myofibers with centrally located nuclei. In the control group (**Fig. 41 a**), this regenerative response became less pronounced over time as only isolated myofibers within the scar tissue were visible at day 28. At day 56, the myofibers were only visible at the periphery of the scar tissue (indicated by arrow). Similar observations were also made for the GF only group; i.e. myofibers could be seen within the scar tissue regions at day 7, but were only visible at the periphery of the scar tissue regions at day 28 (**Fig. 41 b**). For the MSC group, at 28 days, groups of regenerated myofibers, rather than isolated ones, were observed in between patches of scar tissue (**Fig. 41 c**). At the last time point, groups of myofibers were still detectable in between areas of scar tissue. This was also true for the GF+MSC group, except that at day 56, most of the scar tissue areas had been reduced to small islands and the surrounding areas of the scar were rich in myofibers with centrally located nuclei (**Fig. 41 d**). This is indicative of active tissue remodeling.

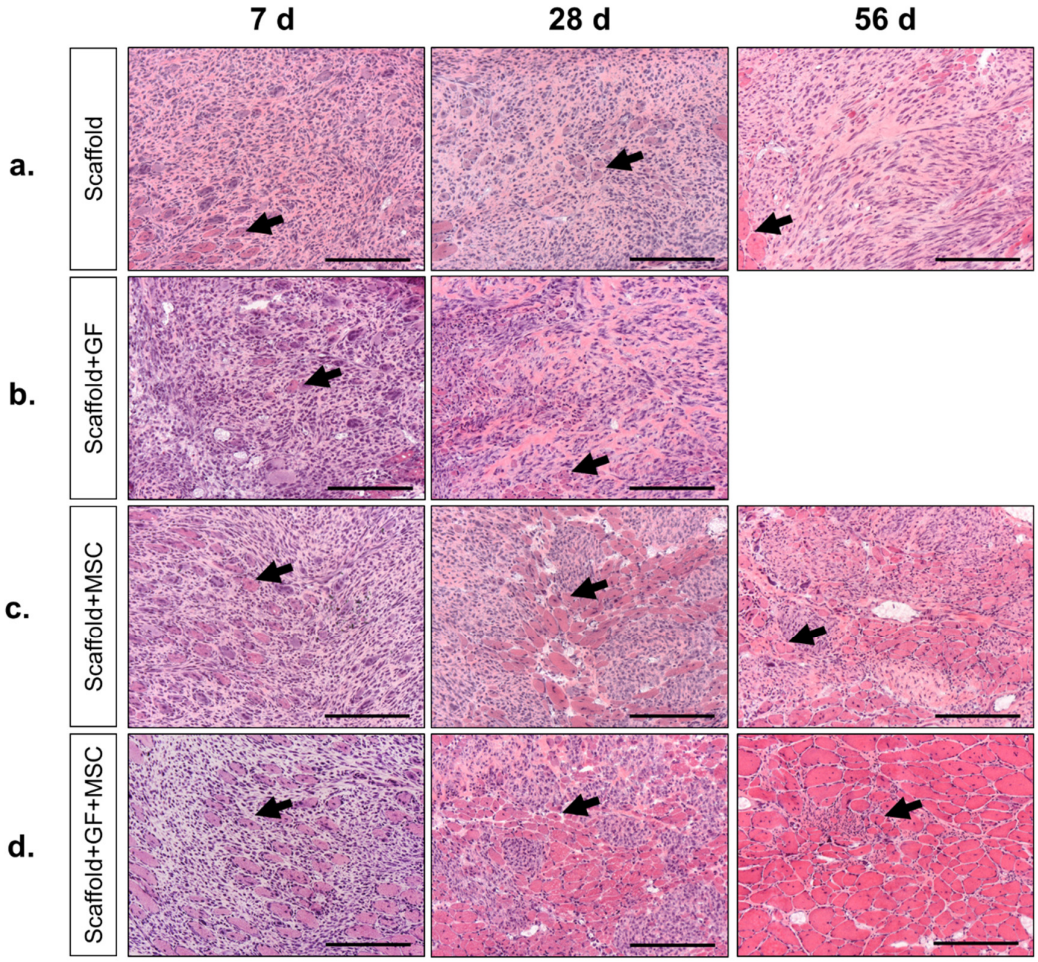

Fig. 41: Myogenic response in scar tissue regions.

Tissue remodeling via new myofiber formation and concurrent scar tissue reduction. Representative images of muscle cross-sections stained with hematoxylin and eosin from animals that received (a) scaffold alone, (b) scaffold with growth factors (hIGF and hVEGF), (c) scaffold with MSCs, and (d) scaffold with MSCs and growth factors. Assessment time points from left to right: 7 days, 28 days, and 56 days. Arrows point towards regenerated myofibers that exhibit a centrally located nuclei [Scale bar = 200 µm].

Regenerated myofibers that was observed in and around the scar tissue area in the different groups could not have been formed without the supply of nutrients to support their growth. Therefore, CD31+ stained muscle sections were re-examined to determine whether CD31+ blood vessels infiltrated the scar tissue areas especially at early time points, and whether the density of blood vessels differed between the groups.

Figure 42 shows regions of scar tissue in the muscle cross sections that were stained with CD31 (red = blood vessels). At the early time point (7 days), comparatively fewer blood vessels were observed in the control and GF groups (**Fig. 42 a, b**) whereas visibly higher density of CD31+ blood vessels were observed infiltrating the scar tissue regions in the MSC and GF+MSC groups (**Fig. 42 c, d**). Over time, blood vessels were still visible in the control and GF groups, but they were located near existing myofibers and very few could be detected infiltrating through the scar tissue area. In comparison, even at later time points, a number of CD31+ blood vessels were observed in the scar tissue area in the MSC and GF+MSC groups. Furthermore, it seemed that in the GF+MSC group, the CD31+ blood vessels increased in diameter and matured over time; this was especially noticeable at the 56 day time point. Concurrent with this maturation was the remodeling and gradual reduction of the scar tissue and its replacement by newly formed myofibers.

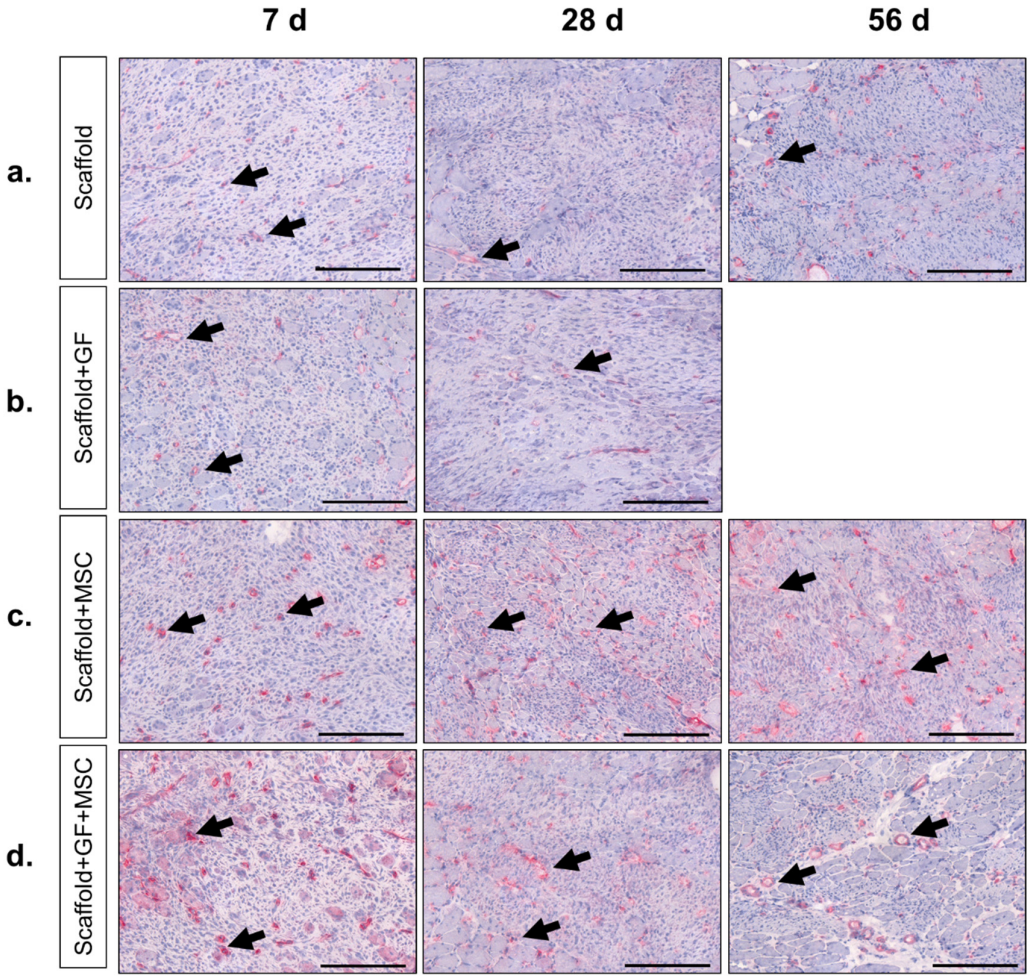

Fig. 42: Angiogenic response in scar tissue regions.

New fiber formation during tissue remodeling is supported by early angiogenesis in scar tissue regions. Representative images of CD31 stained muscle cross-sections from animals that received (a) scaffold alone, (b) scaffold with growth factors (hIGF and hVEGF), (c) scaffold with MSCs, and (d) scaffold with MSCs and growth factors. Assessment time points from left to right: 7 days, 28 days, and 56 days. Arrows point towards CD31+ blood vessels in or around the scar tissue region [Scale bar = 200 µm].

5. Discussion

This thesis demonstrates that porous biomaterial scaffolds enhance the paracrine function of bone marrow derived MSCs by promoting N-cadherin mediated cell-cell contacts. The secreted factors exert strong effects on C2C12 myoblast functions. Furthermore, the results show that N-cadherin also enhances the propensity of MSCs to be stimulated by soluble cues such as hVEGF and hIGF, and enhances their paracrine secretion in response. This strong modulation of MSC paracrine function was not evident when MSCs were encapsulated in 3D hydrogels that prevented physical interaction between the cells. Based on the *in vitro* results, a 3D porous scaffold with the ability to release stimulatory factors was utilized as a carrier to transplant MSCs in a severe muscle injury model. The paracrine effects of the MSCs significantly enhanced muscle contractile forces, and effectively remodeled tissue structure, thereby ensuring that the muscle tissue overcame damage endured due to trauma. Thus, the outcomes of this thesis demonstrate that biomaterial based engineered microenvironments can regulate the regenerative potential of MSCs and induce skeletal muscle regeneration via paracrine effects.

5.1. Paracrine secretion of MSCs

MSCs have received immense scientific interest over the past decade, particularly as a cell type capable of inducing regeneration of musculoskeletal tissues such as bone and cartilage. In addition to their multipotent differentiation potential, MSCs can exert therapeutic benefits via the release of chemokines, cytokines, growth factors, and proteases [149]. Such bioactive factors have been implicated in immune modulation, prevention of apoptosis and fibrotic scarring, angiogenesis, and stimulation of progenitor cell function [150]. Studies from a number of groups have demonstrated that conditioned media derived from MSCs can influence the behavior and function of various cell types including neurons, osteoblasts, and fibroblasts [151, 152]. Generally, MSC-CM exerts positive effects on target cells by enhancing their proliferation and differentiation although this can vary with cell type being investigated and the source of MSCs [153].

Although it is known that dynamic, 3D culture significantly alters the secretion profile of MSCs [154, 155], the vast majority of studies investigating MSC secretome have been carried out with conditioned media from MSCs seeded on tissue culture plastic substrates under static conditions [156, 157]. A discrepancy can therefore arise between the secretion profile characterized *in*

vitro on stiff culture substrates and what the MSCs actually secrete *in vivo*. This is especially plausible because MSCs are known to be responsive to environmental stimuli, and could encounter a wide spectrum of *in vivo* environments with different stiffness (e.g. infarcted myocardium), chemical composition (e.g. variation in ECM composition in different tissues), shear stresses (e.g. after systemic administration) and immune environment (e.g. immune-deficient vs. immune-competent animal models). Moreover, cells encounter a complex, 3D microenvironment not only when injected *in vivo*, but also in biomaterials used for transplantation [158, 159].

Therefore, the characterization of MSC secretion profiles in different environments is crucial to: (1) predict how the secretion will change when cells encounter an *in vivo* microenvironment significantly different to standard 2D culture conditions, and (2) to correlate favorable secretion patterns with different substrate properties, allowing the design of optimized biomaterial systems for MSC delivery.

5.1.1. Modulation of paracrine secretion by substrate microenvironment

Currently, *in vivo* transplantation of cells is largely carried out via bolus injections. An unfortunate reality of this approach is the dramatically low percentage of transplanted cells that survive the hostile injury environment and an even lower percentage of cells that eventually engraft onto the injured tissue [6, 40]. Biomaterials in general, and hydrogels in particular, represent an effective alternative to bolus injection, because they provide a dedicated space for cells to adhere and perform their basic functions, and protect the cells during transplantation. Due to the almost exponential rise in the development of new biomaterials, each claiming a unique advantage over all others, the selection of a biomaterial carrier for cell transplantation can be a confusing one. To keep matters as simple as possible, in this study alginate was used in its most basic form, only modified with cell-adhesive peptides to facilitate cell attachment and viability.

The three alginate based substrates used to study the paracrine behavior of MSCs in this study (2D film, 3D hydrogel, 3D scaffold) had well defined chemical compositions (alginate molecular weight, RGD concentration), and similar cross-linker concentrations were used to ensure no differences in mechanical properties existed. This allowed the investigation of MSC paracrine effects on substrates that differed based on their structural properties i.e. microenvironment. The 3D hydrogels consisted of nanopores that allowed cytokine diffusion

into the conditioned medium, but inhibited cell spreading. 3D scaffolds consisted of macropores which allowed cell movement and spreading.

For the *in vivo* part of this work, the decision to use an open porous scaffold rather than an injectable hydrogel was informed by differences in secretion profiles and paracrine effects observed for MSCs cultured on these substrates. Cytokine array analysis of MSC secretion pattern indicated that the secretion of almost every cytokine was enhanced in MSCs cultured on porous scaffolds. This was further confirmed using more precise rat specific ELISA kits to detect muscle relevant growth factors such as rIGF, rFGF, and rHGF. Interestingly, while high concentrations of rIGF were detected in 3D scaffold-CM, very low concentrations were detected in the 3D hydrogel-CM. To ensure that the secreted cytokines were not being sequestered inside the nanoporous matrix, preliminary experiments were carried out by analyzing the presence of hIGF and hVEGF in solutions of dissolved hydrogels. No remnant factors were detected, which confirmed that the alginate matrix did not inhibit cytokine diffusion into the conditioned media, and further demonstrated that the secretion of certain molecular factors strongly depends on the cells' microenvironment.

Furthermore, small molecules such as hIGF have been reported to diffuse rapidly from injectable alginate hydrogels [160]. A number of groups have utilized sulfated, heparin binding variants of alginate to physically conjugate bioactive factors [161]. Freeman et al. reported that sulfated alginate, but not unmodified alginate, could strongly bind proteins such as FGF [162]. Modified, heparin binding materials have found utility in stabilizing growth factors for controlled delivery systems [163, 164], but are not desirable in a system that is designed to maximize the delivery and outward diffusion of cytokines secreted by MSCs.

Morphological evaluation of MSCs on the different substrates indicated that culture on 2D films and 3D scaffolds promoted cell clustering. CM from these two substrates also showed the highest secretion intensities and exerted stronger paracrine effects on myoblasts. This was an intriguing correlation, and was pursued further by testing the hypothesis that changes in MSC secretion and its effects on myoblast function were due to formation of N-cadherin mediated cell-cell contacts between the MSCs.

There is a paucity of literature on biomaterials based regulation of N-cadherin mediated cell-cell contacts. However, a number of groups have shown that MSC spheroids and aggregates, with high expression of cadherin proteins, exhibit enhanced expression and secretion of

cytokines and growth factors [165]. Lee et al. further demonstrated that blocking E-cadherin in umbilical cord blood derived MSC spheroids reduced the secretion levels to that observed for monolayer cultures [166]. Similarly, aggregation or clustering of MSCs has been shown to modify the anti-inflammatory properties of MSCs [167, 168].

Lee and colleagues, in a different study, proposed that among a group of MSCs derived from different donors, those that had a higher expression of N-cadherin exerted greater therapeutic effects *in vivo* [135]. Blocking and overexpressing N-cadherin correlated with reduced and enhanced levels of secreted VEGF, respectively. The interesting aspect of Lee's study is that they observed N-cadherin related paracrine effects on monolayer cultures, and did not propose or investigate the formation of spheroids or aggregates of MSCs as a requirement for differences in therapeutic effects.

In line with the findings of Lee et al., the outcomes reported in this thesis showed that MSCs cultured on 3D scaffolds did not form spheroids, but clustered together while maintaining adhesion to the alginate matrix. Moreover, blocking N-cadherin reduced the protein secretion of MSCs and subsequently their paracrine effects on myoblasts. This effect was most pronounced in the 2D film and 3D scaffold groups. Immunofluorescent staining for N-Cadherin revealed that apart from 3D hydrogels, MSCs on all other substrates expressed N-cadherin. This was further confirmed by qPCR. MSCs in 3D scaffolds displayed a 9-fold higher expression of the N-cadherin gene Cdh2 compared to encapsulated cells, whereas E-cadherin was not detected on any substrate. Contrary to expectations, N-cadherin was downregulated in 2D films compared to TCP, despite immunofluorescent images suggesting the MSCs on 2D films clustered together while staining positive for N-cadherin. While Lee et al. showed that differences in N-cadherin expression in biological donors correlated with their individual therapeutic efficacy, the results presented here demonstrate that N-cadherin expression and associated paracrine effects from the same biological donors can be altered by varying culture substrates. While the outcomes identify a role for N-cadherin in modulation of paracrine effects, the intricate underlying mechanisms of how these and other cell adhesion molecules alter cellular signaling pathways, gene expression, and eventual function remain unknown. Future studies must therefore attempt to elucidate the exact role of N-cadherin in MSCs cultured on porous scaffolds.

Although the role of cell-matrix interactions in regulation of MSC differentiation has attracted immense attention, it is surprising that not much work has been carried out in trying to modulate the paracrine secretion of MSCs using biomaterials. The outcomes of this thesis as well as other

studies suggest that biomaterials should be viewed as powerful tools that can be used to enhance or modulate MSC secretion. For instance, Seib et al. showed that human MSCs cultured on soft (2 kPa) or stiff (20 kPa) substrates secreted varying levels of IL-8, SDF-1, and VEGF [169]. In particular a 90 fold upregulation of IL-8 was observed on stiff substrates, suggesting that MSCs transplanted via soft or stiff biomaterials may exert different levels of immunomodulatory effects at the site of injury. Similarly other studies have also concluded, using different materials, that stiffer substrates enhance the pro-angiogenic signaling of MSCs, translating into increased capillary tube formation and HUVEC proliferation [170, 171]. Along with stiffness, ECM composition can also influence the paracrine effects of MSCs. For example, Silva et al. showed that MSCs cultured in RGD modified gellan gum hydrogels, rather than unmodified gels, significantly increased the proliferation, metabolic activity and survival of neurons via their secreted factors [172]. Likewise, Jose and colleagues demonstrated that alginate hydrogels modified with GHK, a peptide fragment of osteonectin, significantly enhanced the secretion of VEGF and FGF from encapsulated MSCs [173].

In a translational context, where 3D hydrogels and 3D scaffolds are the two most feasible choices, the results presented here provide strong evidence supporting the use of 3D scaffolds for MSC transplantations. Indeed, appropriate biomaterials must be chosen based on the desired regenerative function of MSCs *in vivo* – whether this is differentiation into a specialized cell type or enhanced paracrine function. The presented results do not suggest that injectable hydrogels, in general, would suppress paracrine effects. Optimization of mechanical and physicochemical properties of the encapsulating biomaterial may alter MSC function. Some work in this area was recently reported by Cai et al. who showed that injectable hydrogels with a stiffness range of 200-400 Pa enhances the paracrine secretion of pro-angiogenic factors from adipose derived stem cells, compared to more compliant gels [174]. Similarly, Thomas et al. reported that microstructural changes of hydrogel microbeads associated with changes in collagen concentration leads to a modulation of the angiogenic and inflammatory responses from human MSCs [175]. Interestingly, a report by Follin and colleagues showed that adipose tissue derived MSCs encapsulated in RGD modified alginate hydrogels showed cell spreading and enhanced expression of paracrine factors compared to monolayer cultures [176]. Closer inspection of the paper revealed that the authors had utilized a very low molecular weight alginate (VLVG), which was recently shown by Chaudhuri and colleagues to facilitate cell spreading and regulate MSC activity and fate [177, 178]. These observations by others further reaffirm that cell spreading leading to cell-cell contacts plays a role in enhancing paracrine

secretion of MSCs. However, specific molecular signaling cascades that link chemical composition, mechanical stiffness, and other properties of the biomaterial with regenerative function of MSCs remain to be elucidated, and would provide important mechanistic insights.

5.1.2. Modulation of paracrine secretion by stimulation with growth factors

Cells that are transplanted *in vivo* encounter a number of different cytokines and growth factors that are secreted by tissue resident or immune cells at the site of injury. These soluble factors can bind to receptors of the cells' surface and trigger various signaling pathways [179, 180]. For example, supplementation of dexamethasone, ascorbic acid, and ß-glycerophosphate can induce the osteogenic differentiation of MSCs [181]. Therefore, it is likely that MSCs may alter their paracrine function in response to soluble cues in the injury environment. While inflammatory cytokines at the site of injury can negatively influence MSC function [182], others that induce endogenous tissue repair may improve the effects of MSCs [183]. In either case, the outcome of an MSC therapy may highly depend on the complex interaction between MSCs and other cell types present in the *in vivo* milieu. This involves not only processing soluble signals secreted by other cells, but also secreting appropriate factors in response.

Based on the differences in secretion profile and paracrine effects of the MSCs observed on 3D scaffolds and 3D hydrogels, two intriguing questions were raised. First, does 3D encapsulation of MSCs put them at a disadvantage with regards to perceiving paracrine signals from others cells in the injury environment? Put another way, do MSCs in 3D scaffolds have a distinct advantage of paracrine communication *in vivo*? Secondly, do soluble cues such as growth factors alter the paracrine effects of MSCs? Both of these questions promised to have major implications on the design of a regenerative strategy.

It was examined whether hIGF and hVEGF, which are growth factors that may be prevalent in a regenerating muscle environment, could modulate the secretion of paracrine factors from MSCs cultured in 3D hydrogels or 3D scaffolds. Encouraging preliminary investigations on MSCs seeded on TCP substrates showed that stimulation with hVEGF+hIGF (GF) enhanced the secretion of cytokines that are well known to play a regenerative role in skeletal muscle (rHGF, rFGF, and rVEGF). When the studies were extended to 3D substrates, a remarkable difference in paracrine response was observed. MSCs in 3D scaffolds showed a significant enhancement in secretion profile when stimulated with hIGF and the combination of hIGF+hVEGF compared to unstimulated MSCs. Stimulation with hVEGF registered a

relatively weaker response. In comparison, stimulation of MSCs in 3D hydrogels did not reach comparable levels even after GF stimulation.

ELISAs were then employed to more precisely detect the secretion level of muscle relevant cytokines such as rFGF, rIGF, and rVEGF. Remarkably, after GF stimulation the secretion levels of all cytokines did not reach the same levels in 3D hydrogel-CM as in 3D scaffold-CM. As discussed before, GF diffusion through the nanoporous alginate matrix was not a limiting factor. Thus, the results indicated that the propensity of MSCs to be stimulated by soluble cues is enhanced in 3D scaffolds that permit cell-cell contacts compared to 3D hydrogels. Furthermore, stimulation with hIGF and hVEGF emerged as a potentially effective strategy to enhance the paracrine secretion, and thus the therapeutic potential, of MSCs.

Due to the ever-growing appreciation for MSC paracrine effects in regeneration, scientists have increasingly focused on trying to gain the ability to modulate or enhance the secretome of MSCs [184]. Two of the major ways this has been explored is via (1) genetic modification [185-187], and (2) pre-conditioning regimes [188-190]. Previous studies have reported that pre-conditioning or stimulating MSCs using soluble cues (mostly different doses of inflammatory cytokines) can improve their regenerative performance via enhancing paracrine factor secretion [191-193]. The results reported in this thesis further contributes to existing knowledge in this emerging area of research, and proposes a simple yet effective strategy to enhance the paracrine secretion of MSCs without any genetic manipulation or harsh pre-conditioning.

In summary, the results discussed in this section indicate that MSCs transplanted in 3D scaffolds are more likely than those in 3D hydrogels to actively participate in tissue regeneration by communicating with other cells in a paracrine fashion.

5.2. Paracrine effects of MSCs on myoblast function

In vivo, muscle resident satellite cells are the primary enablers of repair and regeneration after both minor and major injuries [194]. The post-injury muscle environment is rich with signaling molecules that are either actively secreted by cells or released after structural damage. In this information rich environment, satellite cells become activated, undergo proliferation to produce muscle progenitor cells, migrate to the site of injury, and undergo differentiation to fuse with

surviving myofibers or to form new ones. This set of functions performed by satellite cells and their progeny are essential to induce muscle regeneration.

In vitro work carried out in this thesis was performed using C2C12 myoblasts, a commonly used cell line from mouse muscle. There were two primary reasons for this:

(1) Satellite cells are notoriously sensitive to their microenvironmental niche, and changes in the mechanical or chemical properties of the niche triggers satellite cell activation. A number of challenges exist in the *in vitro* culture of satellite cells. When harvested from skeletal muscle biopsies and cultured on tissue culture treated plastic substrates (TCP), satellite cells lose their 'stemness' and differentiate into a myogenic progenitors. In the past few years, efforts have been made to recapitulate the properties of the satellite cell niche in biomaterial systems, thus allowing extended *in vitro* satellite cell culture without triggering its spontaneous differentiation. For example, Gilbert et al. showed that culturing primary satellite cells on hydrogels that mimic the elasticity (stiffness) of skeletal muscle allowed relatively long term culture of satellite cells and retained their regenerative potential. More recently, a biomaterial based niche together with a well-defined culture media was used to maintain the quiescence of satellite cells *in vitro* for long durations [195]. Due to these existing challenges, investigating the paracrine interaction between MSCs and satellite cells was not a feasible direction for this thesis.

(2) C2C12 myoblasts are able to perform the same basic functions (migration, fusion to form myotubes, expression of typical myogenic markers) as primary myoblasts. The wide-spread use of C2C12 myoblasts in basic research studies also allows a better comparison of the results obtained in this thesis with that of others.

Successful skeletal muscle regeneration is characterized by efficient migration, proliferation, and fusion of satellite cells and their myoblast progenitors to form new muscle fibers (**Fig. 43**) [196-198]. How strongly the paracrine factors secreted by MSCs stimulates these cellular functions may determine the outcome of an MSC based therapeutic approach. Therefore, in this work, *in vitro* assays were established so that the paracrine effects of MSCs on myoblasts could be investigated.

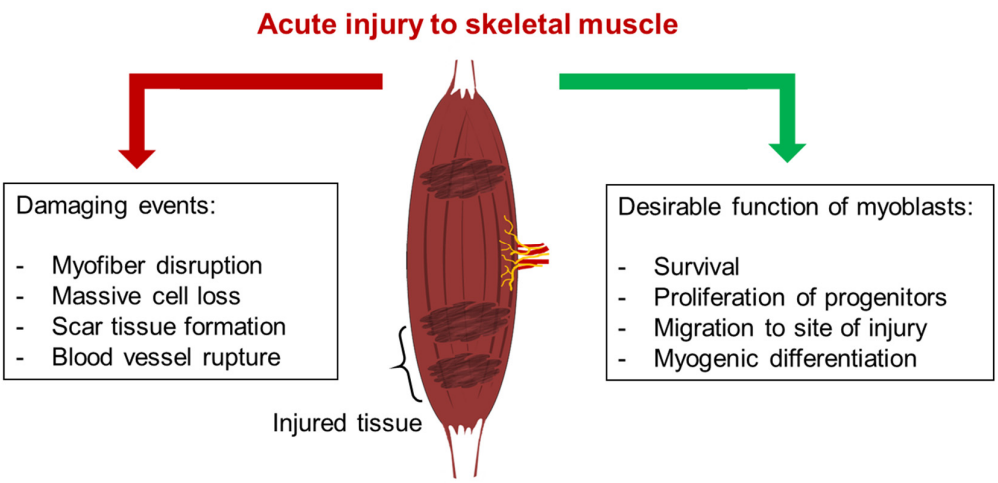

Fig. 43: Undesirable effects of acute injury, and cellular functions required for repair.
In the aftermath of acute injury, the muscle experiences massive loss of cells, necrosis of functional myofibers, disruption of the blood vessel network, and formation of scar tissue. In order to successfully restore muscle function and structure, muscle progenitor myoblasts must be able to survive, undergo proliferation, migrate to the site of injury, and undergo myogenic differentiation. The in vitro assays in this thesis were designed keeping in mind these functions.

In native skeletal muscle, cell migration is more complex because the cells migrate in a 3D environment, may respond to chemical gradients, and have anisotropic contact guidance cues from the muscle ECM [199-201]. Nevertheless, due to the challenges associated with recapitulating the complex environment that cells encounter *in vivo*, a simple, repeatable, widely used, scratch assay was considered a sufficient setup that could provide vital information on the migratory behavior of myoblasts. The readouts analyzed were (1) rate of scratch closure, (2) empty scratch area remaining at a defined time point (or scratch area coverage), (3) migration speed, (4) total migrated distance, (5) net displacement, and (6) directionality. The experiments were performed in serum free conditions because the addition of as low as 1% serum masked the effects of MSC-CM in preliminary experiments. CM that stimulated a high rate of scratch closure, a lower empty area remaining at the end of the experiment, a faster migration speed, a greater distance migrated, a greater net displacement, and a directionality close to 1, were considered superior than those that did not [202, 203]. Without any growth factor stimulation, the 2D-film and the 3D scaffold-CM stimulated favorable migration behavior in myoblasts. Among the growth factor stimulated groups, MSCs in 3D scaffolds stimulated with hIGF alone, or a combination of hIGF+hVEGF, induced favorable migration

behavior in myoblasts. This was likely because the CM of these groups contained enhanced levels of rHGF, rFGF, and rIGF, which are known to stimulate cell motility [145, 204, 205].

Satellite cells in the skeletal muscle often undergo cell death in the event of acute injury [206]. Due to the already minute population of satellite cells in adult skeletal muscles (< 5%), cell death greatly reduces the total population of progenitor myoblasts that can be derived from self-renewing satellite cells, and that eventually participate in regeneration [207, 208]. Therefore the ability of paracrine factors to prevent cells from undergoing apoptosis, and to stimulate their proliferation was assessed *in vitro*. In summary, 3D scaffold-CM supported greater cell survival, and stimulated higher proliferation of myoblasts. Upon stimulation with growth factors, hIGF and hIGF+hVEGF stimulated MSCs in 3D scaffolds induced the most favorable outcomes. In agreement with previous reports, the bolus supplementation of growth factors alone or in combination did not improve cell proliferation relative to controls [209]. This is likely because the experiment was conducted in serum free conditions and the presence of only two growth factors did not trigger a proliferative response in the myoblasts. At the same time, the conditioned media contained a wide range of secreted cytokines which, in an apparently synergistic effect, led to large increases in cell number over the duration of the experiment. Similar conclusions have been drawn by others using direct co-cultures of MSCs and myoblasts [210], but it remained unclear whether physical contact between the two cell types is necessary to induce the effect. The results presented here demonstrate that MSC-CM effectively stimulates myoblast behavior in an indirect co-culture setup. This may imply that MSCs need not engraft onto host tissue in order to induce a therapeutic effect, and that MSCs that are in the near vicinity of the injured tissue can also mount a potent regenerative effect.

Fusion of individual progenitor myoblasts into elongated, multinucleated myotubes marks the beginning of a process that leads to the formation of new myofibers. In the wake of muscle injury, the primary requirements for regeneration involve survival of myoblasts, their migration and sufficient proliferation at the site of injury. Once an adequate number of cells are present, differentiation is initiated by the fusion of myoblasts which leads to the formation of contractile myofibers. *In vivo*, this series of processes is tightly regulated by a complex interaction between multiple cell types. Proliferation and migration of satellite cell progeny usually takes place in the pro-inflammatory phase of muscle healing in the presence of M1 type (classically activated) macrophages. The switch from M1 to M2 macrophages at the onset of the anti-inflammatory phase is associated with the secretion of cytokines and other soluble signals that induce the

differentiation of myoblasts. The myogenic differentiation assays carried out in this work, without co-culture with immune cells, therefore may not provide a complete picture of what may happen *in vivo*. However, the outcomes of the assay provide insights into the role of paracrine factors in modulating myoblast cell cycle withdrawal and myogenic differentiation. Without GF stimulation, 3D scaffold-CM was found to inhibit myotube formation, which agrees with the hypothesis that premature differentiation of myoblasts should be avoided in the immediate aftermath of injury. In contrast, hIGF stimulated 3D scaffold-CM significantly enhanced myotube formation compared to control, despite the neutralization of recombinant hIGF present in the CM. The neutralization was confirmed using ELISA measurements, and was also evident in the hIGF stimulated 3D hydrogel-CM which had a significantly lower fusion index. Thus, the most plausible explanation for enhanced myotube formation in GF stimulated 3D scaffold-CM is the heightened secretion of rIGF along with potentially other myogenic factors, very few of which were secreted by MSCs in 3D hydrogels.

It is clear that MSCs are capable of secreting proliferative as well as differentiative factors at the same time. The results also show that the induction of differentiation can be modulated by soluble factor stimulation of MSCs in a 3D scaffold setting, but not in a 3D hydrogel setting.

Overall, analysis of paracrine effects on myoblasts show that employing a porous biomaterial could increase the likelihood of MSCs exerting a strong therapeutic effect during muscle regeneration, especially in a system which could locally stimulate MSCs with hIGF and hVEGF.

5.3. In vivo observations

5.3.1. Injury model

The utilized injury model consisted of multiple crush trauma applied along the length of the hindlimb soleus muscle of female Sprague Dawley rats (**Fig. 44**). To be translationally relevant, it is important to use immune competent animal models, especially keeping in mind the role of the immune system and its potential modulation by MSCs in muscle regeneration [211, 212]. For instance, Ninagawa et al. found no difference in the long term functional forces generated by injured muscles with or without MSCs transplantation in immunodeficient mice after crush trauma [213]. Compared to other commonly used injury models [214], this injury model is considered more relevant to the impact trauma cases regularly witnessed in the clinic. Left

untreated, injured muscles show the development of fibrotic scar tissue that persists in the long term, severely hampering muscle function [215]. At the same time, there is insufficient revascularization of the injured tissue that in turn does not support the formation of new muscle fibers. These long term negative effects of the injury mimic what has been reported in severe injury cases in human patients [216].

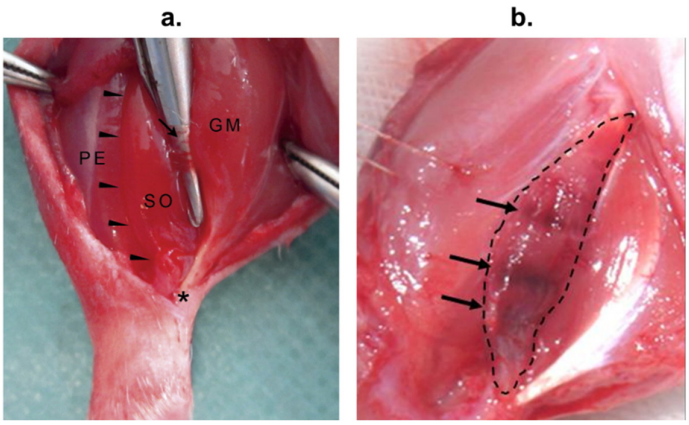

Fig. 44: Clinically relevant muscle injury model.
(a) The opened hindlimb of Sprague Dawley rats consisting of soleus muscle (SO), gastrocnemius muscle (GM), and peritoneal muscles (PE). Arrow heads outline the edge of the soleus muscle. Asterisk indicated Achilles tendon. (b) Acute crush trauma (areas indicated by arrows) was induced along the length of the soleus muscle (dashed outline).

5.3.2. Restoration of function

Functional performance of injured muscles was determined by measuring the fast twitch and tetanic forces generated by the muscle upon electrical stimulation of the sciatic nerve. The fiber composition in soleus muscles vary dramatically between species and even rodents. Whereas the soleus is pre-dominantly composed of fast type fibers in mouse, it mostly consists of slow fibers in rat [217]. Treated with an empty scaffold (control), the fast twitch and tetanic (slow twitch) contraction forces remained stunted at 60 % and 40 % of the contralateral, respectively. This lack of any improvement in muscle forces over 8 weeks represents the inability of the native healing processes of skeletal muscle to induce regeneration following severe trauma, and is consistent with previous observations in this injury model [215].

The delivery of recombinant growth factors hVEGF and hIGF via the scaffold did not lead to an improvement in either fast twitch or tetanic forces. This was slightly surprising because hVEGF is a potent angiogenic factor that can lead to revascularization of injured tissue and pave the way for subsequent myofiber formation that can be triggered by hIGF. Drug release profiles suggested that hVEGF was released within one week whereas hIGF was released over a period of 30 days. This kinetic of drug release is well suited to the regeneration process where the restoration of blood supply is a pre-requisite for myofiber formation and growth. These exact two growth factors were previously reported to have induced functional muscle regeneration in an ischemic injury model [160]. Indeed the primary reason for loss of function in that model is the disturbance in blood flow, which was shown to be restored by delivery of pro-angiogenic factors. In the severe trauma model, lack of benefit with delivery of growth factors may therefore be due to the extent of damage where blood vessel damage is only one of many issues. Such a severe injury may potentiate the need to deliver multiple therapeutic growth factors that can support the various biological processes required for efficient regeneration.

Significant improvement in muscle forces were observed with the transplantation of MSCs. In a previous study, Winkler et al. reported a dose-response relationship between number of intramuscularly transplanted MSCs and the contractile forces measured after treatment [62]. They recorded a maximum of 70% fast twitch forces and 55% of tetanic forces after transplanting 10 million autologous MSCs. In comparison, the results reported in this thesis show that a similar fast twitch force (70%) and a much improved tetanic force outcome (65%) could be obtained with cell numbers that are at least 10 times lower, and not delivered intramuscularly. The pronounced effect with a lower cell number is likely due to the enhanced survival of MSCs when transplanted using a biomaterial scaffold, and the enhanced secretion profile observed for MSCs in 3D scaffolds. Along with pro-angiogenic cytokines like VEGF, MSCs can secrete a myriad of other beneficial bioactive factors, essentially acting as live ‘drug factories’. Because the scaffolds were placed beside the muscle and *in vitro* data suggested minimal outward migration of seeded cells from the scaffold, it is highly likely that the beneficial effect on muscle regeneration was exerted by the multitude of paracrine factors secreted by MSCs while staying inside the scaffold.

In vitro investigations showed that the paracrine secretion of MSCs can be considerably enhanced simply by exposing them to growth factors. Accordingly, the highest muscle contraction forces (both fast twitch and tetanic) were observed for the group where MSCs and

GFs were delivered together. This lends further credence to the hypothesis that the paracrine factors secreted by GF stimulated MSCs can lead to marked improvements in functional regeneration compared to unstimulated MSCs.

5.3.3. Restoration of structure

Based on the differences in the functional performance of injured muscle tissues, a detailed structural assessment was performed. Due to the fact that the crush injury was inflicted at multiple locations along the length of the soleus muscle, the analyses represented the mean values obtained from sections taken from three locations. Our analysis consisted of myofiber density, regenerated myofiber density, blood vessel density, and scar tissue area.

The dynamic nature of muscle tissue remodeling involves the sequential yet overlapping processes of vascularization, myofiber formation, and scar tissue remodeling. Especially at early stages after trauma, re-vascularization of injured tissue is an essential process for successful tissue regeneration [218, 219], as progenitor cells are unable to survive if the nutrient source is more than 150 μm away [220]. At the earliest evaluated time point, animals that received the combination of growth factors and MSCs showed the highest blood vessel density comparable to that induced by the delivery of growth factors alone. At all tested time points, the control group showed the lowest blood vessel density in muscle cross-sections. Re-vascularization in the GF group, however, did not lead to high myofiber densities and showed comparatively higher scar tissue formation. In contrast to our results, previous reports have implicated VEGF as a potent regulator of myoblast function and *in vivo* muscle regeneration [209, 221]. However, it is important to note that these investigations were largely carried out using ischemic injury and toxin induced injury models. Artery lacerations (ischemic injury) and toxin/venom injections are commonly employed in animal models to investigate muscle regeneration. Although these injuries result in acute damage to the muscle, the endogenous healing capacity of the muscle is able to repair and remodel the injured tissues without intervention one month post injury [222]. Our findings suggest that while the absence of sufficient vasculature may contribute to lower fiber densities, lack of tissue remodeling, and reduced contractile function of the tissue, improved vessel formation may not be the sole requirement for muscle regeneration, especially in our injury model.

Moreover, it has been reported that stimulation of vascularization is likely regulated by the action of multiple growth factors and cytokines [223, 224], and the delivery of only hVEGF or

hIGF may have been insufficient. In line with this, and perhaps more importantly for tissue remodeling, a higher presence of CD31+ blood vessels was observed in areas predominantly composed of scar tissue in the GF+MSC and MSC groups. Scar tissue is thought to establish a permanent presence in injured tissues, but the existence of a vascular network within fibrotic regions pointed towards imminent remodeling, and indicated that newly formed myofibers would find nutritional support in areas that are particularly difficult to remodel. Whereas the scar tissue decreased as the tissue remodeled itself in the MSC+GF group, a gradual increase in the scar area was observed in the control group. This could imply that the natural healing mechanisms of skeletal muscle fail to curb or mitigate scar tissue formation in the absence of soluble cues from the MSCs.

In all groups, an early regenerative response in terms of new myofiber formation was observed within scar tissue regions. This is likely due to the inherent regenerative potential of skeletal muscle and the response of resident satellite cells to injury. Interestingly, over time, maturation and multiplication of myofibers in the control and GF groups ceased to exist, whereas an increase in the number of regenerated fibers and myofiber density was observed for MSC and GF+MSC groups. At the last time point evaluated, there were a significantly higher number of regenerated myofibers in the MSC+GF group compared to the other groups, which indicated that active tissue remodeling continued in the long term as newly formed myofibers replaced remaining scar tissue.

Despite the lowest scar tissue presence, highest number of regenerated myofibers, and the highest myofiber density in the GF+MSC group, one might question why the contractile forces were not closer to those of the contralateral uninjured muscles. As observed in the analysis of regenerated fibers, about 35 % of the muscle cross sectional area in the GF+MSC group was occupied by newly formed myofibers with centrally located nuclei. Some of these likely may have not reached full maturity because highly contractile mature myofibers are characterized by the peripheral location of their nuclei. It is probable that further maturation of the regenerated myofibers over time would lead to enhanced contractile properties.

6. Summary and Major Conclusions

In the work presented in this thesis, modulation of MSC paracrine effects by microenvironmental and soluble cues is shown to promote skeletal muscle regeneration.

MSCs are a rich source of bioactive factors, and this property has been harnessed to promote the repair and regeneration of tissues that would otherwise not heal properly. In skeletal muscle, the functional performance of myogenic progenitor cells after injury determines the regenerative outcome. Therefore in the first phase of the project, *in vitro* behavior of myoblasts in the presence of MSC-CM was characterized. The outcomes revealed that paracrine factors secreted by MSCs can improve cell survival, migration, and proliferation.

In keeping with the ultimate goal of delivering cells *in vivo*, MSCs were cultured in 3D alginate based biomaterials and their paracrine function was investigated. Injectable gels and porous scaffolds represent the two most commonly employed biomaterial formulations to transplant cells. MSCs encountered distinct microenvironments in 3D hydrogels (nanoporous) and 3D scaffolds (macorporous), and accordingly adopted different morphologies during culture. MSCs exhibited enhanced secretion of a wide range of cytokines, including ones desirable for muscle regeneration, when cultured in 3D scaffolds compared to 3D hydrogels. As a result, 3D scaffold-CM exerted more potent paracrine effects on myoblast functions. On a mechanistic level, the enhanced paracrine effects of MSCs was found to depend on N-cadherin mediated cell-cell contacts. While 3D hydrogels prevented physical interaction between encapsulated MSCs, 3D scaffolds provided a spacious microenvironment (interconnected pores in the size range 100-200 μm) that was conducive to the formation of cell clusters. Blocking N-cadherin negatively affected the paracrine effects of MSCs on myoblasts. The major conclusion from this part of the study is that variations in biomaterial structure can significantly affect the paracrine function of MSCs, and can modify their ability to influence the behavior and function of target progenitor cells. The results also indicate that biomaterials can be used as powerful tools to modulate the MSC secretome. These findings will have major implications for any tissue engineering strategy that utilizes MSCs. It further stresses the point that while mode of MSC delivery was considered important, it should now be considered critical for the outcome of the regenerative therapy.

In the second part of the thesis, the paracrine response of MSCs to soluble cues was assessed. MSCs in 3D hydrogels or 3D scaffolds were exposed to hIGF and hVEGF and the resulting paracrine effects were investigated. MSCs on 3D scaffolds reacted strongly to GF stimulation,

especially to hIGF, by enhancing their paracrine secretion. The effect was significantly weaker in 3D hydrogels. GF stimulated MSC-CM from 3D scaffolds strongly influenced myoblast proliferation, migration, and differentiation. However, the same effect was not observed for GF stimulated MSC-CM from 3D hydrogels. The stimulatory effects of soluble growth factors were also dependent on cell-cell interaction and N-cadherin expression, as blocking N-cadherin nullified the benefits of GF stimulation. These results suggest that MSCs become highly sensitive to stimulation by soluble cues in porous environments that facilitate physical interaction between MSCs. The major conclusions from this part of the thesis is that transient growth factor exposure is sufficient to enhance the paracrine effects of MSCs, but not every growth factor has a potent effect. This provides a simple yet effective alternative to enhance the therapeutic benefit of MSCs compared to commonly employed strategies such as pre-conditioning via hypoxia or via genetic modification. Additionally, the results suggest that encapsulating MSCs in 3D hydrogels that inhibit cell movement and spreading may reduce their ability to actively communicate with other cells in the injury environment via paracrine signaling.

Finally, 3D scaffolds were used to transplant MSCs *in vivo* near an injured skeletal muscle to assess whether paracrine effects alone can induce muscle regeneration. A variant of the scaffold was able to release incorporated growth factors hIGF and hVEGF to locally stimulate seeded MSCs. The results of functional and histological characterization of treated muscles showed that the delivery of MSCs in GF eluting scaffolds induced robust functional and structural regeneration. Skeletal muscles treated with MSCs and GFs showed the highest contractile strengths, the highest early stage angiogenic response, the highest percentage of regenerated myofibers, the highest myofiber density, and the lowest scar tissue formation after 8 weeks. The major conclusion from the *in vivo* study was that when provided an optimal microenvironment, MSCs possess the ability to regenerate even severe injuries. That they can do this from afar confirmed the paracrine hypothesis, and opens up new possibilities for the regeneration of other tissues. Similar experiments in the future may challenge the long held belief that engraftment of MSCs at sites of tissue damage is an essential criterion to achieve MSC mediated therapeutic benefit.

7. Future Outlook

With almost 5 research articles published per day containing the words "mesenchymal stem cells" or "mesenchymal stromal cells" [www.ncbi.nlm.nih.gov/pubmed/], it would be an understatement to say that MSCs continue to be relevant and widely used for biomedical applications. Already, MSCs are being tested in hundreds of registered clinical trials. Yet, new knowledge regarding their biology, properties, applications, and interactions continues to come through. An increasingly important aspect of MSCs is their interaction with materials. In the body, MSCs interact with ECMs with varying composition, bioactivity, and mechanical compliance. Recognizing this, the last decade has seen multiple breakthrough studies on how cell-matrix interactions can be harnessed to direct cell fate [75, 178, 225-229]. In a large majority of the cases, it is the ability of MSCs to differentiate into different lineages, especially the osteogenic lineage, that is the focus of interest. Outside the realm of the musculoskeletal system (and even within it), therapeutic and regenerative effects of MSCs are primarily derived from their ability to secrete paracrine signals. It is therefore imminent that the field turns towards understanding how MSC paracrine signaling can be modulated and harnessed using biomaterials.

The work reported in this thesis demonstrates at least two ways in which cell-matrix interactions can be used to modulate the paracrine function of MSCs. However, this is a platform that must be built on. To begin with, the intracellular signaling pathways that are activated in response to changes in substrate microenvironment, dimensionality, or growth factor stimulation should be investigated. This can identify major signaling complexes that regulate factor secretion, and that may be targeted in future strategies.

In this work, a correlation was observed between paracrine factor secretion and cell clustering on alginate materials. Because attachment on alginate is mediated by integrin binding RGD peptide sequences, it would be interesting to investigate if the degree of cell clustering can be modulated by altering the amount of adhesive peptides and their distribution on the cell-material interface. Mechanical properties, especially stiffness, has been a focus of intense interest as a modulator of MSC fate. Some studies suggest that paracrine signaling, especially the secretion of angiogenic factors, can be enhanced by increasing the stiffness of substrates. However, *in vivo*, MSCs present in skeletal muscle experience a softer ECM environment than the MSCs present in a calcified bone ECM. Does this imply that MSCs in bone ECM secrete more angiogenic cytokines than those in muscle, despite both tissues being highly vascularized?

Along this line of thought, it would be interesting to distinguish whether MSCs cultured on substrates that mimic the mechanical properties of skeletal muscle secrete paracrine factors that more strongly modulate the function of myoblasts compared to factors from MSCs on a bone mimicking substrate.

Studies on growth factor stimulation of MSCs showed that hIGF leads to a more potent paracrine response from MSCs compared to hVEGF. Experimentally, the MSCs were exposed to the growth factors for 24 hours, but the degradation of the growth factors and their bioactivity due to short half lives in solution was not taken into account. Furthermore, it is at the moment unclear how long the effects of the growth factor stimulation on the MSCs would last if the growth factors are removed from solution. Preliminary experiments (data not shown) indicated that it is likely the MSCs require a more sustained stimulation. In that case, strategies to chemically immobilize relevant growth factors on the surface of the biomaterial could be useful. Chemical immobilization would not only prevent degradation of the growth factor that is normally observed in solution, but it is conceivable that less of the growth factor is required for equal if not enhanced stimulation.

Relevant to skeletal muscle, future studies should investigate the paracrine interaction between MSCs and muscle resident satellite cells or their progenitors. This would require that a well-characterized, standardized substrate that allows long term culture of quiescent satellite cells is used. The substrate properties can then be systematically altered to mimic those of scar tissue or aged muscle tissue.

As mentioned earlier, the regenerating skeletal muscle comprises a complex biological environment where multiple cell types are working in a synchronous fashion. MSCs likely exert paracrine effects on FAP cells, fibroblasts, or the immune system that determines the switch of key molecular and cellular events. All of these interactions can add to the existing knowledge on MSC mediated muscle regeneration, and can likely be transferred to that of other tissues and diseases. Scar formation affects all tissues in the body except bone and liver. MSCs are known for their anti-scarring properties but it is unknown whether MSCs do this by altering ECM deposition by fibroblasts, or whether they alter the concentration, orientation or other aspects of deposited collagen or ECM. Perhaps it is a combination of all these aspects, keeping in mind that FAP cells for instance have been reported to create a pro myogenic differentiation niche in the skeletal muscle. This implies that myogenic progenitor cells likely process a number of unique signals in the ECM that FAP cells or fibroblasts deposit.

8. Appendices

Appendix A: List of Materials, Reagents, Antibodies, Detection kits

Table 3: List of materials and reagents.

Product/Reagent/Material	Catalogue number	Company/Supplier
Normal Goat Serum	S-1000	Biozol
Sodium hydroxide	182158.1211	Applichem
Alginate	PRONOVA UP MVG, PRONOVA UP LVG	Novamatrix
Anti-mouse horseradish peroxidase	NA931	GE Healthcare
C2C12 myoblasts	ATCC® CRL-1772™	ATCC
Calcium chloride dihydrate	C3306	Sigma-Aldrich
Calcium sulfate dihydrate	C3771	Sigma-Aldrich
Caspase-Glo® 3/7 assay	G8091	Promega
Coomassie Plus Protein assay Reagent	1856210	Thermo-Scientific
CyQUANT® kit	C7026	Thermo Fischer
DAPI	32670	Sigma-Aldrich
DC™ Protein Assay kit	5000111	Bio-Rad
Dialysis tubes	734-0653	VWR Spectra/Por®
Dulbecco's modified eagle's medium (high glucose)	D6429	Sigma-Aldrich
Dulbecco's modified eagle's medium (low glucose)	D5546	Sigma-Aldrich
Activated charcoal	C9157	Sigma-Aldrich
Ethylene glycol	24407.292	VWR
FBS Superior	S 0615	Biochrome
Full-Range rainbow markers	RPN800E	GE Healthcare
G_4RGDSP	Custom designed	Peptide 2.0
GAPDH (western blot)	ab8245	Abcam
Glutamax	35050	GIbco
Hydroxylamine hydrochloride	26103	Thermo Scientific
LIVE/DEAD kit	L3224	Thermo Fischer
Luminol enhancer solution	RPN2232V1	GE Healthcare
MES hydrate	M8250	Sigma-Aldrich
Methanol	1.06009	Merck
MOPS SDS running buffer	NO0001	Life technologies
NHS (N-hydroxysuccinimide)	130672	Sigma-Aldrich
Nitrocellulose membrane	LC2001	Life technologies

Non-fat dried milk powder	A0830.0500	Applichem
NuPAGE® Bis-Tris Mini Gels	NP0336BOX	ThermoFisher Scientific
PBS (Dulbecco's phosphate buffered saline)	14190094	Gibco
Penicillin-Streptomycin	P0781	Sigma-Aldrich
Peroxidase solution	RPN2232V2	GE Healthcare
Alexa Fluor® 488 Phalloidin	A12379	Thermo Fisher Scientific
Presto Blue™ Cell viability reagent	A13262	Life technologies
Recombinant human IGF-1	291-G1	R&D systems
Recombinant human $VEGF_{165}$	293-VE	R&D systems
Restore™ Western Blot Stripping Buffer	21059	Thermo Scientific
Sodium chloride	P029.3	Merck
Sodium periodate	311448	Sigma-Aldrich
TBS		
TBST		
Triton X-100	T8787	Sigma-Aldrich
Trizma® base	T6066	Sigma
Trypan Blue Stain	15250061	Gibco
Alkaline Phosphatase Substrate kit	AK5000	Vector Labs
Red Alkaline Phosphatase Substrate kit	SK-5100	Vector Labs
Hematoxylin (Harris)	1.09253.0500	Merck
Eosin	2C140	Chroma
Tissue-Tek® O.C.T. Compound	25608-930	VWR

Table 4: List of antibodies.

Antibodies	Catalogue number	Company/Supplier
Anti-N cadherin blocking antibody	C3865	Sigma-Aldrich
Goat anti-mouse IgG Alexa Fluor® 488 secondary antibody	A11029	Invitrogen
Goat anti-rabbit IgG Alexa Fluor® 546	A11035	Invitrogen
MyoD antibody	MA1-41017	Thermo Scientific
Myogenin primary antibody	ab1835	Abcam
Myosin Heavy Chain primary antibody	MAB4470	R&D Systems
N- cadherin primary antibody (Immunofluorescence)	H-63	Santa Cruz Biotechnology
Recombinant human $VEGF_{165}$ blocking antibody	MAB293	R&D systems
Recombinant human IGF-1 blocking antibody	AF-291	R&D systems
ECL™ Anti-mouse IgG, Horeradish peroxidase	NA9310V	GE Healthcare
Factor VIII	CP 039B	Biocare
Biotinylated goat anti-rabbit IgG secondary antibody	BA-1000	Vector Labs
Anti-CD31 antibody	Ab64543	abcam

Table 5: List of cytokine and growth factor detection kits.

Cytokine/Growth factor Detection kits	Catalogue number	Company/Supplier
Rat FGF ELISA	MFB00	R&D systems
Rat HGF ELISA	MHG00	R&D systems
Rat IGF ELISA	MG100	R&D systems
Rat LIF ELISA	LS-F13295	LSBio
Rat VEGF ELISA	RRV00	R&D systems
Rat Cytokine array (34 cytokines)	AAR-CYT-2-8-RB	Ray Biotech
Rat Cytokine array (90 cytokines)	AAR-BLM-1-4-RB	Ray Biotech
Human IGF-1 ELISA	DG100	R&D systems
Human VEGF ELISA	DVE00	R&D systems

Appendix B: Efficacy of hIGF and hVEGF neutralizing antibodies

The effectiveness of neutralization antibodies (nAB) for hVEGF and hIGF was tested by measuring cytokine concentrations in media supplemented with growth factors +/- nAB. Fig a shows that addition of nAB efficiently neutralized recombinant growth factors. To ensure that the neutralization antibodies do not cross-react with rat MSC secreted paracrine factors in MSC-CM, concentrations of rVEGF and rIGF in MSC-CM +/- nAB were measured. Figure b shows that some cross-reactivity existed and the addition of nAB slightly reduced the detection of rVEGF and rIGF.

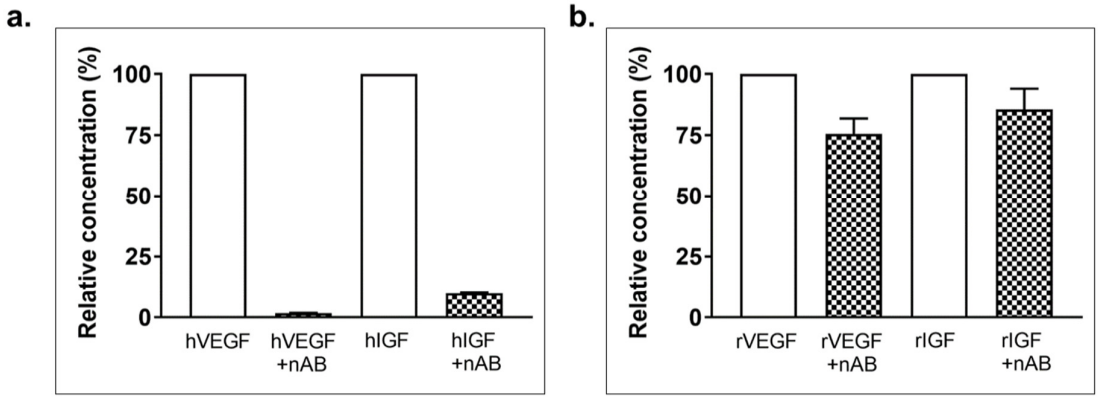

Appendix C: Efficacy of N-cadherin blocking antibody

The figure shows immunofluorescent images of N-cadherin (red) and DAPI (blue) stained MSCs cultured on 3D porous scaffolds without (a), and with (b), N-cadherin blocking [Scale bar =200 µm]. N cadherin blocking was carried out using an antibody produced in mouse (clone GC-4). The primary antibody used for immunofluorescence was produced in a rabbit host.

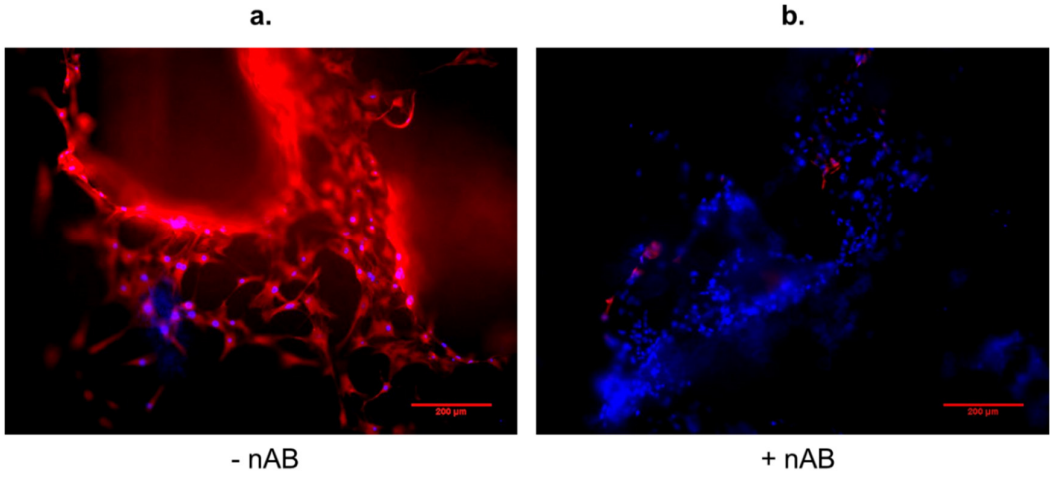

9. References

[1] Baoge L, Van Den Steen E, Rimbaut S, Philips N, Witvrouw E, Almqvist KF, et al. Treatment of Skeletal Muscle Injury: A Review. ISRN Orthopedics. 2012;2012:7.
[2] Järvinen TAH, Järvinen TLN, Kääriäinen M, Kalimo H, Järvinen M. Muscle Injuries: Biology and Treatment. The American journal of sports medicine. 2005;33:745-64.
[3] Sullivan DH, Carter WJ, Warr WR, Williams LH. Side effects resulting from the use of growth hormone and insulin-like growth factor-I as combined therapy to frail elderly patients. The journals of gerontology Series A, Biological sciences and medical sciences. 1998;53:M183-7.
[4] Toth JM, Boden SD, Burkus JK, Badura JM, Peckham SM, McKay WF. Short-term osteoclastic activity induced by locally high concentrations of recombinant human bone morphogenetic protein-2 in a cancellous bone environment. Spine. 2009;34:539-50.
[5] Doorn J, Moll G, Le Blanc K, van Blitterswijk C, de Boer J. Therapeutic applications of mesenchymal stromal cells: paracrine effects and potential improvements. Tissue Eng Part B Rev. 2012;18:101-15.
[6] Fan Y, Maley M, Beilharz M, Grounds M. Rapid death of injected myoblasts in myoblast transfer therapy. Muscle & nerve. 1996;19:853-60.
[7] Law PK, Bertorini TE, Goodwin TG, Chen M, Fang QW, Li HJ, et al. Dystrophin production induced by myoblast transfer therapy in Duchenne muscular dystrophy. Lancet. 1990;336:114-5.
[8] Moll G, Rasmusson-Duprez I, von Bahr L, Connolly-Andersen A-M, Elgue G, Funke L, et al. Are Therapeutic Human Mesenchymal Stromal Cells Compatible with Human Blood? Stem cells (Dayton, Ohio). 2012;30:1565-74.
[9] Gillies AR, Lieber RL. Structure and function of the skeletal muscle extracellular matrix. Muscle & nerve. 2011;44:318-31.
[10] Tedesco FS, Dellavalle A, Diaz-Manera J, Messina G, Cossu G. Repairing skeletal muscle: regenerative potential of skeletal muscle stem cells. The Journal of clinical investigation. 2010;120:11-9.
[11] Schiaffino S, Reggiani C. Fiber types in mammalian skeletal muscles. Physiological reviews. 2011;91:1447-531.
[12] Arnold L, Henry A, Poron F, Baba-Amer Y, van Rooijen N, Plonquet A, et al. Inflammatory monocytes recruited after skeletal muscle injury switch into antiinflammatory macrophages to support myogenesis. The Journal of experimental medicine. 2007;204:1057-69.
[13] Wang H, Melton DW, Porter L, Sarwar ZU, McManus LM, Shireman PK. Altered macrophage phenotype transition impairs skeletal muscle regeneration. The American journal of pathology. 2014;184:1167-84.
[14] Pillon NJ, Bilan PJ, Fink LN, Klip A. Cross-talk between skeletal muscle and immune cells: muscle-derived mediators and metabolic implications. American journal of physiology Endocrinology and metabolism. 2013;304:E453-65.
[15] Pallafacchina G, Blaauw B, Schiaffino S. Role of satellite cells in muscle growth and maintenance of muscle mass. Nutrition, metabolism, and cardiovascular diseases : NMCD. 2013;23 Suppl 1:S12-8.
[16] Starkey JD, Yamamoto M, Yamamoto S, Goldhamer DJ. Skeletal muscle satellite cells are committed to myogenesis and do not spontaneously adopt nonmyogenic fates. The journal of histochemistry and cytochemistry : official journal of the Histochemistry Society. 2011;59:33-46.
[17] Mauro A. Satellite cell of skeletal muscle fibers. The Journal of biophysical and biochemical cytology. 1961;9:493-5.

[18] Yin H, Price F, Rudnicki MA. Satellite cells and the muscle stem cell niche. Physiological reviews. 2013;93:23-67.
[19] Dumont NA, Wang YX, Rudnicki MA. Intrinsic and extrinsic mechanisms regulating satellite cell function. Development (Cambridge, England). 2015;142:1572-81.
[20] Urciuolo A, Quarta M, Morbidoni V, Gattazzo F, Molon S, Grumati P, et al. Collagen VI regulates satellite cell self-renewal and muscle regeneration. Nat Commun. 2013;4:1964.
[21] Montarras D, Morgan J, Collins C, Relaix F, Zaffran S, Cumano A, et al. Direct isolation of satellite cells for skeletal muscle regeneration. Science. 2005;309:2064-7.
[22] Gilbert PM, Havenstrite KL, Magnusson KEG, Sacco A, Leonardi NA, Kraft P, et al. Substrate Elasticity Regulates Skeletal Muscle Stem Cell Self-Renewal in Culture. Science. 2010;329:1078-81.
[23] Joe AWB, Yi L, Natarajan A, Le Grand F, So L, Wang J, et al. Muscle injury activates resident fibro/adipogenic progenitors that facilitate myogenesis. Nat Cell Biol. 2010;12:153-63.
[24] Uezumi A, Fukada S-i, Yamamoto N, Takeda Si, Tsuchida K. Mesenchymal progenitors distinct from satellite cells contribute to ectopic fat cell formation in skeletal muscle. Nat Cell Biol. 2010;12:143-52.
[25] Heredia JE, Mukundan L, Chen FM, Mueller AA, Deo RC, Locksley RM, et al. Type 2 innate signals stimulate fibro/adipogenic progenitors to facilitate muscle regeneration. Cell. 2013;153:376-88.
[26] Bentzinger CF, Wang YX, Dumont NA, Rudnicki MA. Cellular dynamics in the muscle satellite cell niche. EMBO reports. 2013;14:1062-72.
[27] Mackay AM, Beck SC, Murphy JM, Barry FP, Chichester CO, Pittenger MF. Chondrogenic differentiation of cultured human mesenchymal stem cells from marrow. Tissue Eng. 1998;4:415-28.
[28] Pittenger MF, Mackay AM, Beck SC, Jaiswal RK, Douglas R, Mosca JD, et al. Multilineage potential of adult human mesenchymal stem cells. Science. 1999;284:143-7.
[29] Zuk PA, Zhu M, Mizuno H, Huang J, Futrell JW, Katz AJ, et al. Multilineage cells from human adipose tissue: implications for cell-based therapies. Tissue Eng. 2001;7:211-28.
[30] Jackson WM, Nesti LJ, Tuan RS. Potential therapeutic applications of muscle-derived mesenchymal stem and progenitor cells. Expert opinion on biological therapy. 2010;10:505-17.
[31] Barry F, Murphy M. Mesenchymal stem cells in joint disease and repair. Nat Rev Rheumatol. 2013;9:584-94.
[32] Dominici M, Le Blanc K, Mueller I, Slaper-Cortenbach I, Marini FC, Krause DS, et al. Minimal criteria for defining multipotent mesenchymal stromal cells. The International Society for Cellular Therapy position statement. Cytotherapy.8:315-7.
[33] Han F, Wang CY, Yang L, Zhan SD, Zhang M, Tian K. Contribution of murine bone marrow mesenchymal stem cells to pancreas regeneration after partial pancreatectomy in mice. Cell biology international. 2012;36:823-31.
[34] Qian H, Yang H, Xu W, Yan Y, Chen Q, Zhu W, et al. Bone marrow mesenchymal stem cells ameliorate rat acute renal failure by differentiation into renal tubular epithelial-like cells. International journal of molecular medicine. 2008;22:325-32.
[35] Ferrari G, Cusella-De Angelis G, Coletta M, Paolucci E, Stornaiuolo A, Cossu G, et al. Muscle regeneration by bone marrow-derived myogenic progenitors. Science. 1998;279:1528-30.
[36] Horwitz EM, Prockop DJ, Fitzpatrick LA, Koo WW, Gordon PL, Neel M, et al. Transplantability and therapeutic effects of bone marrow-derived mesenchymal cells in children with osteogenesis imperfecta. Nat Med. 1999;5:309-13.

[37] Kuroda R, Ishida K, Matsumoto T, Akisue T, Fujioka H, Mizuno K, et al. Treatment of a full-thickness articular cartilage defect in the femoral condyle of an athlete with autologous bone-marrow stromal cells. Osteoarthritis and cartilage. 2007;15:226-31.
[38] Chen S, Liu Z, Tian N, Zhang J, Yei F, Duan B, et al. Intracoronary transplantation of autologous bone marrow mesenchymal stem cells for ischemic cardiomyopathy due to isolated chronic occluded left anterior descending artery. The Journal of invasive cardiology. 2006;18:552-6.
[39] Prockop DJ, Kota DJ, Bazhanov N, Reger RL. Evolving paradigms for repair of tissues by adult stem/progenitor cells (MSCs). J Cell Mol Med. 2010;14:2190-9.
[40] von Bahr L, Batsis I, Moll G, Hagg M, Szakos A, Sundberg B, et al. Analysis of tissues following mesenchymal stromal cell therapy in humans indicates limited long-term engraftment and no ectopic tissue formation. Stem cells (Dayton, Ohio). 2012;30:1575-8.
[41] Meirelles Lda S, Fontes AM, Covas DT, Caplan AI. Mechanisms involved in the therapeutic properties of mesenchymal stem cells. Cytokine Growth Factor Rev. 2009;20:419-27.
[42] Madrigal M, Rao KS, Riordan NH. A review of therapeutic effects of mesenchymal stem cell secretions and induction of secretory modification by different culture methods. Journal of Translational Medicine. 2014;12:260.
[43] Katagiri W, Osugi M, Kawai T, Hibi H. First-in-human study and clinical case reports of the alveolar bone regeneration with the secretome from human mesenchymal stem cells. Head & face medicine. 2016;12:5.
[44] Osugi M, Katagiri W, Yoshimi R, Inukai T, Hibi H, Ueda M. Conditioned media from mesenchymal stem cells enhanced bone regeneration in rat calvarial bone defects. Tissue Eng Part A. 2012;18:1479-89.
[45] Katagiri W, Osugi M, Kinoshita K, Hibi H. Conditioned Medium From Mesenchymal Stem Cells Enhances Early Bone Regeneration After Maxillary Sinus Floor Elevation in Rabbits. Implant dentistry. 2015;24:657-63.
[46] van Poll D, Parekkadan B, Cho CH, Berthiaume F, Nahmias Y, Tilles AW, et al. Mesenchymal stem cell-derived molecules directly modulate hepatocellular death and regeneration in vitro and in vivo. Hepatology. 2008;47:1634-43.
[47] Linero I, Chaparro O. Paracrine Effect of Mesenchymal Stem Cells Derived from Human Adipose Tissue in Bone Regeneration. PLOS ONE. 2014;9:e107001.
[48] Murry CE, Soonpaa MH, Reinecke H, Nakajima H, Nakajima HO, Rubart M, et al. Haematopoietic stem cells do not transdifferentiate into cardiac myocytes in myocardial infarcts. Nature. 2004;428:664-8.
[49] Caplan AI, Dennis JE. Mesenchymal stem cells as trophic mediators. J Cell Biochem. 2006;98:1076-84.
[50] Shi Y, Su J, Roberts AI, Shou P, Rabson AB, Ren G. How mesenchymal stem cells interact with tissue immune responses. Trends in Immunology. 2012;33:136-43.
[51] Lee RH, Pulin AA, Seo MJ, Kota DJ, Ylostalo J, Larson BL, et al. Intravenous hMSCs improve myocardial infarction in mice because cells embolized in lung are activated to secrete the anti-inflammatory protein TSG-6. Cell stem cell. 2009;5:54-63.
[52] Gao F, Chiu SM, Motan DAL, Zhang Z, Chen L, Ji HL, et al. Mesenchymal stem cells and immunomodulation: current status and future prospects. Cell death & disease. 2016;7:e2062.
[53] Newman RE, Yoo D, LeRoux MA, Danilkovitch-Miagkova A. Treatment of inflammatory diseases with mesenchymal stem cells. Inflammation & allergy drug targets. 2009;8:110-23.
[54] Zimmermann JA, McDevitt TC. Pre-conditioning mesenchymal stromal cell spheroids for immunomodulatory paracrine factor secretion. Cytotherapy. 2014;16:331-45.

[55] Ho SS, Murphy KC, Binder BY, Vissers CB, Leach JK. Increased Survival and Function of Mesenchymal Stem Cell Spheroids Entrapped in Instructive Alginate Hydrogels. Stem cells translational medicine. 2016;5:773-81.
[56] Beier JP, Bitto FF, Lange C, Klumpp D, Arkudas A, Bleiziffer O, et al. Myogenic differentiation of mesenchymal stem cells co-cultured with primary myoblasts. Cell biology international. 2011;35:397-406.
[57] Gang EJ, Jeong JA, Hong SH, Hwang SH, Kim SW, Yang IH, et al. Skeletal myogenic differentiation of mesenchymal stem cells isolated from human umbilical cord blood. Stem cells (Dayton, Ohio). 2004;22:617-24.
[58] Winkler T, von Roth P, Schuman MR, Sieland K, Stoltenburg-Didinger G, Taupitz M, et al. In vivo visualization of locally transplanted mesenchymal stem cells in the severely injured muscle in rats. Tissue Eng Part A. 2008;14:1149-60.
[59] LaBarge MA, Blau HM. Biological progression from adult bone marrow to mononucleate muscle stem cell to multinucleate muscle fiber in response to injury. Cell. 2002;111:589-601.
[60] Matziolis G, Winkler T, Schaser K, Wiemann M, Krocker D, Tuischer J, et al. Autologous bone marrow-derived cells enhance muscle strength following skeletal muscle crush injury in rats. Tissue Eng. 2006;12:361-7.
[61] von Roth P, Duda GN, Radojewski P, Preininger B, Perka C, Winkler T. Mesenchymal stem cell therapy following muscle trauma leads to improved muscular regeneration in both male and female rats. Gender medicine. 2012;9:129-36.
[62] Winkler T, von Roth P, Matziolis G, Mehta M, Perka C, Duda GN. Dose-response relationship of mesenchymal stem cell transplantation and functional regeneration after severe skeletal muscle injury in rats. Tissue Eng Part A. 2009;15:487-92.
[63] Scott M. 32,000 years of sutures. NATNews. 1983;20:15-7.
[64] Bobbio A. The first endosseous alloplastic implant in the history of man. Bulletin of the history of dentistry. 1972;20:1-6.
[65] Huebsch N, Mooney DJ. Inspiration and application in the evolution of biomaterials. Nature. 2009;462:426-32.
[66] Narayan RJ. The next generation of biomaterial development. Philosophical Transactions of the Royal Society A: Mathematical, Physical and Engineering Sciences. 2010;368:1831-7.
[67] Ducheyne P, Cuckler JM. Bioactive ceramic prosthetic coatings. Clinical orthopaedics and related research. 1992:102-14.
[68] Colombo A, Karvouni E. Biodegradable Stents. “Fulfilling the Mission and Stepping Away”. 2000;102:371-3.
[69] Hench LL, Polak JM. Third-Generation Biomedical Materials. Science. 2002;295:1014-7.
[70] Tibbitt MW, Rodell CB, Burdick JA, Anseth KS. Progress in material design for biomedical applications. Proceedings of the National Academy of Sciences. 2015;112:14444-51.
[71] Nair LS, Laurencin CT. Biodegradable polymers as biomaterials. Progress in Polymer Science. 2007;32:762-98.
[72] Hubbell JA, Thomas SN, Swartz MA. Materials engineering for immunomodulation. Nature. 2009;462:449-60.
[73] Li J, Mooney DJ. Designing hydrogels for controlled drug delivery. Nature Reviews Materials. 2016;1:16071.
[74] Zhao X, Kim J, Cezar CA, Huebsch N, Lee K, Bouhadir K, et al. Active scaffolds for on-demand drug and cell delivery. Proceedings of the National Academy of Sciences. 2011;108:67-72.
[75] Engler AJ, Sen S, Sweeney HL, Discher DE. Matrix elasticity directs stem cell lineage specification. Cell. 2006;126:677-89.

[76] Vincent LG, Choi YS, Alonso-Latorre B, del Alamo JC, Engler AJ. Mesenchymal stem cell durotaxis depends on substrate stiffness gradient strength. Biotechnology journal. 2013;8:472-84.
[77] Pumberger M, Qazi TH, Ehrentraut MC, Textor M, Kueper J, Stoltenburg-Didinger G, et al. Synthetic niche to modulate regenerative potential of MSCs and enhance skeletal muscle regeneration. Biomaterials. 2016;99:95-108.
[78] Lutolf MP, Hubbell JA. Synthetic biomaterials as instructive extracellular microenvironments for morphogenesis in tissue engineering. Nat Biotech. 2005;23:47-55.
[79] Balint R, Cassidy NJ, Cartmell SH. Conductive polymers: Towards a smart biomaterial for tissue engineering. Acta Biomaterialia. 2014;10:2341-53.
[80] O'Brien FJ. Biomaterials & scaffolds for tissue engineering. Materials Today. 2011;14:88-95.
[81] Asti A, Gioglio L. Natural and synthetic biodegradable polymers: different scaffolds for cell expansion and tissue formation.37:187.
[82] Kohane DS, Langer R. Polymeric Biomaterials in Tissue Engineering. Pediatr Res. 2008;63:487-91.
[83] Rai R, Tallawi M, Grigore A, Boccaccini AR. Synthesis, properties and biomedical applications of poly(glycerol sebacate) (PGS): A review. Progress in Polymer Science. 2012;37:1051-78.
[84] Malafaya PB, Silva GA, Reis RL. Natural–origin polymers as carriers and scaffolds for biomolecules and cell delivery in tissue engineering applications. Advanced Drug Delivery Reviews. 2007;59:207-33.
[85] Hoare TR, Kohane DS. Hydrogels in drug delivery: Progress and challenges. Polymer. 2008;49:1993-2007.
[86] Nguyen KT, West JL. Photopolymerizable hydrogels for tissue engineering applications. Biomaterials. 2002;23:4307-14.
[87] Tibbitt MW, Anseth KS. Hydrogels as extracellular matrix mimics for 3D cell culture. Biotechnology and Bioengineering. 2009;103:655-63.
[88] Rosales AM, Anseth KS. The design of reversible hydrogels to capture extracellular matrix dynamics. Nature Reviews Materials. 2016;1:15012.
[89] Lee KY, Mooney DJ. Hydrogels for Tissue Engineering. Chemical reviews. 2001;101:1869-80.
[90] Kamelger FS, Marksteiner R, Margreiter E, Klima G, Wechselberger G, Hering S, et al. A comparative study of three different biomaterials in the engineering of skeletal muscle using a rat animal model. Biomaterials. 2004;25:1649-55.
[91] Bandyopadhyay B, Shah V, Soram M, Viswanathan C, Ghosh D. In vitro and in vivo evaluation of L-lactide/ε-caprolactone copolymer scaffold to support myoblast growth and differentiation. Biotechnology Progress. 2013;29:197-205.
[92] Dugan JM, Collins RF, Gough JE, Eichhorn SJ. Oriented surfaces of adsorbed cellulose nanowhiskers promote skeletal muscle myogenesis. Acta Biomaterialia. 2013;9:4707-15.
[93] Huang NF, Patel S, Thakar RG, Wu J, Hsiao BS, Chu B, et al. Myotube Assembly on Nanofibrous and Micropatterned Polymers. Nano Letters. 2006;6:537-42.
[94] Choi JS, Lee SJ, Christ GJ, Atala A, Yoo JJ. The influence of electrospun aligned poly(ε-caprolactone)/collagen nanofiber meshes on the formation of self-aligned skeletal muscle myotubes. Biomaterials. 2008;29:2899-906.
[95] Ma PX, Zhang R. Microtubular architecture of biodegradable polymer scaffolds. J Biomed Mater Res. 2001;56:469-77.
[96] Jana S, Cooper A, Zhang M. Chitosan Scaffolds with Unidirectional Microtubular Pores for Large Skeletal Myotube Generation. Advanced Healthcare Materials. 2013;2:557-61.

[97] Kroehne V, Heschel I, Schügner F, Lasrich D, Bartsch JW, Jockusch H. Use of a novel collagen matrix with oriented pore structure for muscle cell differentiation in cell culture and in grafts. Journal of Cellular and Molecular Medicine. 2008;12:1640-8.
[98] Patel A, Mukundan S, Wang W, Karumuri A, Sant V, Mukhopadhyay SM, et al. Carbon-based hierarchical scaffolds for myoblast differentiation: Synergy between nano-functionalization and alignment. Acta Biomaterialia. 2016;32:77-88.
[99] Chaturvedi V, Naskar D, Kinnear BF, Grenik E, Dye DE, Grounds MD, et al. Silk fibroin scaffolds with muscle-like elasticity support in vitro differentiation of human skeletal muscle cells. Journal of Tissue Engineering and Regenerative Medicine. 2016:n/a-n/a.
[100] Qazi TH, Rai R, Boccaccini AR. Tissue engineering of electrically responsive tissues using polyaniline based polymers: A review. Biomaterials. 2014;35:9068-86.
[101] Jun I, Jeong S, Shin H. The stimulation of myoblast differentiation by electrically conductive sub-micron fibers. Biomaterials. 2009;30:2038-47.
[102] Chen M-C, Sun Y-C, Chen Y-H. Electrically conductive nanofibers with highly oriented structures and their potential application in skeletal muscle tissue engineering. Acta Biomaterialia. 2013;9:5562-72.
[103] Ku SH, Lee SH, Park CB. Synergic effects of nanofiber alignment and electroactivity on myoblast differentiation. Biomaterials. 2012;33:6098-104.
[104] Patel A, Xue Y, Mukundan S, Rohan LC, Sant V, Stolz DB, et al. Cell-Instructive Graphene-Containing Nanocomposites Induce Multinucleated Myotube Formation. Annals of Biomedical Engineering. 2016;44:2036-48.
[105] Cezar CA, Mooney DJ. Biomaterial-based delivery for skeletal muscle repair. Adv Drug Deliv Rev. 2015;84:188-97.
[106] Borselli C, Cezar CA, Shvartsman D, Vandenburgh HH, Mooney DJ. The role of multifunctional delivery scaffold in the ability of cultured myoblasts to promote muscle regeneration. Biomaterials. 2011;32:8905-14.
[107] Hill E, Boontheekul T, Mooney DJ. Designing scaffolds to enhance transplanted myoblast survival and migration. Tissue Eng. 2006;12:1295-304.
[108] Hill E, Boontheekul T, Mooney DJ. Regulating activation of transplanted cells controls tissue regeneration. Proceedings of the National Academy of Sciences of the United States of America. 2006;103:2494-9.
[109] Borselli C, Cezar CA, Shvartsman D, Vandenburgh HH, Mooney DJ. The role of multifunctional delivery scaffold in the ability of cultured myoblasts to promote muscle regeneration. Biomaterials. 2011;32:8905-14.
[110] Ma J, Holden K, Zhu J, Pan H, Li Y. The application of three-dimensional collagen-scaffolds seeded with myoblasts to repair skeletal muscle defects. J Biomed Biotechnol. 2011;812135:12.
[111] Huang NF, Patel S, Thakar RG, Wu J, Hsiao BS, Chu B, et al. Myotube assembly on nanofibrous and micropatterned polymers. Nano Lett. 2006;6:537-42.
[112] Dugan JM, Collins RF, Gough JE, Eichhorn SJ. Oriented surfaces of adsorbed cellulose nanowhiskers promote skeletal muscle myogenesis. Acta Biomater. 2013;9:4707-15.
[113] Beier JP, Klumpp D, Rudisile M, Dersch R, Wendorff JH, Bleiziffer O, et al. Collagen matrices from sponge to nano: new perspectives for tissue engineering of skeletal muscle. BMC Biotechnol. 2009;9:1472-6750.
[114] Choi JS, Lee SJ, Christ GJ, Atala A, Yoo JJ. The influence of electrospun aligned poly(epsilon-caprolactone)/collagen nanofiber meshes on the formation of self-aligned skeletal muscle myotubes. Biomaterials. 2008;29:2899-906.
[115] Aviss KJ, Gough JE, Downes S. Aligned electrospun polymer fibres for skeletal muscle regeneration. Eur Cell Mater. 2010;19:193-204.

[116] Jun I, Jeong S, Shin H. The stimulation of myoblast differentiation by electrically conductive sub-micron fibers. Biomaterials. 2009;30:2038-47.
[117] Chen MC, Sun YC, Chen YH. Electrically conductive nanofibers with highly oriented structures and their potential application in skeletal muscle tissue engineering. Acta Biomater. 2013;9:5562-72.
[118] Ku SH, Lee SH, Park CB. Synergic effects of nanofiber alignment and electroactivity on myoblast differentiation. Biomaterials. 2012;33:6098-104.
[119] Page RL, Malcuit C, Vilner L, Vojtic I, Shaw S, Hedblom E, et al. Restoration of skeletal muscle defects with adult human cells delivered on fibrin microthreads. Tissue Eng Part A. 2011;17:2629-40.
[120] Huang NF, Lee RJ, Li S. Engineering of aligned skeletal muscle by micropatterning. Am J Transl Res. 2010;2:43-55.
[121] Neumann T, Hauschka SD, Sanders JE. Tissue engineering of skeletal muscle using polymer fiber arrays. Tissue Eng. 2003;9:995-1003.
[122] Hosseini V, Ahadian S, Ostrovidov S, Camci-Unal G, Chen S, Kaji H, et al. Engineered contractile skeletal muscle tissue on a microgrooved methacrylated gelatin substrate. Tissue Eng Part A. 2012;18:2453-65.
[123] Monge C, Ren K, Berton K, Guillot R, Peyrade D, Picart C. Engineering muscle tissues on microstructured polyelectrolyte multilayer films. Tissue Eng Part A. 2012;18:1664-76.
[124] Zhao Y, Zeng H, Nam J, Agarwal S. Fabrication of skeletal muscle constructs by topographic activation of cell alignment. Biotechnol Bioeng. 2009;102:624-31.
[125] Natsu K, Ochi M, Mochizuki Y, Hachisuka H, Yanada S, Yasunaga Y. Allogeneic bone marrow-derived mesenchymal stromal cells promote the regeneration of injured skeletal muscle without differentiation into myofibers. Tissue Eng. 2004;10:1093-112.
[126] Wang L, Cao L, Shansky J, Wang Z, Mooney D, Vandenburgh H. Minimally invasive approach to the repair of injured skeletal muscle with a shape-memory scaffold. Mol Ther. 2014;22:1441-9.
[127] Liu J, Xu HH, Zhou H, Weir MD, Chen Q, Trotman CA. Human umbilical cord stem cell encapsulation in novel macroporous and injectable fibrin for muscle tissue engineering. Acta Biomater. 2013;9:4688-97.
[128] Rossi CA, Flaibani M, Blaauw B, Pozzobon M, Figallo E, Reggiani C, et al. In vivo tissue engineering of functional skeletal muscle by freshly isolated satellite cells embedded in a photopolymerizable hydrogel. Faseb J. 2011;25:2296-304.
[129] Beier JP, Stern-Straeter J, Foerster VT, Kneser U, Stark GB, Bach AD. Tissue engineering of injectable muscle: three-dimensional myoblast-fibrin injection in the syngeneic rat animal model. Plast Reconstr Surg. 2006;118:1113-21.
[130] Kim MH, Hong HN, Hong JP, Park CJ, Kwon SW, Kim SH, et al. The effect of VEGF on the myogenic differentiation of adipose tissue derived stem cells within thermosensitive hydrogel matrices. Biomaterials. 2010;31:1213-8.
[131] Liu J, Zhou H, Weir MD, Xu HH, Chen Q, Trotman CA. Fast-degradable microbeads encapsulating human umbilical cord stem cells in alginate for muscle tissue engineering. Tissue Eng Part A. 2012;18:2303-14.
[132] Kuraitis D, Zhang P, Zhang Y, Padavan DT, McEwan K, Sofrenovic T, et al. A stromal cell-derived factor-1 releasing matrix enhances the progenitor cell response and blood vessel growth in ischaemic skeletal muscle. Eur Cell Mater. 2011;22:109-23.
[133] Rowley JA, Madlambayan G, Mooney DJ. Alginate hydrogels as synthetic extracellular matrix materials. Biomaterials. 1999;20:45-53.
[134] Kong HJ, Kaigler D, Kim K, Mooney DJ. Controlling rigidity and degradation of alginate hydrogels via molecular weight distribution. Biomacromolecules. 2004;5:1720-7.

[135] Lee EJ, Choi EK, Kang SK, Kim GH, Park JY, Kang HJ, et al. N-cadherin determines individual variations in the therapeutic efficacy of human umbilical cord blood-derived mesenchymal stem cells in a rat model of myocardial infarction. Mol Ther. 2012;20:155-67.
[136] Liang CC, Park AY, Guan JL. In vitro scratch assay: a convenient and inexpensive method for analysis of cell migration in vitro. Nature protocols. 2007;2:329-33.
[137] Geback T, Schulz MM, Koumoutsakos P, Detmar M. TScratch: a novel and simple software tool for automated analysis of monolayer wound healing assays. BioTechniques. 2009;46:265-74.
[138] Geisler S, Textor M, Schmidt-Bleek K, Klein O, Thiele M, Ellinghaus A, et al. In serum veritas[mdash]in serum sanitas[quest] Cell non-autonomous aging compromises differentiation and survival of mesenchymal stromal cells via the oxidative stress pathway. Cell death & disease. 2013;4:e970.
[139] Fiaschi T, Cirelli D, Comito G, Gelmini S, Ramponi G, Serio M, et al. Globular adiponectin induces differentiation and fusion of skeletal muscle cells. Cell Res. 2009;19:584-97.
[140] Floss T, Arnold HH, Braun T. A role for FGF-6 in skeletal muscle regeneration. Genes & development. 1997;11:2040-51.
[141] Hiatt K, Lewis D, Shew M, Bijangi-Vishehsaraei K, Halum S. Ciliary neurotrophic factor (CNTF) promotes skeletal muscle progenitor cell (MPC) viability via the phosphatidylinositol 3-kinase-Akt pathway. J Tissue Eng Regen Med. 2014;8:963-8.
[142] Hunt LC, White J. The Role of Leukemia Inhibitory Factor Receptor Signaling in Skeletal Muscle Growth, Injury and Disease. Advances in experimental medicine and biology. 2016;900:45-59.
[143] Kurek JB, Bower JJ, Romanella M, Koentgen F, Murphy M, Austin L. The role of leukemia inhibitory factor in skeletal muscle regeneration. Muscle & nerve. 1997;20:815-22.
[144] Song YH, Song JL, Delafontaine P, Godard MP. The therapeutic potential of IGF-I in skeletal muscle repair. Trends in endocrinology and metabolism: TEM. 2013;24:310-9.
[145] Gal-Levi R, Leshem Y, Aoki S, Nakamura T, Halevy O. Hepatocyte growth factor plays a dual role in regulating skeletal muscle satellite cell proliferation and differentiation. Biochimica et Biophysica Acta (BBA) - Molecular Cell Research. 1998;1402:39-51.
[146] Sheehan SM, Allen RE. Skeletal muscle satellite cell proliferation in response to members of the fibroblast growth factor family and hepatocyte growth factor. J Cell Physiol. 1999;181:499-506.
[147] Sart S, Tsai AC, Li Y, Ma T. Three-dimensional aggregates of mesenchymal stem cells: cellular mechanisms, biological properties, and applications. Tissue Eng Part B Rev. 2014;20:365-80.
[148] Zhang Q, Nguyen AL, Shi S, Hill C, Wilder-Smith P, Krasieva TB, et al. Three-dimensional spheroid culture of human gingiva-derived mesenchymal stem cells enhances mitigation of chemotherapy-induced oral mucositis. Stem cells and development. 2012;21:937-47.
[149] Ranganath Sudhir H, Levy O, Inamdar Maneesha S, Karp Jeffrey M. Harnessing the Mesenchymal Stem Cell Secretome for the Treatment of Cardiovascular Disease. Cell stem cell. 2012;10:244-58.
[150] Zullo JA, Nadel EP, Rabadi MM, Baskind MJ, Rajdev MA, Demaree CM, et al. The Secretome of Hydrogel-Coembedded Endothelial Progenitor Cells and Mesenchymal Stem Cells Instructs Macrophage Polarization in Endotoxemia. Stem cells translational medicine. 2015;4:852-61.
[151] Wu Y, Peng Y, Gao D, Feng C, Yuan X, Li H, et al. Mesenchymal stem cells suppress fibroblast proliferation and reduce skin fibrosis through a TGF-beta3-dependent activation. The international journal of lower extremity wounds. 2015;14:50-62.

[152] Sun H, Benardais K, Stanslowsky N, Thau-Habermann N, Hensel N, Huang D, et al. Therapeutic potential of mesenchymal stromal cells and MSC conditioned medium in Amyotrophic Lateral Sclerosis (ALS)--in vitro evidence from primary motor neuron cultures, NSC-34 cells, astrocytes and microglia. PLoS One. 2013;8:e72926.
[153] Hsieh JY, Wang HW, Chang SJ, Liao KH, Lee IH, Lin WS, et al. Mesenchymal stem cells from human umbilical cord express preferentially secreted factors related to neuroprotection, neurogenesis, and angiogenesis. PLoS One. 2013;8:e72604.
[154] Teixeira FG, Panchalingam KM, Assunção-Silva R, Serra SC, Mendes-Pinheiro B, Patrício P, et al. Modulation of the Mesenchymal Stem Cell Secretome Using Computer-Controlled Bioreactors: Impact on Neuronal Cell Proliferation, Survival and Differentiation. Scientific Reports. 2016;6:27791.
[155] Glaeser JD, Geissler S, Ode A, Schipp CJ, Matziolis G, Taylor WR, et al. Modulation of matrix metalloprotease-2 levels by mechanical loading of three-dimensional mesenchymal stem cell constructs: impact on in vitro tube formation. Tissue Eng Part A. 2010;16:3139-48.
[156] Schinkothe T, Bloch W, Schmidt A. In vitro secreting profile of human mesenchymal stem cells. Stem cells and development. 2008;17:199-206.
[157] Xu J, Wang B, Sun Y, Wu T, Liu Y, Zhang J, et al. Human fetal mesenchymal stem cell secretome enhances bone consolidation in distraction osteogenesis. Stem Cell Res Ther. 2016;7:134.
[158] Fischbach C, Kong HJ, Hsiong SX, Evangelista MB, Yuen W, Mooney DJ. Cancer cell angiogenic capability is regulated by 3D culture and integrin engagement. Proc Natl Acad Sci U S A. 2009;106:399-404.
[159] Abdeen AA, Weiss JB, Lee J, Kilian KA. Matrix composition and mechanics direct proangiogenic signaling from mesenchymal stem cells. Tissue Eng Part A. 2014;20:2737-45.
[160] Borselli C, Storrie H, Benesch-Lee F, Shvartsman D, Cezar C, Lichtman JW, et al. Functional muscle regeneration with combined delivery of angiogenesis and myogenesis factors. Proceedings of the National Academy of Sciences. 2010;107:3287-92.
[161] Arlov Ø, Aachmann FL, Sundan A, Espevik T, Skjåk-Bræk G. Heparin-Like Properties of Sulfated Alginates with Defined Sequences and Sulfation Degrees. Biomacromolecules. 2014;15:2744-50.
[162] Freeman I, Kedem A, Cohen S. The effect of sulfation of alginate hydrogels on the specific binding and controlled release of heparin-binding proteins. Biomaterials. 2008;29:3260-8.
[163] Chinen N, Tanihara M, Nakagawa M, Shinozaki K, Yamamoto E, Mizushima Y, et al. Action of microparticles of heparin and alginate crosslinked gel when used as injectable artificial matrices to stabilize basic fibroblast growth factor and induce angiogenesis by controlling its release. J Biomed Mater Res A. 2003;67:61-8.
[164] Li Z, Qu T, Ding C, Ma C, Sun H, Li S, et al. Injectable gelatin derivative hydrogels with sustained vascular endothelial growth factor release for induced angiogenesis. Acta Biomater. 2015;13:88-100.
[165] Rettinger CL, Fourcaudot AB, Hong SJ, Mustoe TA, Hale RG, Leung KP. In vitro characterization of scaffold-free three-dimensional mesenchymal stem cell aggregates. Cell and tissue research. 2014;358:395-405.
[166] Lee EJ, Park SJ, Kang SK, Kim GH, Kang HJ, Lee SW, et al. Spherical bullet formation via E-cadherin promotes therapeutic potency of mesenchymal stem cells derived from human umbilical cord blood for myocardial infarction. Mol Ther. 2012;20:1424-33.
[167] Bartosh TJ, Ylostalo JH, Mohammadipoor A, Bazhanov N, Coble K, Claypool K, et al. Aggregation of human mesenchymal stromal cells (MSCs) into 3D spheroids enhances their antiinflammatory properties. Proc Natl Acad Sci U S A. 2010;107:13724-9.

[168] Bartosh TJ, Ylostalo JH, Bazhanov N, Kuhlman J, Prockop DJ. Dynamic compaction of human mesenchymal stem/precursor cells into spheres self-activates caspase-dependent IL1 signaling to enhance secretion of modulators of inflammation and immunity (PGE2, TSG6, and STC1). Stem cells (Dayton, Ohio). 2013;31:2443-56.
[169] Seib FP, Prewitz M, Werner C, Bornhauser M. Matrix elasticity regulates the secretory profile of human bone marrow-derived multipotent mesenchymal stromal cells (MSCs). Biochem Biophys Res Commun. 2009;389:663-7.
[170] Chandler EM, Berglund CM, Lee JS, Polacheck WJ, Gleghorn JP, Kirby BJ, et al. Stiffness of photocrosslinked RGD-alginate gels regulates adipose progenitor cell behavior. Biotechnol Bioeng. 2011;108:1683-92.
[171] Marklein RA, Soranno DE, Burdick JA. Magnitude and presentation of mechanical signals influence adult stem cell behavior in 3-dimensional macroporous hydrogels. Soft Matter. 2012;8:8113-20.
[172] Silva NA, Moreira J, Ribeiro-Samy S, Gomes ED, Tam RY, Shoichet MS, et al. Modulation of bone marrow mesenchymal stem cell secretome by ECM-like hydrogels. Biochimie. 2013;95:2314-9.
[173] Jose S, Hughbanks ML, Binder BY, Ingavle GC, Leach JK. Enhanced trophic factor secretion by mesenchymal stem/stromal cells with Glycine-Histidine-Lysine (GHK)-modified alginate hydrogels. Acta Biomater. 2014;10:1955-64.
[174] Cai L, Dewi RE, Goldstone AB, Cohen JE, Steele AN, Woo YJ, et al. Regulating Stem Cell Secretome Using Injectable Hydrogels with In Situ Network Formation. Adv Healthc Mater. 2016;5:2758-64.
[175] Thomas D, Fontana G, Chen X, Sanz-Nogués C, Zeugolis DI, Dockery P, et al. A shape-controlled tuneable microgel platform to modulate angiogenic paracrine responses in stem cells. Biomaterials. 2014;35:8757-66.
[176] Follin B, Juhl M, Cohen S, Pedersen AE, Gad M, Kastrup J, et al. Human adipose-derived stromal cells in a clinically applicable injectable alginate hydrogel: Phenotypic and immunomodulatory evaluation. Cytotherapy. 2015;17:1104-18.
[177] Chaudhuri O, Gu L, Darnell M, Klumpers D, Bencherif SA, Weaver JC, et al. Substrate stress relaxation regulates cell spreading. Nature Communications. 2015;6:6365.
[178] Chaudhuri O, Gu L, Klumpers D, Darnell M, Bencherif SA, Weaver JC, et al. Hydrogels with tunable stress relaxation regulate stem cell fate and activity. Nat Mater. 2016;15:326-34.
[179] Nava MM, Raimondi MT, Pietrabissa R. Controlling Self-Renewal and Differentiation of Stem Cells via Mechanical Cues. Journal of Biomedicine and Biotechnology. 2012;2012:12.
[180] Dingal PCDP, Discher DE. Combining insoluble and soluble factors to steer stem cell fate. Nat Mater. 2014;13:532-7.
[181] Jaiswal N, Haynesworth SE, Caplan AI, Bruder SP. Osteogenic differentiation of purified, culture-expanded human mesenchymal stem cells in vitro. J Cell Biochem. 1997;64:295-312.
[182] Liu Y, Wang L, Kikuiri T, Akiyama K, Chen C, Xu X, et al. Mesenchymal stem cell-based tissue regeneration is governed by recipient T lymphocytes via IFN-[gamma] and TNF-[alpha]. Nat Med. 2011;17:1594-601.
[183] Baraniak PR, McDevitt TC. Stem cell paracrine actions and tissue regeneration. Regen Med. 2010;5:121-43.
[184] Sart S, Ma T, Li Y. Preconditioning stem cells for in vivo delivery. BioResearch open access. 2014;3:137-49.
[185] Xue X, Liu Y, Zhang J, Liu T, Yang Z, Wang H. Bcl-xL Genetic Modification Enhanced the Therapeutic Efficacy of Mesenchymal Stem Cell Transplantation in the Treatment of Heart Infarction. Stem Cells Int. 2015;2015:176409.

[186] Kim SH, Moon HH, Kim HA, Hwang KC, Lee M, Choi D. Hypoxia-inducible vascular endothelial growth factor-engineered mesenchymal stem cells prevent myocardial ischemic injury. Mol Ther. 2011;19:741-50.
[187] Haider H, Jiang S, Idris NM, Ashraf M. IGF-1-overexpressing mesenchymal stem cells accelerate bone marrow stem cell mobilization via paracrine activation of SDF-1alpha/CXCR4 signaling to promote myocardial repair. Circ Res. 2008;103:1300-8.
[188] Saparov A, Ogay V, Nurgozhin T, Jumabay M, Chen WCW. Preconditioning of Human Mesenchymal Stem Cells to Enhance Their Regulation of the Immune Response. Stem Cells International. 2016;2016:10.
[189] Zhang J, Chen GH, Wang YW, Zhao J, Duan HF, Liao LM, et al. Hydrogen peroxide preconditioning enhances the therapeutic efficacy of Wharton's Jelly mesenchymal stem cells after myocardial infarction. Chinese medical journal. 2012;125:3472-8.
[190] Crisostomo PR, Wang Y, Markel TA, Wang M, Lahm T, Meldrum DR. Human mesenchymal stem cells stimulated by TNF-α, LPS, or hypoxia produce growth factors by an NFκB- but not JNK-dependent mechanism. American Journal of Physiology - Cell Physiology. 2008;294:C675-C82.
[191] Linares GR, Chiu CT, Scheuing L, Leng Y, Liao HM, Maric D, et al. Preconditioning mesenchymal stem cells with the mood stabilizers lithium and valproic acid enhances therapeutic efficacy in a mouse model of Huntington's disease. Experimental neurology. 2016;281:81-92.
[192] Herrmann JL, Wang Y, Abarbanell AM, Weil BR, Tan J, Meldrum DR. Preconditioning mesenchymal stem cells with transforming growth factor-alpha improves mesenchymal stem cell-mediated cardioprotection. Shock (Augusta, Ga). 2010;33:24-30.
[193] Mirotsou M, Jayawardena TM, Schmeckpeper J, Gnecchi M, Dzau VJ. Paracrine mechanisms of stem cell reparative and regenerative actions in the heart. Journal of molecular and cellular cardiology. 2011;50:280-9.
[194] Relaix F, Zammit PS. Satellite cells are essential for skeletal muscle regeneration: the cell on the edge returns centre stage. Development (Cambridge, England). 2012;139:2845-56.
[195] Quarta M, Brett JO, DiMarco R, De Morree A, Boutet SC, Chacon R, et al. An artificial niche preserves the quiescence of muscle stem cells and enhances their therapeutic efficacy. Nat Biotech. 2016;34:752-9.
[196] Griffin CA, Kafadar KA, Pavlath GK. MOR23 promotes muscle regeneration and regulates cell adhesion and migration. Developmental cell. 2009;17:649-61.
[197] Musarò, A. The Basis of Muscle Regeneration. Advances in Biology. 2014;2014:16.
[198] Alwes F, Enjolras C, Averof M. Live imaging reveals the progenitors and cell dynamics of limb regeneration. eLife. 2016;5:e19766.
[199] Griffin CA, Apponi LH, Long KK, Pavlath GK. Chemokine expression and control of muscle cell migration during myogenesis. J Cell Sci. 2010;123:3052-60.
[200] Webster Micah T, Manor U, Lippincott-Schwartz J, Fan C-M. Intravital Imaging Reveals Ghost Fibers as Architectural Units Guiding Myogenic Progenitors during Regeneration. Cell stem cell.18:243-52.
[201] Stark DA, Karvas RM, Siegel AL, Cornelison DD. Eph/ephrin interactions modulate muscle satellite cell motility and patterning. Development (Cambridge, England). 2011;138:5279-89.
[202] Jansen KM, Pavlath GK. Mannose receptor regulates myoblast motility and muscle growth. J Cell Biol. 2006;174:403-13.
[203] Bentzinger CF, von Maltzahn J, Dumont NA, Stark DA, Wang YX, Nhan K, et al. Wnt7a stimulates myogenic stem cell motility and engraftment resulting in improved muscle strength. The Journal of Cell Biology. 2014;205:97-111.

[204] Siegel AL, Atchison K, Fisher KE, Davis GE, Cornelison DD. 3D timelapse analysis of muscle satellite cell motility. Stem cells (Dayton, Ohio). 2009;27:2527-38.
[205] Neuhaus P, Oustanina S, Loch T, Kruger M, Bober E, Dono R, et al. Reduced mobility of fibroblast growth factor (FGF)-deficient myoblasts might contribute to dystrophic changes in the musculature of FGF2/FGF6/mdx triple-mutant mice. Molecular and cellular biology. 2003;23:6037-48.
[206] Jejurikar SS, Marcelo CL, Kuzon WM, Jr. Skeletal muscle denervation increases satellite cell susceptibility to apoptosis. Plast Reconstr Surg. 2002;110:160-8.
[207] Mauro A. SATELLITE CELL OF SKELETAL MUSCLE FIBERS. The Journal of biophysical and biochemical cytology. 1961;9:493-5.
[208] Yoshida T, Galvez S, Tiwari S, Rezk BM, Semprun-Prieto L, Higashi Y, et al. Angiotensin II inhibits satellite cell proliferation and prevents skeletal muscle regeneration. J Biol Chem. 2013;288:23823-32.
[209] Arsic N, Zacchigna S, Zentilin L, Ramirez-Correa G, Pattarini L, Salvi A, et al. Vascular endothelial growth factor stimulates skeletal muscle regeneration in vivo. Mol Ther. 2004;10:844-54.
[210] Sassoli C, Pini A, Chellini F, Mazzanti B, Nistri S, Nosi D, et al. Bone Marrow Mesenchymal Stromal Cells Stimulate Skeletal Myoblast Proliferation through the Paracrine Release of VEGF. PLOS ONE. 2012;7:e37512.
[211] Sciorati C, Rigamonti E, Manfredi AA, Rovere-Querini P. Cell death, clearance and immunity in the skeletal muscle. Cell Death Differ. 2016;23:927-37.
[212] Sadtler K, Estrellas K, Allen BW, Wolf MT, Fan H, Tam AJ, et al. Developing a pro-regenerative biomaterial scaffold microenvironment requires T helper 2 cells. Science. 2016;352:366-70.
[213] Ninagawa NT, Isobe E, Hirayama Y, Murakami R, Komatsu K, Nagai M, et al. Transplantated mesenchymal stem cells derived from embryonic stem cells promote muscle regeneration and accelerate functional recovery of injured skeletal muscle. BioResearch open access. 2013;2:295-306.
[214] Harris JB, Vater R, Wilson M, Cullen MJ. Muscle fibre breakdown in venom-induced muscle degeneration. Journal of anatomy. 2003;202:363-72.
[215] Winkler T, von Roth P, Matziolis G, Schumann MR, Hahn S, Strube P, et al. Time course of skeletal muscle regeneration after severe trauma. Acta orthopaedica. 2011;82:102-11.
[216] Sicari BM, Rubin JP, Dearth CL, Wolf MT, Ambrosio F, Boninger M, et al. An acellular biologic scaffold promotes skeletal muscle formation in mice and humans with volumetric muscle loss. Science translational medicine. 2014;6:234ra58.
[217] Wigston DJ, English AW. Fiber-type proportions in mammalian soleus muscle during postnatal development. Journal of neurobiology. 1992;23:61-70.
[218] Madeddu P. Therapeutic angiogenesis and vasculogenesis for tissue regeneration. Experimental Physiology. 2005;90:315-26.
[219] Qazi TH, Mooney DJ, Pumberger M, Geißler S, Duda GN. Biomaterials based strategies for skeletal muscle tissue engineering: Existing technologies and future trends. Biomaterials. 2015;53:502-21.
[220] Dennis RG, Kosnik PE, 2nd. Excitability and isometric contractile properties of mammalian skeletal muscle constructs engineered in vitro. In Vitro Cell Dev Biol Anim. 2000;36:327-35.
[221] Germani A, Di Carlo A, Mangoni A, Straino S, Giacinti C, Turrini P, et al. Vascular endothelial growth factor modulates skeletal myoblast function. The American journal of pathology. 2003;163:1417-28.

[222] Hardy D, Besnard A, Latil M, Jouvion G, Briand D, Thépenier C, et al. Comparative Study of Injury Models for Studying Muscle Regeneration in Mice. PLOS ONE. 2016;11:e0147198.
[223] Carmeliet P. Angiogenesis in health and disease. Nat Med. 2003;9:653-60.
[224] Brudno Y, Ennett-Shepard AB, Chen RR, Aizenberg M, Mooney DJ. Enhancing microvascular formation and vessel maturation through temporal control over multiple pro-angiogenic and pro-maturation factors. Biomaterials. 2013;34:9201-9.
[225] Li CX, Talele NP, Boo S, Koehler A, Knee-Walden E, Balestrini JL, et al. MicroRNA-21 preserves the fibrotic mechanical memory of mesenchymal stem cells. Nat Mater. 2016;advance online publication.
[226] Cosgrove BD, Mui KL, Driscoll TP, Caliari SR, Mehta KD, Assoian RK, et al. N-cadherin adhesive interactions modulate matrix mechanosensing and fate commitment of mesenchymal stem cells. Nat Mater. 2016;15:1297-306.
[227] Khetan S, Guvendiren M, Legant WR, Cohen DM, Chen CS, Burdick JA. Degradation-mediated cellular traction directs stem cell fate in covalently crosslinked three-dimensional hydrogels. Nat Mater. 2013;12:458-65.
[228] Trappmann B, Gautrot JE, Connelly JT, Strange DG, Li Y, Oyen ML, et al. Extracellular-matrix tethering regulates stem-cell fate. Nat Mater. 2012;11:642-9.
[229] Benoit DS, Schwartz MP, Durney AR, Anseth KS. Small functional groups for controlled differentiation of hydrogel-encapsulated human mesenchymal stem cells. Nat Mater. 2008;7:816-23.